

NEW SIGNAL PROCESSING  
ALGORITHMS FOR AUTOMATED  
EXTERNAL DEFIBRILLATORS

BY

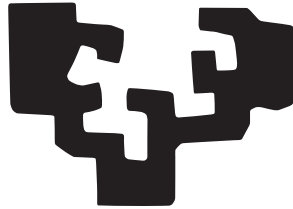
UNAI IRUSTA ZARANDONA

SUPERVISOR

JESÚS MARÍA RUIZ OJEDA

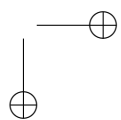
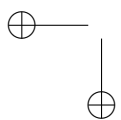
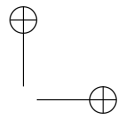
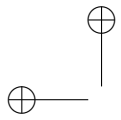
SUBMITTED IN PARTIAL FULFILLMENT  
FOR THE REQUIREMENTS FOR THE DEGREE  
OF DOCTOR OF SCIENCE

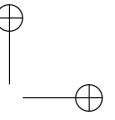
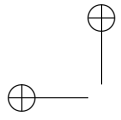
eman ta zabal zazu



UPV EHU

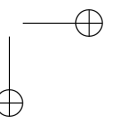
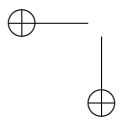
DEPARTMENT OF ELECTRONICS AND TELECOMMUNICATIONS  
BILBAO, JULY 2010

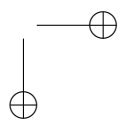
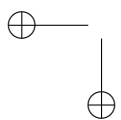
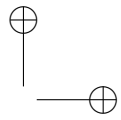
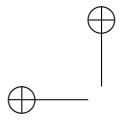




*Dedicated to my loving wife, Cristina, for her  
endless support, patience and encouragement.*

*Thanks for looking so well after your cocodrilos.*







## ABSTRACT

Life is a journey sometimes interrupted in a sudden and unexpected way.

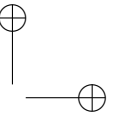
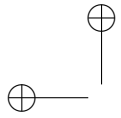
In 40% of sudden out-of-hospital cardiac arrest (OHCA) cases the initially recorded heart rhythm is ventricular fibrillation (VF). The only effective way to treat VF is by procuring a defibrillating electrical shock to the heart. In an out-of-hospital setting, the shock is delivered using an automated external defibrillator (AED), a device capable of analyzing the victim's electrocardiogram (ECG) to detect if a shockable rhythm is present. Survival from OHCA depends largely on two factors: early defibrillation and early cardiopulmonary resuscitation (CPR), which prolongs the window of opportunity for defibrillation. CPR must be stopped for a reliable AED rhythm analysis because chest compressions introduce artifacts in the ECG. Unfortunately, interrupting CPR adversely affects defibrillation success.

The use of AEDs in 1 to 8 year olds was approved in 2003. AEDs, which were originally designed for adult patients, must accurately discriminate pediatric arrhythmias to be safely used in children. Several AEDs have been adapted for pediatric use, either by demonstrating that existing adult algorithms accurately diagnose pediatric arrhythmias or by creating specific algorithms to diagnose pediatric arrhythmias.

This thesis presents a new AED algorithm designed for adult and pediatric patients together. The algorithm is thoroughly tested using pediatric and adult arrhythmia databases compliant with the American Heart Association (AHA) statements, and on real resuscitation data with and without CPR artifacts.

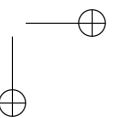
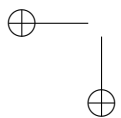
The work started with a long experimental phase in which 1090 pediatric rhythms were retrospectively collected and classified to create a comprehensive database of pediatric arrhythmias. Additionally, an existing adult database was revised and 928 new adult rhythms were collected and classified. The complete dataset is composed of 2782 registers, 1270 were used to develop the algorithm and 1512 to test it.

Then, a new AED shock advice algorithm composed of four sub-algorithms was designed. These sub-algorithms are based on a set of new arrhythmia detection features derived from several signal domains such as time, frequency, slope or the autocorrelation function. The algorithm exceeded the AHA performance goals for



the detection of shockable and non-shockable rhythms both on adult and pediatric arrhythmias.

The work concluded with the analysis of the performance of the algorithm for real resuscitation data extracted from a comprehensive database of OHCA episodes. All AHA performance goals were met for artifact-free OHCA rhythms. Then, the performance of the algorithm during chest compressions was assessed, before and after the suppression of the CPR artifact. The CPR artifact was suppressed using a new methodology developed as part of this thesis work. Although shockable rhythms were accurately identified after filtering, non-shockable rhythms were not.



## LABURPENA

Bizitza bidaia da, batzuetan bat-batean eta ezustean eteten den bidaia.

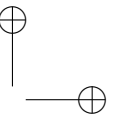
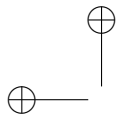
Ospitaletik kanpo gertatzen diren bat-bateko bihotz-biriketako geldiketa-kasuen % 40an lehendabizi grabatutako bihotz-erritmoa fibrilazio bentrikularra (FB) da. Bihotzean desfibrilazioa eragingo duen deskarga elektrikoa ematea da FBa tratatzeko modu eraginkor bakarra. Ospitaletik at, kanpoko desfibrilagailu automatikoa (KDA) erabiltzen da deskarga emateko, pazientearen elektrokardiograma (EKG) aztertu eta desfibrilagarriak diren erritmoak detektatzeko gaitasuna duen aparagailua, alegia. Kasu horietan, biziraupena bi faktore hauen menpekoa da: desfibrilazio goiztiarraren menpekoa eta bihotz-biriketako berpizte (BBB) goiztiarraren menpekoa (desfibrilazioa emateko aukera-lehioa luzatzen duena). BBBan ematen diren bular-sakadak interferentzia sortzen dute EKGan; ondorioz, BBBa gelditu behar da KDAk bihotz erritmoa egokiro azter dezan. Tamalez, geldiketa horiek desfibrilazioaren arrakasta maila txikiagotzen dute.

KDA-aren erabilera 1 eta 8 urte bitarteko umeekin 2003an onartu zen. Ordura arte paziente helduak tratatzeko diseinutako KDAk modu zehatzean identifikatu behar dituzte arritmia pediatrikoak, umeekin erabili ahal izateko. Zenbait KDA umeekin erabiltzeko egokitu dira, bi eratarata: helduekin erabiltzen diren algoritmoak umeekin ere zehatzak direla frogatuz, eta umeen arritmiak identifikatzeko algoritmo bereziak erabiliz.

Tesi honetan KDA algoritmo berri bat garatu da, diseinua paziente heldu eta pediatrikoekin batera eginez. Algoritmoa sakon egiaztatu da. Batetik, American Heart Association (AHA) erakundeak ezarritako baldintzak betetzen dituzten helduen eta umeen arritmia datu-baseak erabiliz, eta, bestetik, bihotz-geldiketetan grabatutako arritmiak erabiliz, BBB interferentziaz kutsatutako eta interferentziarik gabeko kasuetan.

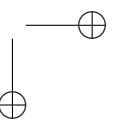
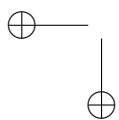
Tesi-lana atal experimental luze batekin hasi zen. Fase horretan 1090 arritmia pediatriko bildu eta klasifikatu ziren, arritmia pediatrikoen datu-base zabal bat sortuz. Horrez gain, helduen datu-base oso bat berraztertu eta 928 helduen arritmia berri bildu eta klasifikatu ziren. Datu-base osoak 2782 erregistro ditu: 1270 algoritmoa garatzeko erabili ziren eta 1512 algoritmoa egiaztatzeko.

Ondoren, lau azpialgoritmoz osatutako algoritmo berria garatu zen. Azpialgoritmoek seinalearen zebait eremutan kalkulaturako



parametro berriak erabiltzen dituzte arritmiak detektatzeko; adibidez, denbora, maiztasuna, pendiza edo autokorrelazio-funtzioa. Algoritmo berriak AHAK ezarritako mailak gainditzen ditu erritmo desfibrilagarri eta ez-desfibrilagarriak detektatzeko, paziente pediatriko zein helduekin.

Lanaren azken atalean, algoritmo berriak bihotz-geldiketan grabatutako erregistroak identifikatzeko duen ahalmena aztertu zen. BBB interferentziarik gabeko erritmoetan, algoritmoak AHAK ezarritako mailak gainditzen ditu. Ondoren, erritmoak aztertu ziren bular-sakadak ematen ziren bitartean, BBB interferentzia ezabatu aurretik eta ezabatu ondoren. Interferentzia ezabatzeko, tesian zehar garatutako metodo berri bat erabili zen. BBB interferentzia ezabatu ondoren, erritmo desfibrilagarriak modu zehatzean identifikatu ziren; erritmo ez-desfibrilagarriak, ez.







## RESUMEN

La vida es un viaje que a veces se interrumpe de forma súbita e inesperada.

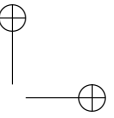
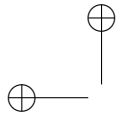
La fibrilación ventricular (VF) es el primer ritmo registrado en el 40% de las muertes súbitas por paro cardiorrespiratorio extrahospitalario (PCRE). El único tratamiento eficaz para la FV es la desfibrilación mediante una descarga eléctrica. Fuera del hospital, la descarga se administra mediante un desfibrilador externo automático (DEA), que previamente analiza el electrocardiograma (ECG) del paciente y comprueba si presenta un ritmo desfibrilable. La supervivencia en un caso de PCRE depende fundamentalmente de dos factores: la desfibrilación temprana y la resucitación cardiopulmonar (RCP) temprana, que prolonga la FV y por lo tanto la oportunidad de desfibrilación. Para un correcto análisis del ritmo cardiaco es necesario interrumpir la RCP, ya que, debido a las compresiones torácicas, la RCP introduce artefactos en el ECG. Desafortunadamente, la interrupción de la RCP afecta negativamente al éxito en la desfibrilación.

En 2003 se aprobó el uso del DEA en pacientes entre 1 y 8 años. Los DEA, que originalmente se diseñaron para pacientes adultos, deben discriminar de forma precisa las arritmias pediátricas para que su uso en niños sea seguro. Varios DEAs se han adaptado para uso pediátrico, bien demostrando la precisión de los algoritmos para adultos con arritmias pediátricas, o bien mediante algoritmos específicos para arritmias pediátricas.

Esta tesis presenta un nuevo algoritmo DEA diseñado conjuntamente para pacientes adultos y pediátricos. El algoritmo se ha probado exhaustivamente en bases de datos acordes a los requisitos de la American Heart Association (AHA), y en registros de resucitación con y sin artefacto RCP.

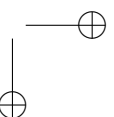
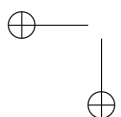
El trabajo comenzó con una larga fase experimental en la que se recopilaban y clasificaban retrospectivamente un total de 1090 ritmos pediátricos. Además, se revisó una base de arritmias de adultos y se añadieron 928 nuevos ritmos de adultos. La base de datos final contiene 2782 registros, 1270 se usaron para diseñar el algoritmo y 1512 para validarlo.

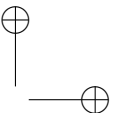
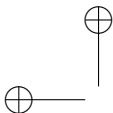
A continuación, se diseñó un nuevo algoritmo DEA compuesto de cuatro subalgoritmos. Estos subalgoritmos están basados en un conjunto de nuevos parámetros para la detección de arritmias, calculados en diversos dominios de la señal, como el tiempo,



la frecuencia, la pendiente o la función de autocorrelación. El algoritmo cumple las exigencias de la AHA para la detección de ritmos desfibrilables y no-desfibrilables tanto en pacientes adultos como en pediátricos.

El trabajo concluyó con el análisis del comportamiento del algoritmo con episodios reales de resucitación. En los ritmos que no contenían artefacto RCP se cumplieron las exigencias de la AHA. Posteriormente, se estudió la precisión del algoritmo durante las compresiones torácicas, antes y después de filtrar el artefacto RCP. Para suprimir el artefacto se utilizó un nuevo método desarrollado a lo largo de la tesis. Los ritmos desfibrilables se detectaron de forma precisa tras el filtrado, los no-desfibrilables sin embargo no.





*Life is a journey not a destination.*

— Ralph Waldo Emerson

## ACKNOWLEDGMENTS

This is the culmination of six years of dedicated work. Sometimes I was lost, other times I walked down the wrong alley. At times I felt I did not know where I was heading but I was always sure the path was right. And I never walked alone. It is my pleasure to thank the people who inspired me to follow this path and those who helped me walk this way.

I thank my parents, Maite and Joseba, for teaching me the value of hard and honest work and for showing me the pleasure of doing things well. My brothers and sisters, Aritz, Olatz and Naiara for making our house a fun place to live and for putting up with my bossy and distant character. My uncle Sabin, for so many inspiring books, surely you were not joking.

I am grateful to the Electronics and Telecommunications department and to the University of the Basque Country for their support. To the Spanish Ministry of Science and Osatu SCoop for financial support. Thanks to the people in Osatu's R&D department for giving us interesting problems to work on.

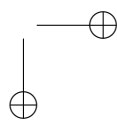
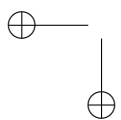
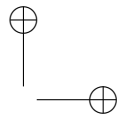
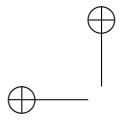
I am indebted to Joseba Zubia, who introduced me to the art and craft of scientific research, and who kindly accepted that I looked at research from a different optic. To Trygve Eftestøl for his willingness to cooperate, this thesis would have been different had I never enjoyed sharing interests with you. My gratitude to Drs. Brugada, Benito, Bodegas, Pastor, Porres and López-Herce for their contribution to the ECG databases.

To the people in the GSC group, thanks for making me feel home. Special thanks to Eli and Sofia for all the shared hard work and moments, good and bad. Many thanks for all those unrewarded hours spent working on ECG databases, and thank you both for being an essential part of this work.

To my supervisor and friend, Jesús, words can't describe how I feel. This thesis is our work. Thank you for the privilege of knowing a wonderful teacher, a role model of inspiration, insight, outlook and hard work. But most of all, thanks for the company.

To Cristina and Eneko, thank you for making these last two years the most wonderful experience in my life.

— Unai Irusta



# CONTENTS

List of Figures	xv
List of Tables	xvii
List of Acronyms	xix
1 INTRODUCTION	1
1.1 The ECG signal . . . . .	1
1.2 Sudden cardiac death . . . . .	3
1.3 The chain of survival . . . . .	4
1.4 The automated external defibrillator . . . . .	7
1.4.1 The shock advice algorithm . . . . .	8
1.4.2 The use of AEDs in children . . . . .	11
1.5 New milestones in the design of AED shock advice algorithms . . . . .	13
1.5.1 Shock advice algorithms for pediatric use . . . . .	14
1.5.2 CPR artifacts and shock advice algorithms . . . . .	15
1.6 Objectives of the thesis . . . . .	16
2 BACKGROUND	19
2.1 AED shock advice algorithms . . . . .	19
2.1.1 Feature extraction . . . . .	20
2.1.2 Decision algorithms . . . . .	23
2.2 Review of five VF detection algorithms . . . . .	23
2.2.1 Comparison of five VF detection algorithms . . . . .	27
2.3 Pediatric shock advice algorithms . . . . .	30
2.4 Shock advice during CPR . . . . .	33
2.4.1 First animal models . . . . .	33
2.4.2 First experiments on human VF . . . . .	35
2.4.3 First study on real OHCA episodes . . . . .	37
2.4.4 Simplifying rhythm analysis during CPR . . . . .	39
2.4.5 Comparative assessment on OHCA registers . . . . .	42
2.5 Contributions of the thesis work . . . . .	44
3 ECG REGISTER DATABASES	45
3.1 Databases for AED rhythm analysis . . . . .	45
3.1.1 The collection of the ECG registers . . . . .	46
3.1.2 The classification of the ECG registers . . . . .	49
3.1.3 Databases of adult registers . . . . .	52
3.1.4 The pediatric database . . . . .	54
3.1.5 Databases for the development and testing of AED shock advice algorithms . . . . .	56
3.2 Database of OHCA episodes . . . . .	57
4 SHOCK ADVICE ALGORITHM	63

4.1	Overview of the shock advice algorithm . . . . .	63
4.1.1	Basic design principles . . . . .	63
4.1.2	Block diagram of the decision algorithm . . .	64
4.2	Asystole algorithm . . . . .	67
4.3	QRS algorithm . . . . .	70
4.3.1	Slope domain: <i>bCP</i> parameter . . . . .	71
4.3.2	Frequency domain: <i>bW</i> parameter . . . . .	72
4.3.3	Time domain: <i>bWT</i> parameter . . . . .	75
4.3.4	Decision algorithm . . . . .	78
4.4	Regularity algorithm . . . . .	83
4.4.1	Signal analysis using the ACF . . . . .	84
4.4.2	Classification results . . . . .	89
4.5	SVT/VT algorithm . . . . .	92
4.5.1	Features in the frequency domain . . . . .	93
4.5.2	Decision algorithm . . . . .	95
4.6	Classification results . . . . .	99
4.6.1	Segment type classification . . . . .	99
4.6.2	Shock/Noshock classification . . . . .	101
4.6.3	Results for the adult and pediatric patients .	104
4.6.4	Graphical examples of classification errors .	107
5	OHCA RHYTHM ANALYSIS . . . . .	113
5.1	Structure of the OHCA episodes . . . . .	113
5.2	Diagnosing clean OHCA rhythms . . . . .	115
5.3	Rhythm analysis during CPR . . . . .	120
5.3.1	Characteristics of the CPR artifact . . . . .	120
5.3.2	Adaptive filter based on the frequency of the chest compressions . . . . .	123
5.3.3	Sensitivity and specificity of the new AED algorithm . . . . .	130
6	CONCLUSIONS . . . . .	143
7	BIBLIOGRAPHY . . . . .	149

## LIST OF FIGURES

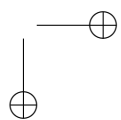
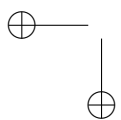
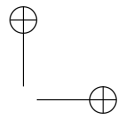
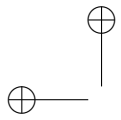
Figure 1.1	The electrical system of the heart . . . . .	1
Figure 1.2	A typical ECG recording . . . . .	2
Figure 1.3	Subgroups at risk for sudden cardiac death	4
Figure 1.4	The chain of survival . . . . .	5
Figure 1.5	Basic operation steps of an AED . . . . .	8
Figure 1.6	Defibrillation pad placement . . . . .	13
Figure 2.1	Diagram of an AED shock advice algorithm	19
Figure 2.2	ECG in the time and frequency domains . .	21
Figure 2.3	Parameters for the calculation of TCI . . . .	26
Figure 2.4	OHCA rhythms corrupted by a CPR artifact	34
Figure 2.5	Example of the additive noise model . . . .	36
Figure 3.1	Shockable and non-shockable rhythms . . .	47
Figure 3.2	Digitization process of paper ECG strips. . .	49
Figure 3.3	Pediatric VT and SVT . . . . .	51
Figure 3.4	Rhythms from the OHCA register database	60
Figure 4.1	Block diagram of the shock advice algorithm	66
Figure 4.2	Block diagram of the Asystole algorithm . .	67
Figure 4.3	Borderline cases for the Asystole algorithm .	69
Figure 4.4	Block diagram of the QRS algorithm . . . .	70
Figure 4.5	Slope for PR and nPR segments . . . . .	72
Figure 4.6	Analysis in the slope domain . . . . .	73
Figure 4.7	Bandwidth for PR and nPR segments . . . .	74
Figure 4.8	Analysis in the frequency domain . . . . .	75
Figure 4.9	Baseline content for PR and nPR segments .	76
Figure 4.10	Analysis in the time domain . . . . .	77
Figure 4.11	Histograms for the QRS algorithm . . . . .	79
Figure 4.12	Misclassification examples, QRS algorithm .	82
Figure 4.13	Regularity in shockable registers . . . . .	83
Figure 4.14	Block diagram of the Regularity algorithm .	84
Figure 4.15	Regularity of the positive peaks of the ACF	86
Figure 4.16	Peak ordering of the ACF . . . . .	88
Figure 4.17	Analysis in the autocorrelation domain . . .	89
Figure 4.18	Borderline cases for the Regularity algorithm	91
Figure 4.19	Block diagram of the SVT/VT algorithm . .	92
Figure 4.20	PSD for SVT and VT . . . . .	94
Figure 4.21	Histograms for the SVT/VT algorithm . . .	96

Figure 4.22	Borderline cases for the SVT/VT algorithm . . .	98
Figure 4.23	Misclassified VF . . . . .	108
Figure 4.24	Misclassified pediatric VT . . . . .	109
Figure 4.25	Misclassified SVT . . . . .	110
Figure 4.26	Misclassified non-shockable rhythms . . . . .	111
Figure 5.1	Analysis intervals for OHCA episodes. . . . .	114
Figure 5.2	PEA recorded in victims of OHCA . . . . .	116
Figure 5.3	Misclassified OHCA registers . . . . .	119
Figure 5.4	Two CPR artifacts . . . . .	120
Figure 5.5	PSD of the CPR artifacts . . . . .	121
Figure 5.6	Spectral overlap . . . . .	122
Figure 5.7	Estimating the chest-compression frequency . . . . .	124
Figure 5.8	The reference signal . . . . .	126
Figure 5.9	Diagram of the CPR suppression filter . . . . .	127
Figure 5.10	Frequency response of the LMS filter . . . . .	128
Figure 5.11	Se and Sp after filtering for $N = 5$ . . . . .	129
Figure 5.12	VF recovered after filtering . . . . .	134
Figure 5.13	VF identified before and after filtering . . . . .	135
Figure 5.14	VF misclassified after filtering . . . . .	136
Figure 5.15	AS identified before and after filtering . . . . .	137
Figure 5.16	AS misclassified after filtering . . . . .	138
Figure 5.17	PEA identified before and after filtering . . . . .	139
Figure 5.18	PEA misclassified after filtering . . . . .	140
Figure 5.19	PR identified before and after filtering . . . . .	141
Figure 5.20	PR recovered after filtering . . . . .	142



## LIST OF TABLES

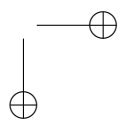
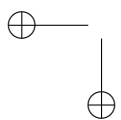
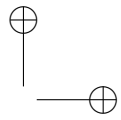
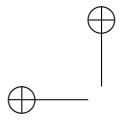
Table 1.1	Percentage of survival in OHCA . . . . .	6
Table 1.2	Contingency table for an AED . . . . .	9
Table 1.3	AHA performance goals for AED algorithms	11
Table 2.1	Comparison of five VF detection methods . .	29
Table 2.2	Summary of published pediatric databases .	32
Table 2.3	Rhythm analysis methods during CPR tested on OHCA episodes . . . . .	43
Table 3.1	Characteristics of the acquisition systems . .	48
Table 3.2	The Reanibex database. . . . .	52
Table 3.3	The Donostia–Emergencias database . . . .	53
Table 3.4	The pediatric database . . . . .	55
Table 3.5	The pediatric database, 1–8 year olds . . . .	56
Table 3.6	Development and test databases . . . . .	58
Table 3.7	The database of OHCA registers . . . . .	61
Table 4.1	Segment classification categories . . . . .	65
Table 4.2	<i>P</i> parameter for the development database .	68
Table 4.3	Classification results, Asystole algorithm . .	68
Table 4.4	Discriminative power, QRS algorithm . . . .	79
Table 4.5	Classification results, QRS algorithm . . . .	81
Table 4.6	Classification results, Regularity algorithm .	90
Table 4.7	Feature selection, SVT/VT algorithm . . . .	95
Table 4.8	Classification results, SVT/VT algorithm . .	97
Table 4.9	Classification results for the segments . . . .	100
Table 4.10	Se and Sp for the segments . . . . .	102
Table 4.11	Se and Sp for the registers . . . . .	103
Table 4.12	Additional performance metrics . . . . .	104
Table 4.13	Se and Sp, pediatric/adult segments . . . .	105
Table 4.14	Se and Sp, pediatric/adult registers . . . .	106
Table 4.15	Performance metrics, pediatric/adult . . . .	107
Table 5.1	Se and Sp for pure OHCA rhythms . . . . .	117
Table 5.2	Mean performance of the LMS filter . . . . .	130
Table 5.3	Se and Sp before and after filtering . . . . .	131

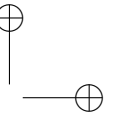
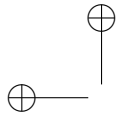




## LIST OF ACRONYMS

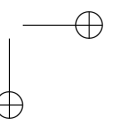
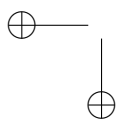
ACF	Autocorrelation function
AED	Automated external defibrillator
AF	Atrial fibrillation
AHA	American heart association
CPR	Cardiopulmonary resuscitation
DF	Dominant frequency
ECG	Electrocardiogram
EMS	Emergency medical services
EP	Electrophysiology
FFT	Fast Fourier transform
ILCOR	International liaison committee on resuscitation
IV	Ideoventricular
LMS	Least mean squares
NSR	Normal sinus rhythm
OHCA	Out-of-hospital cardiac arrest
PAD	Public access defibrillation
PEA	Pulseless electrical activity
PR	Pulse-giving rhythm
PSD	Power spectral density
PVC	Premature ventricular contractions
ROSC	Return of spontaneous circulation
SB	Sinus bradycardia
SCD	Sudden cardiac death
SNR	Signal-to-noise ratio
SVT	Supraventricular tachycardia
VF	Ventricular fibrillation
VT	Ventricular tachycardia
bpm	beats per minute
cpm	compressions per minute
dB	decibel
et al.	and others (et alia)
i. e.	that is (id est)

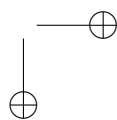
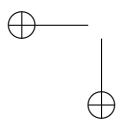
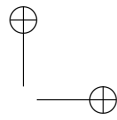
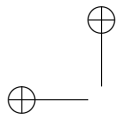




*Defibrillators are for hearts too good to die.*

— Claude S Beck





# 1 | INTRODUCTION

## 1.1 The ECG signal

The heart is a hollow muscular organ that pumps blood through the blood vessels by repeated and rhythmic contractions. The human heart has four chambers: the two on the right pump blood to the lungs to pick up oxygen, and the two on the left pump the oxygenated blood to the body. On each side, there is an upper low-pressure chamber called the atrium, and a lower high-pressure chamber called the ventricle that provides the main pumping function.

The cardiac cycle consists of two phases: a filling phase called diastole and a contracting or pumping phase called systole. To pump blood effectively, the cardiac muscle must contract in a highly synchronized way. This contraction is triggered by an electric impulse automatically generated in the heart and propagated through an elaborate conduction system, shown in Figure 1.1. This is possible because the myocardium, the heart's muscular

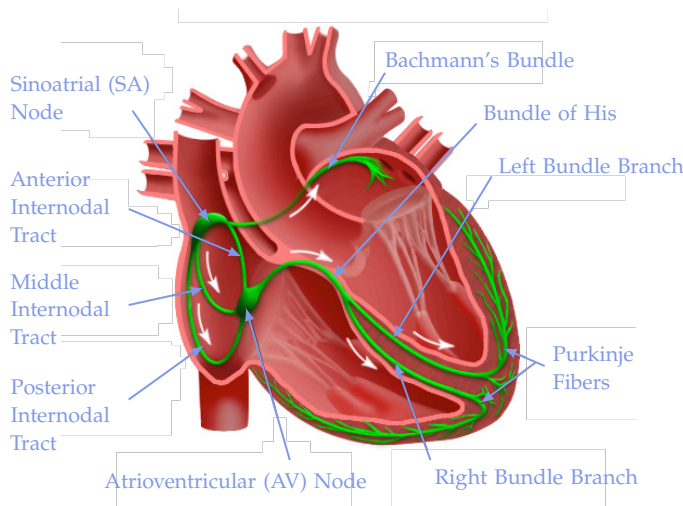


**Figure 1.1:** The electrical system of the heart. Downloaded and adapted from [www.ohsuhealth.com](http://www.ohsuhealth.com).

wall, contains specialized cells with the capacity to generate and conduct an electrical impulse.<sup>†</sup>

In a healthy heart, the initiation of the cardiac cycle occurs in a cluster of pacemaker cells, called sinoatrial (SA) node, located in the right atrium. Acting as the natural pacemaker of the heart, the SA node initiates the impulse at regular intervals 60 to 100 times per minute. The electrical impulse propagates through the internodal pathways, activating — depolarizing — the atria. This causes the atria to contract; thus, pumping blood into the ventricles. The atrioventricular (AV) node collects and delays the impulse, allowing the ventricles time to finish filling with blood. The impulse then traverses the wall between the ventricles through the bundle of His and divides into the right and left bundle branches, and further into a network of conducting fibers called the Purkinje fibers. The impulse propagates rapidly through this network, depolarizing the ventricles and producing a unified contraction. The cardiac cells then return to their original state — repolarize — following a refractory period, during which they cannot be depolarized again. The refractory period prevents the impulse from traveling back to the atria.

The electrical activity of the heart recorded by electrodes placed on the body surface is called an electrocardiogram or ECG. Figure 1.2 shows an ECG record of a normal beat of the heart, called

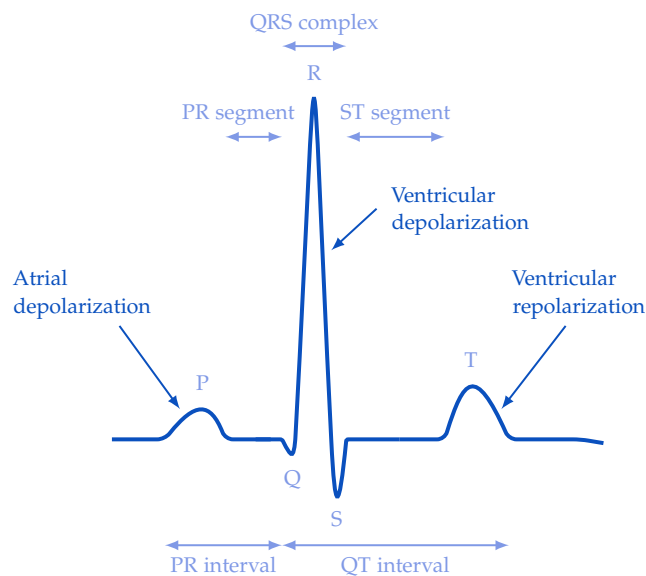


**Figure 1.2:** A typical ECG recording of a normal sinus rhythm.

<sup>†</sup> The myocardium is primarily composed of contractile muscle cells.



the normal sinus rhythm. It consists of a P wave, a QRS complex, and a T wave, caused by atrial depolarization, ventricular depolarization, and ventricular repolarization, respectively. Atrial repolarization is masked by the QRS complex and is not visible in the ECG.

## 1.2 Sudden cardiac death

The sudden cessation of the mechanical activity of the heart, confirmed by the absence of signs of circulation, is called sudden cardiac arrest (SCA).<sup>69</sup> Death resulting from SCA is called sudden cardiac death (SCD) and is usually defined as the unexpected natural death from a cardiac cause within a short time, generally less than one hour from the onset of the symptoms.<sup>152</sup>

SCD is the single most important cause of death in the adult population of the industrialized world. The precise incidence of SCD is not known. Estimates of the annual incidence among the United States (US) adult population range from 184 000 to 450 000, depending on the definition of SCD and the inclusion criteria used in each study.<sup>35,151</sup> The most widely accepted estimate of 300 000 annual deaths accounts for an average of 100 to 200 deaths per 100 000 adults over 35 years of age and represents 50% of all heart-related deaths.<sup>104</sup>

The most frequent cause of SCD is fatal ventricular arrhythmias: ventricular fibrillation (VF) and ventricular tachycardia (VT).<sup>40</sup> In fact, VT degenerating to VF appears to be the mechanism for the large majority of cardiac arrests.<sup>97</sup> During VF, the ventricles rapidly depolarize and repolarize, and the heart loses its coordinated function and stops pumping blood efficiently. The only effective way to terminate VF and to restore a perfusing cardiac rhythm is defibrillation, procured through the delivery of an electrical shock to the heart.<sup>23</sup>

One of the highest priorities in cardiovascular research today is the prediction and prevention of the occurrence of SCD. Currently, the most predictive risk factors for the occurrence of SCD are the presence and severity of an underlying heart disease. Unfortunately, at least two thirds of all SCDs occur as a first clinical event or among subgroups of patients thought to be at relatively low risk for SCD.<sup>105</sup> Only 35–45% of the cases, the first three subgroups in Figure 1.3, present sufficient risk for effective preventive strategies.<sup>104</sup> This is why emphasis is put on the development of safe, low-cost interventions that can be applied to the population at large.

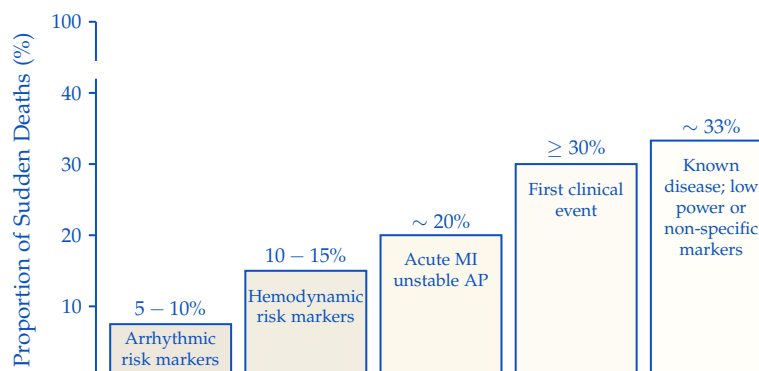


**Figure 1.3:** Subgroups at risk for sudden cardiac death. At least two-thirds of all SCDs occur as a first clinical event or among subgroups of patients thought to be at relatively low risk for SCD. AP = Angina pectoris; MI = Myocardial infarction. Derived from Myerburg and Castellanos.<sup>105</sup>

However, most SCDs occur out of hospital,<sup>151</sup> and the emergency medical services (EMS) only treat 60% of out of hospital cardiac arrests (OHCA).<sup>30</sup> In fact, the estimated annual incidence of OHCA treated by EMS in the US is 55 per 100 000 population, with VF as the initially recorded rhythm in 40% of those cases.<sup>116</sup> Although many more victims present VF or VT at the time of collapse, by the time the first ECG is recorded, their rhythm has deteriorated to asystole,<sup>135</sup> characterized by the absence of electrical activity.

The deterioration of the heart function in prolonged cardiac arrest leads to lower survival rates. For instance, the estimated survival rate in all cases of OHCA is a poor 8.4%, but rises to 17.7% when the victim presents VF as the initial rhythm.<sup>116</sup> Consequently, early intervention for victims of OHCA is critical for survival and has led to the definition of the concept of the *chain of survival*.

### 1.3 The chain of survival

In the early 1990s, the American Heart Association (AHA) established the chain of survival metaphor to describe the sequence of actions for a successful resuscitation in the event of an OHCA. The chain of survival, depicted in Figure 1.4, consists of four interdependent links.

1. *Early access*. The resuscitation chain starts with early access, which includes all steps between the initiation of the

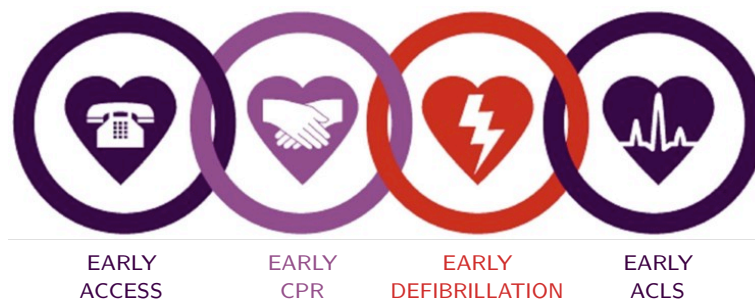


**Figure 1.4:** The chain of survival and its four interdependent links: Early Access, Early CPR, Early Defibrillation, and Early ACLS. Downloaded and adapted from <http://cprftlauderdale.com>.

cardiac arrest and the arrival of EMS personnel. First, the medical emergency is recognized either by the person with symptoms or by a witness, and then the EMS are accessed and activated. Finally, the responder reaches the scene and locates the patient to provide adequate care.

2. *Early cardiopulmonary resuscitation (CPR)*. Bystander CPR is the second link in the chain of survival. CPR consists of chest compressions and ventilations that maintain a minimal blood flow to sustain a sufficient perfusion before the arrival of the EMS personnel.
3. *Early defibrillation*. Most SCA victims are in VF, which can only be restored to a perfusing rhythm through defibrillation. In an out-of-hospital setting, defibrillation is normally administered using an automated external defibrillator (AED). The AED is a portable user-friendly device that analyzes the victim's ECG to determine whether a shockable rhythm is present. When the AED detects a shockable rhythm, it charges, then prompts the rescuer to press a shock button to deliver a defibrillating shock.
4. *Early advanced cardiac life support (ACLS)*. The last critical link in the management of cardiac arrest is early ACLS, the treatment provided by qualified health care personnel after defibrillation. ACLS includes intubation and the administration of medication.

Although the four links in the chain of survival are important, most differences in SCA survival rates are explained by two variables: the time intervals from collapse to CPR and from collapse to defibrillation.<sup>93,133</sup> If no CPR is provided, survival rates

in VF cardiac arrest decrease by 7% to 10% with every minute that defibrillation is delayed.<sup>93</sup> On the contrary, when bystander CPR is provided, the decrease is smaller: it averages 3% to 4% for every minute from collapse to defibrillation.<sup>93,133</sup> At most time intervals to defibrillation, CPR can double<sup>93,133</sup> or triple<sup>60</sup> survival from witnessed SCA. The data shown in Table 1.1 best summarize the importance of the interaction between bystander CPR and defibrillation. Without CPR starting within 5 minutes and defibrillation occurring within 10 minutes, the value of early defibrillation degrades, and the value of early CPR is lost.

Immediate bystander CPR is important for two reasons: many adults in VF survive with intact neurologic function if CPR is performed and defibrillation administered within 5 minutes after collapse,<sup>36,145</sup> and CPR prolongs VF: that is, the window of opportunity for defibrillation.<sup>59,136</sup> However, CPR alone is unlikely to terminate VF. The restoration of an adequate perfusing rhythm requires defibrillation.

When immediate access to defibrillation is available, the survival rates are very high. For instance, survival rates greater than 90% have been reported for patients defibrillated within the first minute of collapse.<sup>98</sup> However, in prolonged arrests (>5 min), several studies suggest that administering CPR before defibrillation may improve survival.<sup>36,145</sup> When EMS personnel do not witness the OHCA, the duration of the arrest is difficult to estimate, and CPR as the initial treatment may be beneficial. The evidence was not conclusive when the resuscitation guidelines were last revised in 2005, and the decision on initial treatment (CPR/defibrillation) was left to EMS directors.<sup>41</sup>

A current model of VF cardiac arrest explains the differences in treatment.<sup>139</sup> During the first or electrical phase of the arrest (<4 min), defibrillation is the crucial intervention. However, during the second or circulatory phase (i. e., for prolonged arrests: 4–10 min), the generation of adequate cerebral and coronary perfusion

Collapse to CPR	Collapse to defibrillation	
	< 10 min	> 10 min
< 5 min	37%	7%
> 5 min	20%	0%

**Table 1.1:** Percentage of survival to hospital discharge in OHCA, showing the influence of early CPR and early defibrillation.<sup>37</sup>

through chest compressions is the key intervention. Several recent studies advocate two minutes of uninterrupted chest compressions before defibrillation for prolonged arrests.<sup>79,48,78</sup>

The AHA supported the concept of public access defibrillation (PAD) in 1995<sup>140</sup> as an effort to shorten time to defibrillation. Through PAD programs, the community has access to the AED and is trained in its use. More recently, AEDs have been placed in a variety of settings,<sup>†</sup> making immediate defibrillation available and significantly increasing survival rates. The advances in AED technology over the past two decades have made AED use by non-medical personnel safe and effective, contributing to the feasibility of PAD programs.<sup>98</sup>

## 1.4 The automated external defibrillator

Diack et al. introduced the AED in 1979.<sup>42</sup> Since the early 1990s, there have been important advances in AED technology, particularly in the fields of defibrillation waveform, long-duration batteries, and rhythm analysis algorithms.<sup>131</sup> Current AEDs are low-cost, small and light, simple-to-operate devices that accurately diagnose lethal ventricular arrhythmias. These characteristics are essential in PAD programs where AEDs are operated by first-time users with minimal training. Manufacturers have simplified AED operation, which consists of four universal steps<sup>2,131</sup> (see Figure 1.5).

1. *Power on.* The AED is turned on by pressing the power switch or by lifting the monitor cover. Once switched on, a voice prompt is initiated to guide the operator through the next steps.
2. *Attach electrode pads.* The electrode pads are then placed in an anterolateral position, as indicated in the defibrillation pads in Figure 1.5. The electrode pads serve to record the ECG and to deliver the electric shock when needed. In some cases, drying or shaving the victim's chest will be necessary to guarantee adequate contact between the pads and the skin.
3. *Analyze the rhythm.* In some devices, the operator presses the *analyze* button to initiate rhythm analysis; in other devices, it begins automatically when the pads are placed and

<sup>†</sup> Among others: EMS systems, police departments, casinos, airport terminals, and commercial aircraft.<sup>134,112,143</sup>

connected. Motion artifacts produce errors in the rhythm analysis algorithms; therefore, all movement affecting the victim must be avoided, and CPR must be interrupted.

4. *Advise shock.* If the rhythm analysis algorithm detects a lethal ventricular arrhythmia, the AED will recommend a shock. In a semiautomatic configuration, the rescuer must press the shock button to deliver the shock, while in a fully automatic configuration, the shock is delivered without the intervention of the rescuer. If the algorithm does not detect a lethal ventricular arrhythmia, the AED prompts the rescuer to resume CPR.

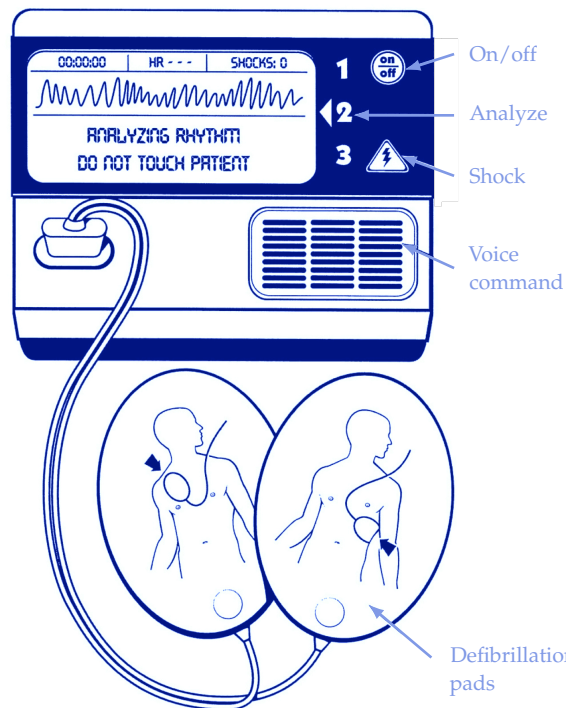


**Figure 1.5:** The automated external defibrillator and its basic operation steps. Adapted from Takata et al.<sup>131</sup>

#### 1.4.1 The shock advice algorithm

AEDs are thought to be operated by rescuers who do not need to recognize or interpret heart rhythms. For this reason, an essential component of the AED is the rhythm analysis or shock advice

algorithm. In 1997, the AHA task force on automatic external defibrillation published a scientific statement<sup>80</sup> that, among other items described how to evaluate the accuracy of the algorithms and the algorithm performance specifications.

The shock advice algorithm of an AED analyzes the ECG to determine whether or not to shock a patient; i. e., the decision of the algorithm is a binary diagnostic test. The accuracy of the algorithm is evaluated by comparing the decisions of the algorithm with the consensus diagnosis of three expert reviewers, as indicated in Table 1.2. It is then possible to calculate the proportions of correctly identified shockable (*Sensitivity*), non-shockable (*Specificity*), and total rhythms (*Accuracy*). The positive and negative predictive values — PPV and NPV — give the probability that a shock is needed when it is recommended by the AED or not needed when it is not recommended by the AED.

		Rhythm classification	
		Shockable	Non-shockable
Algorithm decision	Shock	True Positive = TP	False Positive = FP
	No Shock	False Negative = FN	True Negative = TN
Sensitivity (Se) = $100 \times \frac{TP}{TP + FN}$			
Specificity (Sp) = $100 \times \frac{TN}{TN + FP}$			
Accuracy (Acc) = $100 \times \frac{TN + TP}{TP + FN + TN + FP}$			
Positive predictive value (PPV) = $100 \times \frac{TP}{TP + FP}$			
Negative predictive value (NPV) = $100 \times \frac{TN}{TN + FN}$			

**Table 1.2:** Contingency table for an AED decision algorithm. The rhythm classification is the result of 100% agreement among three expert reviewers of OHCA rhythms.

The AHA task force divided the cardiac rhythms into three broad categories.

- *Shockable rhythms*: lethal ventricular arrhythmias that lead to death unless the patient is defibrillated. These rhythms include coarse VF (peak-to-peak amplitude  $> 200 \mu\text{V}$ <sup>50</sup>)

and rapid VT.<sup>†</sup> Shockable rhythms are associated with an unresponsive and pulseless patient in all cases of VF and in most cases of rapid VT.

- *Non-shockable rhythms*: benign (or even normal) rhythms that must not be shocked, especially in patients with a pulse, because no benefit will follow and deterioration in rhythm may result. These rhythms include: normal sinus rhythm (NSR), supraventricular tachycardia (SVT), sinus bradycardia (SB), atrial flutter or fibrillation (AF), heart blocks, idioventricular (IV) rhythms, premature ventricular contractions (PVC), and other rhythms occurring in a conscious patient with a pulse. Asystole is included in the non-shockable rhythm category. Although patients in asystole are pulseless and unresponsive, there is no evidence of benefits from defibrillating asystole.<sup>99</sup> In fact, the 2005 European resuscitation guidelines do not recommend the interruption in chest compressions to attempt shock delivery for asystole.<sup>41</sup>
- *Intermediate rhythms*: rhythms for which the benefits of defibrillation are limited or uncertain. This category includes fine VF (non-coarse) and slow VT. Fine VF precedes asystole, survival rates are low, and it is associated with a considerable delay since collapse.

The statement mentions that the ECG data used to develop and test the algorithms may be acquired from prehospital or in-hospital events and that the data used to develop the algorithm must be different from the data used to test the algorithm.

The task force also specified the minimum number of ECG samples per category needed to test the algorithm, and the values of the sensitivity and specificity for each rhythm type. These values are compiled in Table 1.3.

The IEC 60601-2-4 standard<sup>64</sup> — which specifies the requirements for the safety of cardiac defibrillators, and particularly the section<sup>‡</sup> that specifies the performance goals of AED shock advice algorithms — is currently under revision. The current draft supports keeping the VF sensitivity goal above 90% and the specificity for non-shockable rhythms above 95%.

The shock advice algorithms of commercial AEDs have been tested extensively in adults, both in vitro against libraries of

<sup>†</sup> The task force did not specify the heart rate above which VT should be shocked because tolerance to VT varies widely among patients. Each manufacturer should specify the criteria for VT used in its algorithm.

<sup>‡</sup> Section: *essential performance data of the rhythm recognition detector*, page 15 of the current standard.



Rhythms	Minimum test sample size	Performance goal	90% lower CI <sup>a</sup>
<b>Shockable</b>			
Coarse VF	200	>90% Se	87%
Rapid VT	50	>75% Se	67%
<b>Non-shockable</b>			
NSR	300	>99% Sp	97%
AF, SB, SVT, blocks, idioventricular, PVC	100	>95% Sp	88%
Asystole <sup>b</sup>	30	>95% Sp	92%
<b>Intermediate</b>			
Fine VF	25	Report only	-
Other VT	25	Report only	-

<sup>a</sup> The confidence interval (CI) is calculated for the minimum sample size and an observed performance equal to the performance goal.

<sup>b</sup> Asystole is included for safety.

**Table 1.3:** Performance goal for AED shock advice algorithms. The samples must be free of artifacts.

recorded cardiac rhythms<sup>103,34</sup> and clinically in many field trials.<sup>138,110,112</sup> These algorithms are extremely accurate in the discrimination of shockable and non-shockable rhythms in the field, with reported sensitivities of 96–100% and specificities of around 100%.

#### 1.4.2 The use of AEDs in children

Sudden death is 10 times less frequent in pediatric (under 21 years of age) patients than in adult patients, and estimates of the annual incidence range between 8.5 and 19.7 per 100 000 children,<sup>47,87,124,53</sup> depending on the inclusion criteria for age and etiology. In the US, an estimated 16 000 children die each year from SCA.<sup>124</sup> Although cardiac arrest in children constitutes less than 10% of all OHCA, the social and emotional impact is enormous because of the greater life expectancy of a child.

Cardiac arrests due to arrhythmias are less frequent in children than in adults.<sup>87,148</sup> Data on the initially recorded rhythm on pediatric SCA show that VF as the initial rhythm is less common in children than in adults and that its occurrence increases with

age. However, VF has been reported as the initial rhythm in 4% to 24% of pediatric OHCA cases.<sup>124,101,58</sup> In-hospital studies also indicate that VF is not a rare rhythm among children. A recent comprehensive study reported VF or pulseless VT as the initial rhythm in 14% of children in cardiac arrest.<sup>106</sup> More importantly, in most pediatric studies, VF is the arrhythmia associated with the highest survival rate.<sup>101,58,148</sup> For example, Mogayzel et al.<sup>101</sup> reported a 17% survival rate with good neurological outcome when VF was the initially recorded rhythm, versus only 2% for patients in asystole or pulseless electrical activity (PEA).<sup>†</sup> Young and Seidel<sup>148</sup> reported that only 5% of children in asystole survived versus a 30% survival rate for children in VF.

As late as 2000, no conclusive study on the use of AEDs in patients under 8 years of age existed. In 1998, Atkins et al.<sup>14</sup> evaluated the accuracy and efficacy of AEDs in adolescents for the first time. However, their study was not conclusive because it only included 18 patients, with a mean age of 12 years. Cecchin et al.<sup>25</sup> in 2001 and Atkinson et al.<sup>16</sup> in 2003 published two independent studies that provided the necessary scientific evidence to recommend the use of AEDs in children. Based on this evidence, in 2003, the International Liaison Committee on Resuscitation (ILCOR) made the following recommendations.<sup>120</sup>

*“Automated external defibrillators (AEDs) may be used for children 1–8 years of age who have no signs of circulation. Ideally, the device should deliver a pediatric dose. The arrhythmia detection algorithm used in the device should demonstrate high specificity for pediatric shockable rhythms, i. e. it will not recommend delivery of a shock for non-shockable rhythms (Class IIb).*

*Currently the evidence is insufficient to support a recommendation for or against the use of AEDs in children <1 year of age.”*

These recommendations were included in the 2005 European resuscitation guidelines.<sup>22</sup> These guidelines mention the most important modifications needed to adapt the AEDs designed for adult patients for pediatric use.

- *Defibrillation pads.* Defibrillation pads must be large enough to provide good contact with the chest walls; however, there should be good separation between the pads. Current guidelines recommend pad diameters of 4.5 cm for children under 10 kg and 8–12 cm diameter for children >10 kg. If the pads in the anterolateral position are too close together, the an-

<sup>†</sup> PEA is characterized by organized, wide complex electrical activity, usually at a slow rate, and absent pulses.<sup>22</sup>

teroposterior position is recommended to avoid electrical arcing (see Figure 1.6).

- *Defibrillation dose.* An AED for pediatric use should deliver a lower dose (50–75J), suitable for children aged 1–8 years. The dose can be adjusted electronically when charging or by an attenuator incorporated into the pediatric defibrillator pads.
- *AED shock advice algorithm.* The shock advice algorithm should be able to discriminate lethal ventricular arrhythmias accurately in the pediatric case and should be tested against a library of pediatric arrhythmias.

Since ILCOR recommended the use of AEDs in children, several case reports of successful pediatric defibrillation<sup>18,90</sup> have provided further evidence of the benefits of extending AED use to the pediatric population.

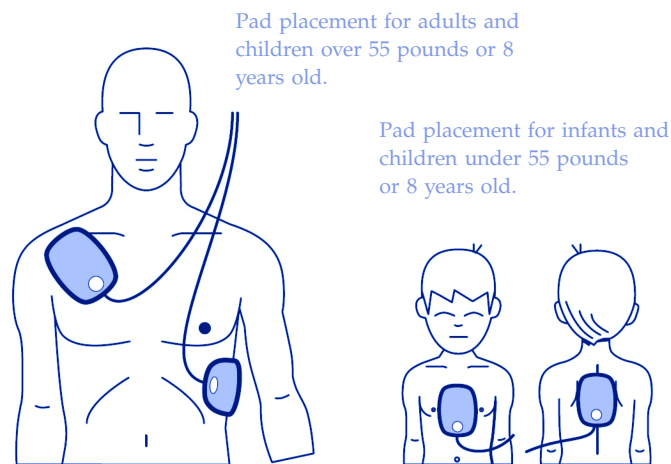


**Figure 1.6:** Defibrillation pad placement. Pads are placed in the anterolateral position in adult patients and in the anteroposterior position in pediatric patients. Adapted from Philips Medical Systems.

## 1.5 New milestones in the design of AED shock advice algorithms

Two important aspects related to the design of AED shock advice algorithms have attracted the attention of the scientific community

in the last years: the design of AED shock advice algorithms valid for adult and pediatric use, and the influence of CPR on AED shock advice algorithms.

### 1.5.1 AED shock advice algorithms for pediatric use

The current resuscitation guidelines mention that the performance of the shock advice algorithm must be tested against a database of pediatric arrhythmias before an AED can be used on children.<sup>22</sup> However, no public database of pediatric arrhythmias exists to test AED shock advice algorithms. In fact, in all published studies to date, researchers have tested the algorithms of several commercial AEDs against proprietary databases of pediatric arrhythmias.<sup>25,16,15</sup>

The compilation of a pediatric database is difficult because fatal ventricular arrhythmias are less frequent in children than in adults. In fact, none of the published studies reported a database that met the AHA specifications summarized in Table 1.3. Although the lack of shockable arrhythmias is the most important difference, there are two other relevant differences between the adult and pediatric cases. First, the heart rate is higher in the pediatric rhythms. In particular, SVT frequently exceeds the shockable rate threshold of adult VT and might be misinterpreted as shockable by adult AEDs.<sup>120,15</sup> Second, the probability of the occurrence of arrhythmias is different in children and adults; for instance, AF rarely occurs in children.<sup>43</sup> The composition of the databases of pediatric arrhythmias reflects these differences, and this may have important implications in the design of shock advice algorithms.

The initial studies on shock advice algorithms for children tried to demonstrate that existing adult algorithms accurately diagnosed pediatric arrhythmias.<sup>25,16</sup> More recently, Atkins et al.<sup>15</sup> showed that an adult algorithm fell below the AHA specification, with an 87.1% specificity on pediatric SVT and a 54.6% sensitivity on pediatric VT, and proposed the use of a pediatric algorithm.

This thesis presents a new approach — a single algorithm designed using a combination of a pediatric and an adult database — which will be suitable for pediatric and adult use.

There could be differences between the adult and pediatric cases. For instance, because a child's heart rate is higher, the threshold for shockable VT could be higher in children.<sup>16</sup> However, using a threshold adapted to each patient group can account for this difference. The appropriate threshold will be activated when the AED identifies the type of patient, which is necessary to decide the defibrillation dose. The identification normally occurs either

through a switch in the AED or because the defibrillation pads are different for adults and children.

### 1.5.2 CPR artifacts and AED shock advice algorithms

As stated in Section 1.3, the most influential factor explaining OHCA survival rates is the interaction between CPR and defibrillation. CPR must be interrupted during AED rhythm analysis because the mechanical activity from the chest compressions introduces artifacts into the ECG that make the rhythm analysis algorithms of current AEDs unreliable.<sup>92,49</sup> The time interval between the end of CPR and the delivery of the shock is known as the *hands-off* interval.

Current evidence suggests that minimizing the hands-off interval is an important determinant of survival from prolonged VF cardiac arrest. An initial study using a swine model of prolonged (7 min) VF cardiac arrest reported a decline in survival rates from 80% to 0% when the hands-off interval was increased from 10 to 20 s.<sup>149</sup> In a later swine study of prolonged (6.5 mins) VF, cardiac arrest survival degraded from 83% to 17% after the introduction of a 40 s hands-off interval.<sup>127</sup>

Eftestøl et al.<sup>45</sup> demonstrated that VF waveforms in humans deteriorated during hands-off intervals and analyzed the relationship between the duration of the hands-off interval and the probability of the restoration of spontaneous circulation (ROSC) after the shock. Shorter hands-off intervals correlated with higher probabilities of ROSC. In a more recent prospective study of human in-hospital and out-of-hospital cardiac resuscitations, shock success<sup>†</sup> declined from 94% to 38% when the hands-off interval increased from under 10 s to over 30 s.<sup>44</sup> In fact, reducing the hands-off intervals motivated a change from the three-shock protocol of the 2000 European resuscitation guidelines to a one shock protocol in the 2005 guidelines.<sup>41</sup> Currently, CPR must be resumed immediately after giving a single shock and without reassessing the rhythm or feeling for a pulse.

In 2004, a study of seven popular AEDs measured hands-off intervals in the range of 5.2 to 28.4 s.<sup>126</sup> A hands-off interval below 10 s was only achieved for one AED. In the light of the published evidence, the design of AED shock advice algorithms should minimize the hands-off interval to increase survival rates.

This thesis work explores two approaches to minimizing the hands-off interval: the design of AED algorithms that will diag-

<sup>†</sup> Defined as removal of VF for at least 5 s following defibrillation.

nose a rhythm in less than 10 s, and the suppression of the CPR artifact from the ECG to allow a reliable diagnosis during CPR.

## 1.6 Objectives of the thesis

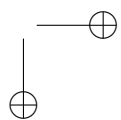
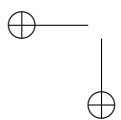
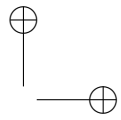
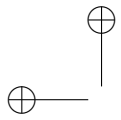
The main objective of this thesis work is to *design an AED shock advice algorithm valid for adult and pediatric patients, and to test its performance on a real resuscitation scenario*. In order to accomplish this objective, a set of intermediate goals have been defined.

- *The compilation of the experimental data.* The AED shock advice algorithm will be developed simultaneously for adult and pediatric patients. The experimental data must contain a representative set of pediatric and adult arrhythmias. The adult database should comply with the AHA statement,<sup>80</sup> while the pediatric data will have fewer shockable samples.<sup>25,16</sup> A database of OHCA episodes composed of time intervals with and without CPR artifacts is necessary to test the algorithm in a real resuscitation scenario.
- *Parametrization of the ECG.* Although commercial AED algorithms are not published in the scientific literature, it is well known that they analyze ECG features derived from several signal domains (time, frequency, and slope).<sup>25,16</sup> The first step in the design of the algorithm is to define a set of discrimination parameters applicable to adult and pediatric patients from several signal domains.
- *Design of the AED shock advice algorithm.* The shock advice algorithm is the result of optimally combining the discrimination parameters to produce an accurate shock/noshock decision. An algorithm designed for universal use will be developed and tested using a representative set of pediatric and adult arrhythmias, and its accuracy will be validated in terms of sensitivity and specificity. In an effort to reduce the hands-off interval, the algorithm should diagnose arrhythmias in less than 10 s.
- *Testing the algorithm in a resuscitation scenario.* AED algorithms are designed to meet AHA performance goals. In an OHCA scenario the rhythms analyzed by the AED might be of different nature; furthermore, they often appear corrupted by a CPR artifact. The performance of the algorithm will therefore be tested for OHCA rhythms both with and without CPR artifacts. During CPR, the AED algorithm will

be tested in combination with a CPR artifact suppression method.

The accomplishment of the objectives of this thesis work will contribute to the advancement of AED algorithms in the following ways.

- An AED shock advice algorithm designed using a combination of adult and pediatric arrhythmias is more reliable than adult algorithms tested on pediatric databases<sup>25,16</sup> and is less complex than using a pediatric and an adult algorithm.<sup>15</sup>
- The assessment of the influence of the CPR artifact on the AED shock advice algorithm will contribute to a better understanding of the limitations of rhythm analysis during CPR.





## 2 | BACKGROUND

This chapter provides the background necessary to put the most important contributions of this thesis work in context. Section 2.1 presents the general structure of AED shock advice algorithms, and then it describes the main methods used to derive the features that serve in the discrimination of shockable rhythms. Emphasis is on the methods for the detection of VF, which have attracted the attention of the scientific community. In 2003, ILCOR approved the use of AEDs in children, and since then, AED shock advice algorithms adapted for pediatric use have gained relevance, as discussed in Section 2.3. The interaction between CPR and the AED shock advice algorithm, and in particular the problems associated with the suppression of the CPR artifact, are covered in Section 2.4. The chapter concludes with a brief description of the main contributions of this thesis work.

### 2.1 AED shock advice algorithms

AED shock advice algorithms analyze a single lead surface ECG<sup>†</sup> to detect fatal ventricular arrhythmias, i. e., VF and fast VT, accurately and reliably. An arrhythmia detection system consists basically of the three blocks shown in Figure 2.1.

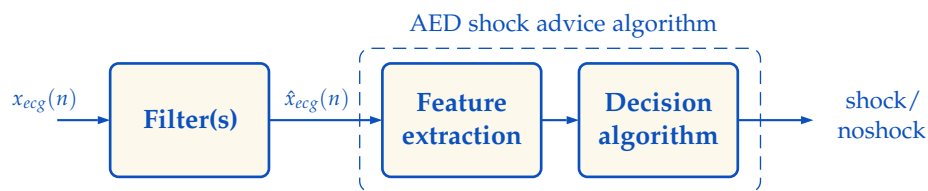


**Figure 2.1:** Building blocks of an AED shock advice algorithm. Filters preprocess the raw ECG signal,  $x_{ecg}(n)$ , to obtain an ECG free of artifacts,  $\hat{x}_{ecg}(n)$ . The shock advice algorithm analyzes  $\hat{x}_{ecg}(n)$  to obtain a shock/noshock diagnosis.

<sup>†</sup> Implantable Cardioverter-Defibrillator algorithms based on intracardiac leads are excluded from this section. For a comprehensive review see Jenkins and Caswell<sup>75</sup> or Aliot et al.<sup>8</sup>

First, the ECG is filtered to eliminate noise, such as baseline wander or muscle noise. AEDs may also have a filter to suppress the CPR artifact, as discussed in Section 2.4. The shock advice algorithm then analyzes the filtered ECG, where a shock/noshock decision is made based on the values of a set of features. These features are designed to quantify the distinctive characteristics of ventricular arrhythmias.

The following subsections review the main features and decision algorithms found in the literature. Then, five algorithms are discussed in detail. These algorithms were chosen for two reasons: they illustrate the most widely accepted approaches to feature extraction in a simple way, and they have been extensively reviewed and tested in the literature.

### 2.1.1 Feature extraction

The first stage in a shock advice algorithm is the computation of a set of features that will serve to discriminate fatal ventricular arrhythmias. These features quantify distinctive characteristics of the arrhythmias, which are generally better observed by transforming the ECG into a new domain. For example, Figure 2.2 shows the time and frequency domain representation of two shockable — VF and VT — and two non-shockable — NSR and SVT — rhythms. Non-shockable rhythms have larger bandwidths and more harmonic content because of the fast-changing QRS complexes. Other characteristics are better observed in the time domain; for instance, the waveform irregularity of VF or the lower content around the isoelectric line of VT.

Four domains have been extensively used to extract features: the time domain, the frequency domain, the time–frequency domain, and the complexity domain.

1. *Time domain features.* The time domain has been used to quantify many different characteristics of ventricular arrhythmias. In 1978, Kuo and Dillman<sup>88</sup> proposed the VF filter leakage, a measure of the similarity of ventricular arrhythmias to a sinusoidal waveform. The autocorrelation function (ACF) was introduced to stress the periodic nature of VT and pulsed rhythms, as opposed to the more irregular VF.<sup>57,17,27</sup> Other authors identified fast ventricular arrhythmias based on heart rate calculations. For instance, Thakor et al.<sup>132</sup> developed the Threshold Crossing Interval (TCI) feature to estimate the inverse of the heart rate; i. e., the mean interval between beats. Later, Chen et al.<sup>29</sup> refined the algorithm by considering the refractory period of the ventricles, and

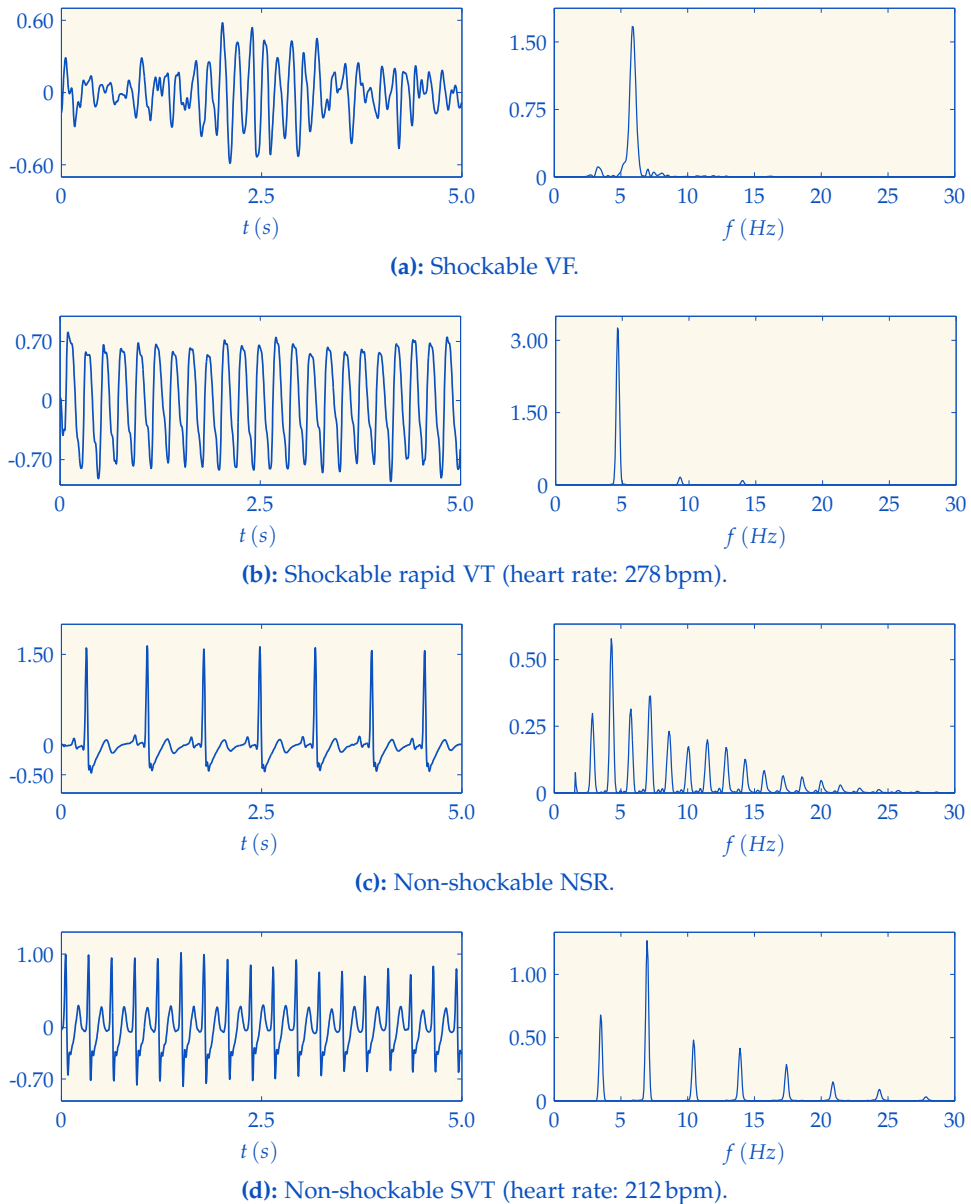


**Figure 2.2:** Time domain (left panel) and frequency domain (right panel) representation of shockable (a–b) and non-shockable (c–d) rhythms. The  $y$  axis is the amplitude of the ECG in mV for the time domain representation, and the normalized power spectral density for the frequency domain representation.

Amann et al.<sup>10</sup> introduced two methods to estimate the heart rate based on exponentially decaying functions. The probability density function (PDF) is an adequate tool to calculate the isoelectric content,<sup>91,113</sup> which is low in ventricular rhythms. Time domain modeling of the ECG based on Prony<sup>28</sup> and autoregressive models<sup>52</sup> has been recently proposed, as well as features derived from the comparison of the ECG with a set of predefined reference signals.<sup>10</sup>

2. *Frequency domain features.* Pulsed rhythms have quasi-periodic and fast-changing QRS complexes, and concentrate their frequency components around the harmonics of the cardiac frequency, with major components up to 25 Hz.<sup>32</sup> The more sinus-like ventricular arrhythmias are narrow-band signals concentrated around the fundamental frequency, with most of their components under 10 Hz.<sup>128</sup> The early researchers on VF detection observed these differences using the Fast Fourier Transform (FFT).<sup>109,108</sup> In 1989, Barro et al.<sup>19</sup> made a more systematic approach and developed a set of four features measuring the concentration of the amplitude spectrum around the fundamental frequency and the relative contributions of the different frequency bands. Clayton et al.<sup>33</sup> analyzed 31 spectral amplitudes separated by 0.5 Hz in the 2–16.6 Hz frequency range and concluded that a combination of the parameters proposed by Barro et al. and the TCI feature provided better results than a brute force approach. Minami et al.<sup>100</sup> successfully detected ventricular arrhythmias by analyzing the frequency content of the QRS complex in five predefined frequency bands. More recently, bispectral analysis<sup>82</sup> has been explored as a tool to identify ventricular arrhythmias.
3. *Time–frequency domain features.* In 1995, Afonso and Tompkins<sup>5</sup> introduced time–frequency distributions in an attempt to track the spectral characteristics of VF over time better. They showed the superiority of the smoothed Wigner–Ville and the cone-shaped kernel distributions over the short-time Fourier transform. Clayton and Murray<sup>31</sup> further explored the smoothed Wigner–Ville distribution. Khadra et al.<sup>81</sup> introduced features based on the continuous wavelet transform (WT), and later al Fahoum and Howitt<sup>7</sup> extended the analysis by including the continuous and discrete WT and various mother functions. The discrete WT has been used to characterize the complexity of VF across different scales.<sup>62,130</sup> Time–frequency distributions provide a powerful framework for arrhythmia discrimination; however,

they demand a high computational cost<sup>†</sup> that limits their applicability in current AED technology.

4. *Complexity domain features.* Ventricular arrhythmias are considered nonlinear physiological processes of varying complexity.<sup>115</sup> Although complexity is not a domain per se, this point summarizes the contributions aimed at quantifying the nonlinear character of those physiological processes. These techniques include methods derived from nonlinear dynamics and chaos theory, such as correlation dimension,<sup>31,125,111</sup> Lyapunov exponents,<sup>111</sup> and phase space plots.<sup>11</sup> Other authors proposed the use of qualitative chaos based on symbolic complexity,<sup>61</sup> multifractality,<sup>137</sup> Hurst indices,<sup>130</sup> and methods based on different types of entropy<sup>121,122,62</sup> to quantify the complexity of VF. Perhaps the best-known contribution is the 1999 paper by Zhang et al.<sup>150</sup> based on the Lemp–Ziv complexity, which is one of the few computationally reasonable methods to estimate the complexity of ventricular arrhythmias.

### 2.1.2 Decision algorithms

In an AED, the values obtained for the features are fed to a decision algorithm that diagnoses the rhythm as shockable or non-shockable. Decision algorithms based on one feature range from single-thresholding<sup>150,10,11</sup> to more elaborate sequential hypothesis testing on consecutive values on the feature.<sup>132,29,26</sup> However, real AED algorithms are based on multiple features because no single feature captures all the variability of ventricular arrhythmias. Many multiple feature classification algorithms have been used, including heuristic decision trees,<sup>19,73,85</sup> multistage thresholding,<sup>28‡</sup> k Nearest Neighbors (kNN),<sup>24,72,74</sup> linear discriminant analysis,<sup>71</sup> and generalized linear models.<sup>52</sup> Clayton et al.<sup>33</sup> introduced an algorithm based on neural networks, which have been frequently used for the detection of ventricular arrhythmias.<sup>7,137</sup>

## 2.2 Review of five VF detection algorithms

This section describes five of the most thoroughly reviewed<sup>32,70,10</sup> and best-known VF detection algorithms. Three are based on

<sup>†</sup> The computational cost is considerably lower in the case of the discrete WT.<sup>62</sup>

<sup>‡</sup> This is actually another form of decision tree: a multiple stage, single-thresholding technique.

the time domain: the VF filter, the algorithm based on the ACF and the TCI method. One is based in the frequency domain, the spectral algorithm. The last one is the method proposed by Zhang et al. to quantify the complexity of VF.

#### *VF filter*

In 1978, Kuo and Dillman introduced a novel time domain feature to identify VF,<sup>88</sup> which various other authors have used since as a benchmark to compare their results.<sup>150,137</sup> The basic idea is that the VF waveform is approximately sinusoidal and can be canceled by applying a narrow-band filter around the fundamental frequency of the waveform. A feature called leakage quantifies the residue after filtering.

For an ECG data segment of  $m$  samples,  $V_i$ , the leakage,  $l$ , is defined as:

$$l = \frac{\sum_{i=1}^m |V_i + V_{i-T/2}|}{\sum_{i=1}^m (|V_i| + |V_{i-T/2}|)}, \quad (2.1)$$

where  $T$ , the number of samples in a mean period, is estimated assuming a sinusoidal waveform:

$$T = 2\pi \frac{\sum_{i=1}^m |V_i|}{\sum_{i=1}^m |V_i - V_{i-1}|}. \quad (2.2)$$

Sinusoidal waveforms yield low values of  $l$  because samples separated by a half period cancel each other. In the original contribution, the leakage was calculated if no QRS complexes or paced beats were detected. However, later implementations have not considered a QRS detection stage and have identified VF for  $l < 0.625$ .<sup>32,70,10</sup>

#### *Algorithm based on the autocorrelation*

The ACF of a periodic signal has peaks of decreasing amplitude separated by multiples of the period. Therefore, the ACF is a proper tool to discriminate periodic ECGs from the more irregular VF.

Chen et al.<sup>27</sup> ordered the ACF peaks by their amplitude. Then, they fitted a linear regression equation to the integer order,  $x_i$ , and the corresponding lag,  $y_i$ , of the first  $m$  peaks of the ACF:

$$y_i = a + bx_i, \quad (2.3)$$

with

$$a = \bar{y} - b\bar{x} \quad \text{and} \quad b = \frac{\sum_{i=1}^m (x_i - \bar{x})y_i}{\sum_{i=1}^m (x_i - \bar{x})^2}, \quad (2.4)$$

where  $\bar{x}$  and  $\bar{y}$  are the mean values of  $x_i$  and  $y_i$ .

The goodness of the linear regression fit is measured by computing the variance ratio,  $VR$ :

$$VR = \frac{b}{[R/(m-2)]}, \quad \text{with} \quad (2.5)$$

$$R = \sum_{i=1}^m (y_i - \bar{y} - b(x_i - \bar{x}))^2. \quad (2.6)$$

When  $VR > F_{1,m-2;0.05}$  (the F-test at level 0.05),<sup>†</sup> a linear relationship exists between  $y_i$  and  $x_i$ , the peaks are well ordered and the rhythm is not VF.

#### Spectral algorithm

In 1989, Barro et al.<sup>19</sup> introduced a set of four spectral features based on the amplitude<sup>‡</sup> of the FFT of the Hamming windowed ECG.

First, the reference frequency ( $F$ ) is identified as the frequency where the amplitude of the FFT is maximum in the 0.5–9 Hz range and all the components below 5% of the peak amplitude are made zero. Then, four features,  $FSMN$ ,  $A_1$ ,  $A_2$ , and  $A_3$ , are calculated in the 0.5–min(100 Hz, 20F) frequency range.  $FSMN$  is the center of mass of the amplitude spectrum and measures its concentration around  $F$ :

$$FSMN = \frac{1}{F} \frac{\sum a_i f_i}{\sum f_i}, \quad (2.7)$$

where  $a_i$  is the amplitude at frequency,  $f_i$ .  $A_1$  is the ratio of the area in the 0.5–0.5F range to the total area;  $A_2$  is the ratio of the area in the 0.7F–1.4F range to the total area; and  $A_3$  is the ratio of the sum of the areas of the 2<sup>nd</sup> to 8<sup>th</sup> harmonics in bands of 0.6F to the total area.

The algorithm detects VF using a heuristic decision tree when all of the following conditions hold:  $A_1 > 0.19$ ,  $FSMN \leq 1.55$ ,  $A_2 \geq 0.45$  and  $A_3 < 0.09$ .

<sup>†</sup> Although Chen et al.<sup>27</sup> were more restrictive, later authors have used a 0.05 or 95% probability level.<sup>32,70,10</sup>

<sup>‡</sup> Because of computational constraints, Barro et al.<sup>19</sup> calculated the amplitude spectrum as the sum of the absolute values of the real and imaginary parts of the FFT.

### Threshold crossing intervals

The TCI feature, introduced by Thakor et al.,<sup>132</sup> measures the mean interval between consecutive beats of the ECG waveform. First, the ECG is converted to a binary signal by comparing it with a threshold. A heart beat is detected every time the ECG crosses the detection threshold, which adjusts dynamically every second to 20% of the peak value of the signal during that second. The TCI is calculated for every 1 s interval as follows:

$$\text{TCI} = \frac{1000}{(N - 1) + \frac{t_2}{t_1 + t_2} + \frac{t_3}{t_3 + t_4}} \text{ (ms)}, \quad (2.8)$$

where  $N$  is the number of pulses in the 1 s interval, and the  $t_i$  intervals are defined in Figure 2.3.

Fast ventricular arrhythmias present lower interbeat intervals, i. e., TCI values, than pulsed rhythms. NSR is detected when  $\text{TCI} \geq 400 \text{ ms}$ . Although VF and fast VT have low values of TCI, Thakor et al.<sup>132</sup> discriminated VT from VF using a sequential hypothesis testing procedure.

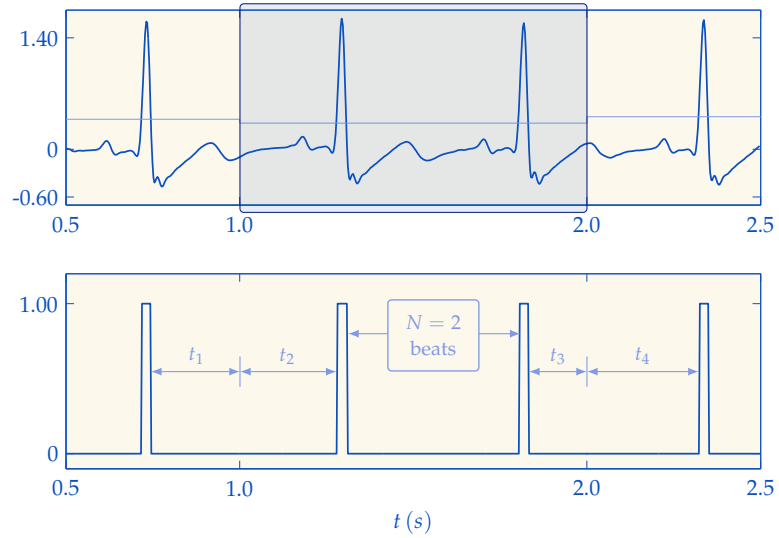


**Figure 2.3:** Basic parameters in the calculation of the TCI for an NSR. The top panel shows the ECG in mV of the NSR, and the bottom panel shows its corresponding binary signal.



### Complexity measure

In 1999, Zhang et al.<sup>150</sup> introduced a new method to quantify the complexity of ventricular arrhythmias based on the Lempel–Ziv Complexity Measure.<sup>94</sup>

First, the  $n$  sample ECG data segment,  $\{x_i\}_{i=1}^n$ , is normalized by subtracting  $x_m$ , the mean value of the samples. The normalized sequence,  $\{\hat{x}_i\}_{i=1}^n$ , is converted to a sequence of 0–1 symbols,  $\{s_i\}_{i=1}^n$ , by comparing it with a threshold,  $T_d$ . The threshold calculation is based on  $P_c$ , the number of datapoints in  $0 < \hat{x}_i < 0.1V_p$ , and  $N_c$ , the number of datapoints in  $0.1V_n < \hat{x}_i < 0$ .  $V_p$  and  $V_n$  are the positive and negative peak values of the normalized data segment. If  $(P_c + N_c) < 0.4n$ , the threshold is set to  $T_d = 0$ . Else if  $P_c < N_c$  then  $T_d = 0.2V_p$ , otherwise  $T_d = 0.2V_n$ .

The Lempel–Ziv complexity is computed by scanning  $\{s_i\}_{i=1}^n$  from left to right and increasing the complexity counter,  $c(n)$ , by one unit every time a new subsequence of consecutive characters is found. Kaspar and Schuster<sup>77</sup> give a detailed description of the computation of  $c(n)$ , including a flow chart description of the algorithm. The upper bound of  $c(n)$  is  $b(n) = n / \log_2 n$ , which is the asymptotic behavior of  $c(n)$  for a random string. The normalized complexity measure is then defined as:

$$C(n) = \frac{c(n)}{b(n)} \quad 0 \leq C(n) \leq 1, \quad (2.9)$$

and it measures the rate of occurrence of new patterns within the sequence  $\{s_i\}_{i=1}^n$ .

Ventricular arrhythmias are inherently more complex than NSR and have higher  $C(n)$  values. Zhang et al.<sup>150</sup> detected NSR when  $C(n) < 0.150$  and separated VT from the more complex VF when  $C(n) < 0.486$ . Some authors<sup>70,10</sup> who reviewed the VF detection method later modified the NSR detection threshold to  $C(n) < 0.173$ .

#### 2.2.1 Comparison of five VF detection algorithms

The methods for the detection of ventricular arrhythmias described in the literature report excellent sensitivity and specificity; for instance, Zhang et al.<sup>150</sup> mention a 100% sensitivity and specificity when the complexity measure is computed on ECG segments longer than 6 s. Most of these results, however, are biased by the data used in the studies; i. e., these methods were developed and tested on proprietary databases that do not meet the AHA criteria described in Section 1.4.1. Furthermore, in many cases, the methods are developed and tested on the same data.<sup>132,150</sup>

Three important review articles that compared the five VF detection algorithms described in the previous section underlined these sources of bias. In 1993, Clayton et al.<sup>32</sup> compared the first four algorithms using a proprietary database of 150 VF segments and 100 VF-like segments, which included recordings of muscle artifacts and atrial flutter. By 2000, Jekova,<sup>70</sup> in a comparative study, had added the method proposed by Zhang et al.<sup>150</sup> in 1999. She used a dataset composed of 71 NSR and 90 VF segments extracted from three standard databases for arrhythmia detection: the AHA database, the CU ventricular tachyarrhythmia database, and the MIT-BIH malignant ventricular arrhythmia database.<sup>†</sup> In their 2005 comparative analysis, Amann et al.<sup>10</sup> used a more comprehensive dataset composed of the complete MIT-BIH arrhythmia database, the complete CU ventricular tachyarrhythmia database, and the subset of ventricular arrhythmias from the AHA database, totaling 333 583 segments of 8 s.

The review articles quite accurately reproduced the original methods, although some differences exist. For example, Jekova and Amann et al. do not use the sequential hypothesis test on the TCI values proposed by Thakor et al. but rather a decision algorithm based on a majority criterion. The authors of the review articles use lower probability levels than the original authors for the F-test in the ACF method; they do not use a QRS detection stage in the VF filter method or they use slightly higher thresholds on the  $C(n)$  value to discriminate NSR. The most important difference between the original contributions and the review articles is the length of the data segments used to compute the discrimination features. The original VF detection methods were not developed using a standard length of the data segment. For instance, Kuo and Dillman computed the VF leakage using 2 s segments, while Zhang et al. obtained the best discrimination results for data segments longer than 6 s. In the review articles, the authors compared the performance of the algorithms using the same length of the data segment for all the methods, 4 s in Clayton et al. and 8 s in Jekova and Amann et al.

Despite these differences, the three review articles illustrate that when the methods are evaluated on datasets other than those used by the original authors, the results degrade substantially. Table 2.1, a summary of the results presented in the review articles, best shows how testing a method on different databases produces large differences in the results. Two important conclusions are derived from the results compiled in Table 2.1.

<sup>†</sup> These databases are described in more detail in section Section 3.1.

- The results presented in the original contributions are biased by the data used in the studies, as confirmed by the large differences in the results reported by the original authors and the review articles. Among the review articles, Jekova reports better sensitivities and specificities because she used a very restrictive database, which only included VF and NSR. When other arrhythmias, or a larger class of VF, are included, the results deteriorate, as shown in Amann et al. Furthermore, the data used in the original studies also biased the detection thresholds. For example, the much higher specificity than sensitivity obtained by all the reviewers of the spectral algorithm showed that the detection thresholds obtained by Barro et al. are biased toward the detection of non-shockable rhythms. The adequate framework to avoid such biases is the AHA statement describing the methodology to test AED shock advice algorithms,<sup>80</sup> which includes a thorough description of the databases and a clear indication to separate test from development (see Section 1.4.1).
- No single feature captures all the morphological variability of ventricular arrhythmias. The methods reviewed are representative of the different techniques and signal analysis domains. The results showed that a single feature or a single domain approach is not sufficient. A robust AED shock advice algorithm must rely on features from several domains to represent such morphological variability better.

	Clayton et al. <sup>32</sup>		Jekova <sup>70</sup>		Amann et al. <sup>10</sup>	
	Se(%)	Sp(%)	Se(%)	Sp(%)	Se(%)	Sp(%)
VF filter	77	55	94	91	19	100
ACF	67	38	78	32	50	49
Spectral	46	72	79	93	29	100
TCI	53	93	98	75	75	84
CM	-	-	66	75	59	92

**Table 2.1:** Sensitivity and specificity reported in the comparative analysis of five VF detection methods.

### 2.3 Pediatric shock advice algorithms

The literature on ventricular arrhythmia detection methods reviewed in the preceding sections is ample, and the methods are well documented. The conclusions and methods presented in those studies, however, are applicable only to the adult case. The use of AEDs in pediatric patients has only recently received attention.

In 1998, Atkins et al.<sup>14</sup> published the first data on AED use in children and adolescents. They analyzed 18 cases, including 9 VF, of patients with a mean age of 12.1 years, and they concluded that AEDs accurately recognize the cardiac rhythms observed in pediatric cardiac arrest. These conclusions, however, were sustained by an insufficient number of rhythms from patients with a high mean age. In 2001, Cecchin et al.<sup>25</sup> published the first comprehensive study. They compiled 696 rhythms, including 73 VF and 58 VT, from 191 pediatric patients, and the segments had a duration of 5 s. The median age of the patients was 3.0 years. Furthermore, the methodology for the classification and compilation of the arrhythmias followed the guidelines indicated by the AHA.<sup>80</sup> A second important contribution came in 2003, when Atkinson et al.<sup>16</sup> published a second study where 1561 pediatric rhythms, 73 VF and 3 VT, from 201 patients with a median age of 11 months were analyzed. The ECG samples had a duration of 15 s.

The contributions by Cecchin et al. and Atkinson et al. demonstrated that two adult algorithms from commercial AEDs accurately identified pediatric non-shockable rhythms and pediatric VF. In both studies, the specificity was above 99% and the VF sensitivity above 95%. They both concluded that the analyzed adult AED algorithms could be used in children and constituted the bulk of evidence needed by ILCOR to recommend AED use on pediatric patients.<sup>120</sup> However, both studies failed to meet AHA criteria on fast VT; Cecchin et al. reported a 71% VT sensitivity, and the results from Atkinson et al. were not significant because their database only contained three instances of shockable VT.

The differences between pediatric and adult arrhythmias might explain the poor VT sensitivity results; in particular, the higher rates of pediatric SVT. A related problem is that, as indicated in the ILCOR statement,<sup>120</sup> heart-rate-oriented AED shock advice algorithms designed for adult patients might identify high-rate pediatric SVT as shockable. Atkins et al.<sup>15</sup> addressed this difficulty when they recently showed how an AED algorithm designed for adult patients failed to identify non-shockable pediatric suprav-

tricular arrhythmias accurately. Using an adult algorithm, Atkins et al. obtained a specificity of 87% for pediatric supraventricular rhythms, well below the 95% AHA specification. They defined a new set of detection criteria adapted to pediatric rhythms to correct those deficiencies and obtained a 99.6% specificity for the pediatric supraventricular rhythms. Unlike the two previous studies, Atkins et al. supported the use of two algorithms: one adult and one pediatric. The pediatric algorithm was automatically used when the pediatric defibrillation pads were attached. Their study was based on 749 strips from 198 children under 8 years of age, and the strips had a duration of 9 s. The database included 42 VF, 78 VT and 348 supraventricular rhythms.

Finally, Aramendi et al.<sup>12</sup> recently assessed the performance of four of the five classical methods for the detection of VF for pediatric and adult rhythms. They showed that features related to the spectral distribution of the ECG power, such as the leakage,  $l$ , or the spectral parameter,  $A_2$ , are less affected by the inclusion of pediatric arrhythmias than are heart-rate-dependent features, such as TCI or  $C(n)$ .<sup>†</sup> The study used a subset of the complete pediatric and adult databases described in Section 3.1, and it is the first study to evaluate such parameters using databases compliant with the AHA statement.

Although there is not a vast literature on pediatric AED algorithms, some important conclusions can be drawn from the published studies described in the preceding paragraphs.

- There is no public database of pediatric arrhythmias to test AED algorithms. To date, the most laborious task of all the studies in this field has been the experimental phase, which comprises the gathering and classification of pediatric rhythms. Table 2.2 displays a summary of the rhythms collected by the three studies described above. Furthermore, none of the databases meets the AHA requirements for the numbers of ventricular arrhythmias, underlining the well-known fact that ventricular arrhythmias in children are not as frequent as in adults. As addressed by Atkins et al., a comprehensive database must include a large number of SVTs in the non-shockable category to test the robustness of the algorithm in the presence of very-high-rate pediatric SVT.
- The values of the discrimination features used in the shock advice algorithms are different in adult and pediatric pa-

<sup>†</sup>  $C(n)$  is aimed at quantifying the complexity of the ECG; however, it depends strongly on the heart rate as a consequence of the signal binarization process that precedes the calculation of the Lempel–Ziv complexity.

tients. The differences between pediatric and adult rhythms — for instance, the higher rate of pediatric rhythms — are reflected in the values of the features used to discriminate ventricular arrhythmias. In their groundbreaking contribution, Cecchin et al. compared the features used in their AED algorithm and reported higher rates for the pediatric database and higher conduction scores for pediatric ventricular arrhythmias; surprisingly, these differences do not alter the performance of the adult algorithm on pediatric rhythms. On the contrary, Atkins et al. had to adapt the detection criteria of the adult algorithm to identify pediatric SVT accurately. Aramendi et al. analyzed the differences for four classical VF detection methods.

- The algorithms are not public. The literature on pediatric AED algorithms has focused on the validation or adaptation of current adult AEDs for pediatric use. Patents protect the algorithms; therefore, they are not published in the scientific literature. The only well-known VF detection methods are those described in the preceding sections for adult patients.

Rhythms	Cecchin et al. <sup>25</sup>	Atkinson et al. <sup>16</sup>	Atkins et al. <sup>15</sup>
<b>Shockable</b>			
VF	73	73	42
VT	58	3	78
<b>Non-shockable</b>			
NSR	173	798	208
SVT	116	378	161
Other	135	217	187
Asystole	39	79	29
<b>Intermediate</b>			
Fine VF	102 <sup>a</sup>	0	0
Slow VT		3	44

<sup>a</sup> The authors do not specify how intermediate rhythms are distributed between fine VF and slow VT.

**Table 2.2:** Number of pediatric rhythms per category reported in the studies that tested AED algorithms in children.

## 2.4 Shock advice during CPR

During CPR, the mechanical activity from the chest compressions introduces artifacts in the ECG. For example, Figure 2.4 shows four OHCA episodes where a CPR artifact corrupts the ECG. These artifacts make the rhythm analysis algorithms of current AEDs unreliable. Therefore, CPR must be discontinued for a reliable diagnosis by the AED.<sup>126</sup> These hands-off intervals adversely affect the probability of ROSC after the delivery of the shock;<sup>45,149,44</sup> furthermore, pauses in chest compressions compromise circulation.<sup>20</sup> The shortening of those intervals, particularly the suppression of the CPR artifact to allow a reliable AED diagnosis during CPR, has been an active field of research during the last 15 years.

The first studies on the suppression of the CPR artifact, described in Section 2.4.1, were conducted on animal models. A multidisciplinary group of Norwegian researchers<sup>†</sup> has led the investigations on CPR artifact removal from the human ECG, treated in Section 2.4.2 and Section 2.4.3. They conducted the first experiments on the suppression of the CPR artifact from human VF and most importantly, the first clinical studies based on a database of OHCA episodes. Their filtering methods use several additional reference channels (multi-channel) besides the surface ECG. Since then, most efforts have focused on the simplification of the filtering methods, either by filtering the artifact using only the surface ECG or by using only one additional reference channel (dual-channel methods). These two approaches are reviewed in Section 2.4.4. A novel alternative to the suppression of the CPR artifact is the direct analysis of the corrupted ECG, an approach also discussed in Section 2.4.4.

### 2.4.1 First animal models

Research on CPR artifact removal was initiated using porcine models. Strohmenger et al.<sup>129</sup> induced VF on pigs using an AC current and after 4 minutes of cardiac arrest administered CPR by means of a mechanically driven piston at a constant chest compression rate of 80 cpm. They computed a set of spectral features correlated with myocardial blood flow and the probability of ROSC and observed a clear spectral separation between the CPR artifact in the lower frequencies and VF in the higher frequencies. The dominant frequency (DF) of VF in pigs falls around 9 Hz,

<sup>†</sup> The group is composed of medical staff from the Ullevål University Hospital, engineers from the University of Stavanger, and researchers from an AED manufacturer, Laerdal Medical AS.



**Figure 2.4:** Examples of CPR artifact in OHCA episodes. During the initial 5 s, the CPR artifact corrupts the ECG. During the following 5 s, CPR is stopped, and the recorded signal shows the underlying heart rhythm. The shock/noshock decisions with and without CPR artifact show how a direct analysis of the corrupted ECG is not reliable (the real analysis interval is longer than 5 s). The y axis shows the ECG in mV.

while CPR administered at 80 cpm has a fundamental frequency of 1.33 Hz. Strohmenger et al. concluded that the CPR artifact could be efficiently suppressed using a constant-coefficient high-pass digital filter with a 4.3 Hz cutoff frequency. Following a similar experimental procedure, several studies have successfully suppressed the CPR artifact from pigs with cutoff frequencies around 4 Hz.<sup>107,114</sup> Unfortunately, the dominant frequencies of human VF are much lower than in pigs; they fall between 3 and 5 Hz.<sup>128</sup> Consequently, there is an important spectral overlap between human VF and the CPR artifacts that makes a simple



constant-coefficient filter inadequate for the suppression of the CPR artifact in humans.<sup>128</sup>

#### 2.4.2 First experiments on human VF: the additive noise model

Research on the suppression of the CPR artifact from the human ECG started with two important papers by Aase et al.<sup>3</sup> and Langhelle et al.<sup>92</sup> Langhelle et al. conjectured that the CPR artifact is an additive noise and identified four possible sources for the artifact: the mechanical stimulation of the heart, the mechanical stimulation of the thoracic muscles, electrode tapping or dragging, and static electricity. The influence of these sources can be measured by recording additional reference channels that can be incorporated into more elaborate adaptive filters. Furthermore, if the noise model is additive, the filtering methods can be tested using independently recorded human VF and CPR artifacts, added at different signal-to-noise ratios (SNRs), to conform the corrupted ECG. Figure 2.5 shows an example of how a human VF and a CPR artifact are combined when the additive noise model is used. The CPR suppression filter estimates the underlying ECG, and the efficiency of the filter is quantified by comparing the estimated ECG with the original ECG; i. e., the SNR at the output of the filter. Langhelle et al. first described this methodology,<sup>†</sup> and Aase et al. later systematized it to test their adaptive filters based on additional reference channels.

Langhelle et al. combined 25 samples of human VF with a CPR artifact recorded from a pig in asystole. CPR was administered with a mechanical chest compression device at a constant rate of 90 cpm (1.5 Hz), and additional reference signals were recorded to model the four sources of the artifact. Two filtering methods were compared: a high-pass constant-coefficient filter with a cutoff frequency of 4.9 Hz that suppressed the first three harmonics of the artifact, and an adaptive filter based on a single reference signal. Although several reference signals were recorded, their conjugate gradient adaptive finite impulse response filter could only accommodate one. Langhelle et al. studied different configurations for the reference signal and concluded that the best results were obtained when two reference signals were mixed together: the thoracic impedance and the compression depth. Adaptive methods were proved superior to constant-coefficient filters which

<sup>†</sup> Although Aase et al. published their results earlier they acknowledged the precedence of Langhelle et al.

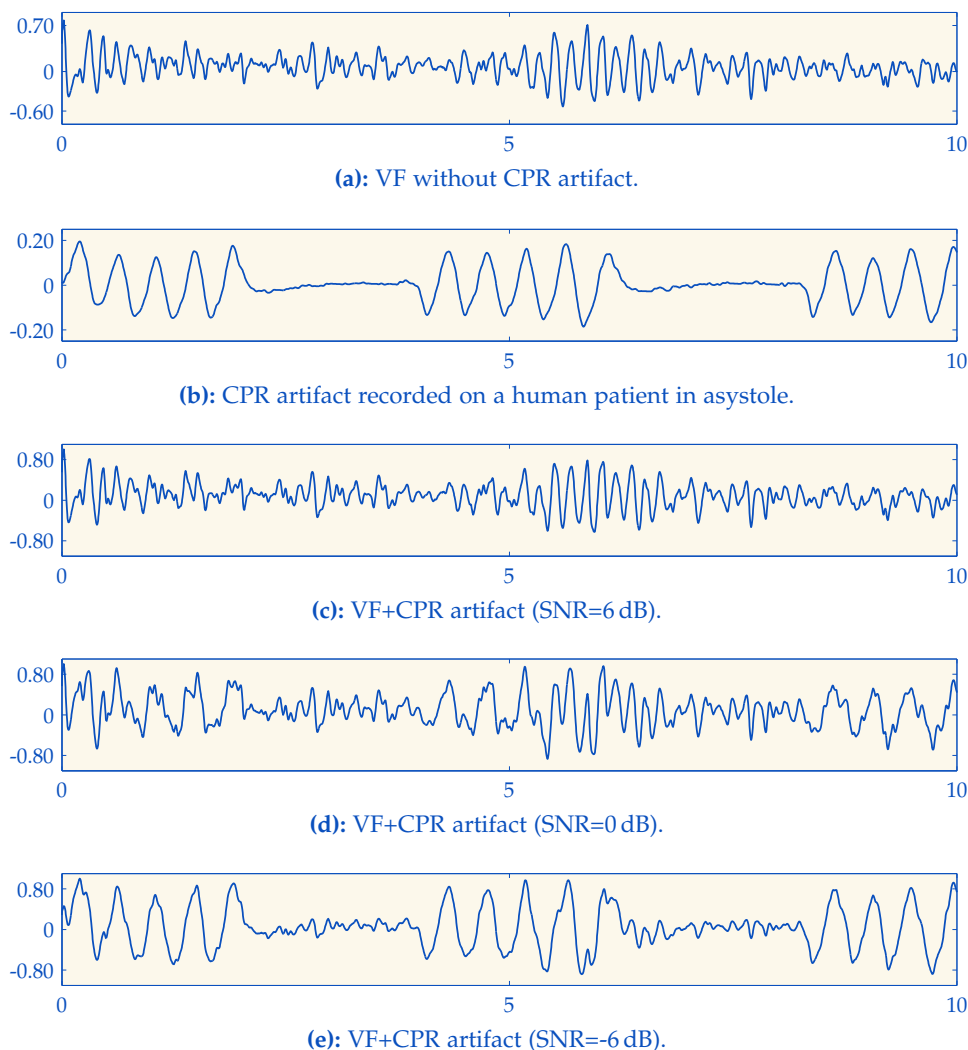


**Figure 2.5:** Additive noise model: combination of a human VF and a human CPR artifact recorded from a patient in asystole at different SNR. The VF+CPR artifact combinations are normalized so that the maximum amplitude is 1 mV.

were discarded thereafter as a CPR artifact suppression method in humans.

The contribution by Aase et al. completed the preliminary adaptive filter presented by Langhelle et al. Aase et al. used a larger database of shockable human rhythms, 200 VF and 75 VT samples, combined with CPR artifacts obtained from two pigs in asystole. CPR was administered by a mechanical chest compression device at 60, 90, and 120 cpm (1, 1.5, and 2 Hz). Furthermore, they pro-

posed an adaptive multi-channel Wiener filter that accommodated an arbitrary number of independent reference signals to reflect the different sources of additive noise better. Aase et al. evaluated not only how the SNR improved but also how the sensitivity of an AED improved after the CPR artifact was suppressed, observing that artifact removal becomes more difficult as the compression rate increases. This was due to the growing spectral overlap, which was highest when chest compressions were administered at 120 cpm. They also observed important differences between VF and VT sensitivities: the AED algorithm performed worse for VT, both before and after filtering the artifact. Aase et al. concluded that the differences were caused by the characteristics of the AED algorithm, which treats organized VT below 180 bpm (3 Hz) as non-shockable. The algorithm misinterpreted the appearance of repetitive lower-rate CPR artifacts as slow VT.

The filtering method proposed by Aase et al. presents important computational limitations, as their method requires the inversion of an autocorrelation matrix for every signal sample. The dimension of the autocorrelation matrix is given by the sum of the filter lengths of each reference signal. Although the method can accommodate many reference channels and use arbitrary filter lengths, the computational cost of inverting the autocorrelation matrix limits its applicability. Furthermore, real reference signals may produce ill-conditioned autocorrelation matrices. In 2002, Husøy et al.<sup>63</sup> proposed a more efficient adaptive filter — a Multi-Channel Recursive Adaptive Matching Pursuit (MC-RAMP) algorithm — that corrected those limitations. They demonstrated that both methods produced similar results in terms of SNR improvement for a database of 200 VF and 71 VT, combined with CPR artifacts recorded from pigs in asystole in the most unfavorable conditions; i. e., at a constant compression rate of 120 cpm. The reference channels were acquired using a modified Heartstart 4000 AED from Laedal Medical AS that recorded the thoracic impedance, the ECG common mode, and the compression acceleration. The compression depth was not directly recorded; it was estimated using the compression acceleration signal in the way described by Aase and Myklebust.<sup>4</sup>

### 2.4.3 First study on real OHCA episodes

The importance of the preceding contributions is unquestionable as they started and perfected the field of CPR artifact cancellation in humans. They all, however, suffered three important limitations: the CPR artifacts originated from mechanically administered CPR

in pigs, therefore ignoring the variability on CPR administration by rescuers in humans; they only contemplated the shockable rhythms rather than all possible rhythms during OHCA; and they were tested on artificial mixtures of clean shockable rhythms and CPR artifacts. All these limitations were overcome in 2004 when Eilevstjønn et al.<sup>46</sup> published the results of a comprehensive study that analyzed a CPR cancellation algorithm on recordings from OHCA victims.

The study by Eilevstjønn et al. was based on data recorded in a clinical study led by Dr. Lars Wik from the Institute for Experimental Medical Research at the Ullevål University Hospital in Oslo.<sup>146</sup> The OHCA episodes were recorded at three sites between 2002 and 2003 (Akershus in Norway, Stockholm in Sweden and London in the United Kingdom (UK)) using the Heartstart 4000 AED from Laedal Medical AS. The AEDs were modified to record additional reference channels, including the thoracic impedance, the ECG common mode, the compression acceleration, and the compression depth, which was derived from the pad pressure and compression acceleration signals. Eilevstjønn et al. extracted ECG segments with a uniform underlying heart rhythm containing an initial 10 s interval corrupted by CPR, immediately followed by 10 s without a CPR artifact. Their database contained 184 shockable rhythms, 178 VF and 6 fast VT,<sup>†</sup> and 348 non-shockable rhythms: 104 asystole, 228 PEA and 16 pulse-giving rhythms (PR). The ECG segments were randomly distributed in two equal subsets for development and testing.

Eilevstjønn et al. modified the MC-RAMP adaptive filter proposed by Husøy et al. to incorporate the four reference signals mentioned in the preceding paragraph. They tested the filter in a more realistic scenario by optimizing and reporting its performance in terms of how the sensitivity and specificity improved after filtering. They also compared the sensitivity and specificity after filtering with those obtained in the intervals without CPR.

Eilevstjønn et al. obtained an excellent sensitivity of 96.7% for the filtered test set, above the 90% AHA performance goal for VF, concluding that CPR artifacts could successfully be cleaned from VF/VT in a clinical scenario. The results for the non-shockable rhythms, however, were disappointing: the specificity was only 79.9%, well below the 95% AHA specification.<sup>‡</sup> Eilevstjønn et al. mentioned the inadequacies of the shock advice algorithm and the manifestation of spontaneous underlying heart activity as possible reasons for the low specificity. The suppression of the CPR artifact

<sup>†</sup> Rate above 150 bpm.

<sup>‡</sup> This figure refers to asystole and other non-shockable rhythms. The specificity performance goal for NSR is 99%, although NSR is rare in OHCA victims.

was found to be more complex for non-shockable rhythms than for shockable rhythms.

#### 2.4.4 Simplifying rhythm analysis during CPR

The major limitation of a CPR filtering technique based on multiple reference signals is that the acquisition of such signals implies AED hardware alterations. Current AEDs only record the surface ECG signal to diagnose the underlying heart rhythm, and in some cases, a limited set of reference channels to improve CPR administration and the delivery of the defibrillation shock. Since the publication of the study by Eilevstjønn et al., several contributions have attempted to reduce or eliminate the need to use reference signals, thus minimizing the AED hardware modifications required to implement the CPR suppression method. This section describes the three main approaches: filters based solely on the surface ECG (no reference channels), filters based on a single reference channel (dual-channel methods), and the direct classification of the corrupted ECG (no filter).

##### *Filters based only on the surface ECG*

In 2007, Aramendi et al.<sup>13</sup> published the first study on the suppression of the CPR artifact from the human VF using only the surface ECG. The method is based on a notch filter centered around the fundamental frequency of the compressions, which was estimated as the frequency where the amplitude spectrum of the corrupted ECG was maximum in the 1–3 Hz band. The filter adapted to the time-varying characteristics of the artifact by updating the estimate of the fundamental frequency every 4.8 s.<sup>†</sup> Aramendi et al. used artificial mixtures of 200 human VF samples and 25 CPR artifacts recorded from OHCA patients in asystole, and reported good SNR improvement and a mean AED sensitivity of 98.1% for all the input corruption levels tested.

In 2008, de Gauna et al.<sup>39</sup> published a more comprehensive work. Although de Gauna et al. used artificial mixtures to design their adaptive CPR suppression filter, they reported their results using data extracted from the database of OHCA episodes used by Eilevstjønn et al. The filter was based on a more elaborate model of the artifact, composed of two harmonically related sinusoids of time-varying amplitude and phase. The parameters of the model were the fundamental frequency of the artifact and its harmonic content, which were estimated using spectral analysis every 4.8 s.

<sup>†</sup> The analysis window of the AED used to test the effectiveness of the filter.

Cleaning the CPR artifact from non-shockable rhythms, asystole in particular, posed the greatest difficulty because the residuals after filtering often resembled low-amplitude VF, which was diagnosed as shockable. Specificity was improved by a prefiltering stage, where asystole corrupted by CPR was detected when the power content percentage of the low frequencies exceeded a threshold.

More recently, Amann et al.<sup>9</sup> investigated the possibility of using a coherent line removal algorithm to suppress the CPR artifact using only the surface ECG. Again, the algorithm starts by estimating the fundamental frequency of the artifact using spectral analysis on the surface ECG. The coherent line removal algorithm then removes the artifact, assuming a periodic artifact of strong harmonic components. The filtering results, however, are not conclusive because the performance of the algorithm was evaluated in terms of SNR improvement for artificial mixtures of 14 human VF and 12 CPR artifacts — compression rate 80–120 cpm — recorded in pigs in asystole.

#### *Dual-channel filters*

Models of the CPR artifact based only on the analysis of the surface ECG are not accurate enough. As discussed later in Section 2.4.5, the filtering results using only the ECG are well below those reported by Eilevstjønn et al.<sup>46</sup> for a multi-channel method. However, intermediate approaches based on a single reference channel can be as accurate as the more elaborate multi-channel methods.

Berger et al.<sup>21</sup> proposed the first dual-channel method in 2007. The study used the force signal to model the CPR artifact, using linear and nonlinear coupling terms.<sup>†</sup> The filter was tested on a porcine experimental setup, and CPR was administered through a mechanical device, the Zoll AutoPulse, which works at a constant frequency of 80 cpm.<sup>55</sup> The sensitivity and specificity of three commercial AED algorithms were tested for 13 NSR, 8 asystole, and 106 VF episodes recorded from 13 pigs. Although the results were promising, they must be considered with care because porcine VF presents larger DF than human VF, and CPR was administered mechanically at a low compression rate.<sup>‡</sup> As stated in Section 2.4.3, suppressing the artifact introduced by human rescuers in human OHCA registers is a much more challenging effort.

<sup>†</sup> The nonlinear coupling term is quadratic and serves to model higher harmonics of the artifact. In fact, Berger et al. mentioned that the filtering results substantially improved after the addition of this term.

<sup>‡</sup> The current guidelines recommend 100 cpm.<sup>56</sup>

A group of Austrian researchers investigated the possibility of using the arterial blood pressure as the reference signal. Rheinberger et al.<sup>117</sup> proposed a Kalman filter based on lagged copies of the arterial blood signal to adjust the time-varying amplitudes and phases of the CPR artifact model. However, the results were not conclusive because they used artificial mixtures with a very limited database composed of 14 CPR porcine artifacts and 14 human VF episodes. Later, Werther et al.<sup>142</sup> used a similar database to adjust a different filtering method based on Gabor multipliers. Werther et al. assumed a known SNR to adjust the amplitude of the reference channel; however, the SNR is not known when the ECG is recorded in a real OHCA setting. This initial effort was later completed by comparing the performance of four dual-channel filtering methods using 395 human ECGs (165 from OHCA settings, and 230 from public databases) combined with 13 CPR artifacts recorded from pigs in asystole.<sup>141</sup> In any case, all these contributions use artificial mixtures and are not based on recordings from human OHCA episodes. Furthermore, recording the arterial blood pressure signal may not be realistic in a resuscitation scenario, although the methods could be adjusted for other reference channels.<sup>141</sup>

Irusta et al.,<sup>67</sup> presented the first dual-channel method tested in human OHCA episodes, the method is described in detail in Chapter 5. The filter estimates a time-varying Fourier series representation of the CPR artifact and uses the instantaneous frequency of the chest compressions as the only additional reference channel. These data are not directly recorded in AEDs but can be easily derived from, for instance, the compression depth or the force signal. The method was tested on 381 OHCA registers: 89 shockable and 292 non-shockable, including 88 asystole. These are the first realistic results for dual-channel methods, and the sensitivities and specificities reported for a commercial AED are comparable to those presented by Eilevstjønn et al. for the MC-RAMP filter, as later discussed in Section 2.4.5.

#### *Classifying the corrupted ECG*

In 2008, Li et al.<sup>95</sup> introduced a new approach to rhythm diagnosis during CPR. All the previous efforts were concentrated on suppressing the CPR artifact to identify the underlying ECG rhythm. Li et al. proposed a method to classify directly the ECG corrupted by a CPR artifact. Their classification algorithm is based on features that are marginally affected by the artifact. These features

were obtained from the wavelet transform, the spectral analysis,<sup>†</sup> and the correlation function. The algorithm was validated on 4580 segments of 10 s duration from 229 victims of OHCA: 2360 uncorrupted and 2220 corrupted by CPR artifacts. The results are promising: Li et al.<sup>95</sup> reported a sensitivity of 93.3% and a specificity of 88.6% for the corrupted registers. However, their database of non-shockable registers only contains 4% asystole corrupted by CPR, which does not reflect the fact that asystole is the most frequent non-shockable rhythm in OHCA.<sup>35</sup> Furthermore, asystole corrupted by CPR has also been identified as the non-shockable rhythm type that is the most difficult to identify.<sup>39</sup>

More recently, Krasteva et al.<sup>86</sup> presented a second attempt at direct classification of the corrupted ECG. Their shock advice algorithm is based on features derived from the corrupted ECG and a reconstructed version of the ECG; i. e., the algorithm combines features obtained from the corrupt and the filtered ECG. The authors used a development and a validation dataset of OHCA registers of 20 s duration: 10 s corrupted by CPR followed by 10 s without artifact. The testing dataset was obtained from 100 OHCA victims and was composed of 172 shockable registers and 721 non-shockable registers, including 330 asystole registers. Their results, 90.1% sensitivity and 86.1% specificity, are worse than those reported by Li et al.,<sup>95</sup> probably because their database contains a much larger proportion of asystole.

#### 2.4.5 Comparative assessment on OHCA registers

Table 2.3 shows a comparison of four methods tested on OHCA registers. Each method represents one of the four approaches to rhythm analysis during CPR described in the preceding sections. The comparison must be accepted with caution for two reasons. First, the composition of the databases was different in each study. There are, for example, large differences among the studies in the proportion of asystole corrupted by CPR: 30% of the non-shockable registers in Eilevstjønn et al., 43% in de Gauna et al., 30% in Irusta et al., and 46% in Krasteva et al. Second, each study assessed the performance of the technique using a different AED algorithm. Eilevstjønn et al. reported a 81.5% sensitivity and a 67.2% specificity before filtering; i. e., the AED algorithm they used has a tendency to identify CPR artifacts as shockable. Conversely, Irusta et al. reported a sensitivity of 58.4% and a

<sup>†</sup> Li et al. use the AMSA parameter, which has been previously used in studies on the prediction of shock success.<sup>114</sup>



specificity of 90.8% before filtering; i. e., CPR artifacts are more frequently classified as non-shockable by their AED algorithm.

The first three studies use data from the same source, the clinical study described in Section 2.4.3. The performance reported by de Gauna et al. for a filter based only on the surface ECG is well below the one reported by Eilevstjønn et al. for a multi-channel filter and Irusta et al. for a dual-channel filter, particularly the sensitivity, which is 5 to 6 points lower. In fact, the best global performance is obtained for the dual-channel method, which suggests that a single reference channel may suffice to model the artifact accurately. The variations in specificity between the dual-channel and multi-channel methods are probably related to the differences in the performance of the AED algorithms when classifying rhythms corrupted by CPR artifacts. Finally, Krasteva et al. reported the lowest sensitivity, similar to the one reported in de Gauna et al., but the highest specificity, half a point above that reported in Irusta et al. Their method, based on the direct analysis of the corrupted ECG, presented an 86% specificity despite the high prevalence of asystole in their database.<sup>†</sup> Filtering based on reference channels presents good sensitivity; therefore,

Authors	Method	Se(%) <sup>a</sup>	Sp(%) <sup>a</sup>	Testing datasets <sup>b</sup>	
				S	NS
Eilevstjønn et al. <sup>46</sup>	MC-RAMP	96.7 (87.6–98.0)	79.9 (73.3–85.2)	92	174
de Gauna et al. <sup>39</sup>	Kalman filter	90.1 (83.6–94.2)	80.4 (75.9–84.3)	131	347
Irusta et al. <sup>67</sup>	LMS filter	95.6 (84.4–99.6)	85.6 (78.9–90.5)	45	146
Krasteva et al. <sup>86</sup>	Direct analysis	90.1 (85.6–94.6)	86.1 (83.6–88.7)	172	721

<sup>a</sup> 95% CI indicated in parenthesis.  
<sup>b</sup> S ≡ shockable, NS ≡ non-shockable.

**Table 2.3:** Comparison of four different approaches to rhythm analysis during CPR tested on OHCA registers. The AED shock advice algorithms used in each study were: the Philips HeartStart 4000 algorithm in Eilevstjønn et al. and the algorithm from the Reanibex 200 in de Gauna et al. and Irusta et al. The datasets used in the first three studies originated from the same original database (see Section 2.4.3). Data reproduced and corrected from Krasteva et al.<sup>86</sup>

<sup>†</sup> The reported specificity for asystole is a poorer 83%.

these methods may be combined with the direct analysis of the corrupted ECG to improve the specificity.

All the studies report a sensitivity above the 90% AHA performance goal for VF. The major limitation of all approaches is the specificity, which is well below the 95% AHA performance goal for all cases. Unfortunately, a reliable rhythm analysis during CPR is not currently a commercial reality;<sup>96</sup> the results compiled in Table 2.3 are still far from the AHA performance goals.

## 2.5 Contributions of the thesis work

The motivation and objectives of the thesis work are described in Section 1.6. At this point, we summarize, in the context of the background presented in this chapter, the main contributions of the thesis work.

1. *A database of pediatric arrhythmias.* Gathering and classifying a sufficient number of pediatric arrhythmias to test AED algorithms is a laborious and complex experimental task, which was initiated by our research group because of the lack of public pediatric arrhythmia databases to test AED algorithms. This database was then combined with an adult database, which served to develop and test the validity of the AED shock advice algorithm for adults and children. The results and methodology followed in the creation of the databases are presented in Section 3.1.
2. *New arrhythmia detection algorithms.* This thesis proposes a new AED shock advice algorithm that is valid for both adults and children. The current literature only covers adult ventricular arrhythmia detection algorithms and the validation of complete AED algorithms on children. No general methods valid for adult and pediatric patients have been described in detail. The method is developed and tested on a combination of adult and pediatric databases designed to reflect the most difficult discrimination cases fully, such as the high-rate pediatric SVT. This point is covered in Chapter 4.
3. *Rhythm analysis for OHCA episodes.* The complete analysis of an AED arrhythmia detection algorithm must include the assessment of its performance for OHCA registers, both with and without CPR artifacts. This is explored in Chapter 5.



# 3 | ECG REGISTER DATABASES

This chapter presents the ECG register databases created to develop and test the algorithms described in Chapter 4 and Chapter 5. The chapter is organized in two sections. The first section introduces the databases of adult and pediatric registers used to develop and test the AED shock advice algorithms. The second section presents the database of OHCA registers used to assess the performance of the AED algorithm in a resuscitation scenario, in both the presence and the absence of CPR artifacts.

## 3.1 Databases for AED rhythm analysis

The AHA scientific statement described in Section 1.4.1 is the framework for the creation of the ECG register databases used to develop and test AED shock advice algorithms. The statement describes, among other things, the composition of the databases in terms of the types of rhythms and the minimum number of registers per rhythm type (see Table 1.3 for a summary). Furthermore, it mentions that the data used to develop the algorithm must be different from the data used to report the performance of the algorithm.

Currently, there exists no public database of ECG registers compliant with the AHA statement. Each AED manufacturer, therefore, must compile its own proprietary database of ECG registers to test their algorithms. Since 2003, when ILCOR recommended the use of AEDs in children 1 to 8 years of age,<sup>120</sup> the database must also include pediatric arrhythmias if the AED will treat children. To date, only three proprietary pediatric databases have been described in the scientific literature,<sup>25,16,15</sup> and none of them meets the minimum requirement for the numbers of shockable registers specified in the AHA statement.

The creation of a database of ECG registers is a complex experimental task that involves EMS (out-of-hospital data), hospitals (in-hospital data), expert cardiologists to classify the registers and biomedical engineers to manage and store the data. First, the registers are collected, either retrospectively or prospectively, and then at least three expert reviewers classify them. The registers

are classified into one of three possible classes: shockable (fast VT and coarse VF), non-shockable (NSR, other non-shockable rhythms, such as SVT, and asystole), and intermediate (slow VT and fine VF). Several examples of shockable and non-shockable ECG registers are shown in Figure 3.1.

Our research group has been involved in research on AED shock advice algorithms since 2000. As a result of several research projects, two databases of adult arrhythmias were available for this thesis work: the Reanibex and the Donostia–Emergencias databases, described in Section 3.1.3. In 2005, we initiated a project to create a pediatric database. The creation of the pediatric database, which constitutes the core of the experimental part of this thesis work, was completed by late 2007.

The following sections present a unified description of the two phases in the creation of the two adult databases and the pediatric database. Section 3.1.1 describes the original sources and the formats of the registers, together with the process followed to obtain the final common storage format. The classification procedure is detailed in Section 3.1.2, with particular attention to the difficulties found when classifying pediatric arrhythmias.

### 3.1.1 The collection of the ECG registers

The databases mentioned in the preceding section are collections of classified surface ECG registers. These registers were obtained from several sources, which can be grouped in the following three broad categories.

- *Public databases of surface ECG registers.* The following publicly available databases of ECG registers were used to build our databases:<sup>102,1</sup>
  - The Massachusetts Institute of Technology-Boston’s Beth Israel Hospital (MIT-BIH) databases, including the arrhythmia, malignant ventricular arrhythmia, atrial fibrillation/flutter, supraventricular arrhythmia, long-term, ST change and noise stress test databases.
  - The Creighton University (CU) ventricular tachyarrhythmia database.
  - The AHA database for evaluation of ventricular arrhythmia detectors.

The registers in these databases are stored in either MIT or AHA file formats. Lead II, equivalent to the defibrillator pads placed in anterior–anterior position, was used to obtain the registers.

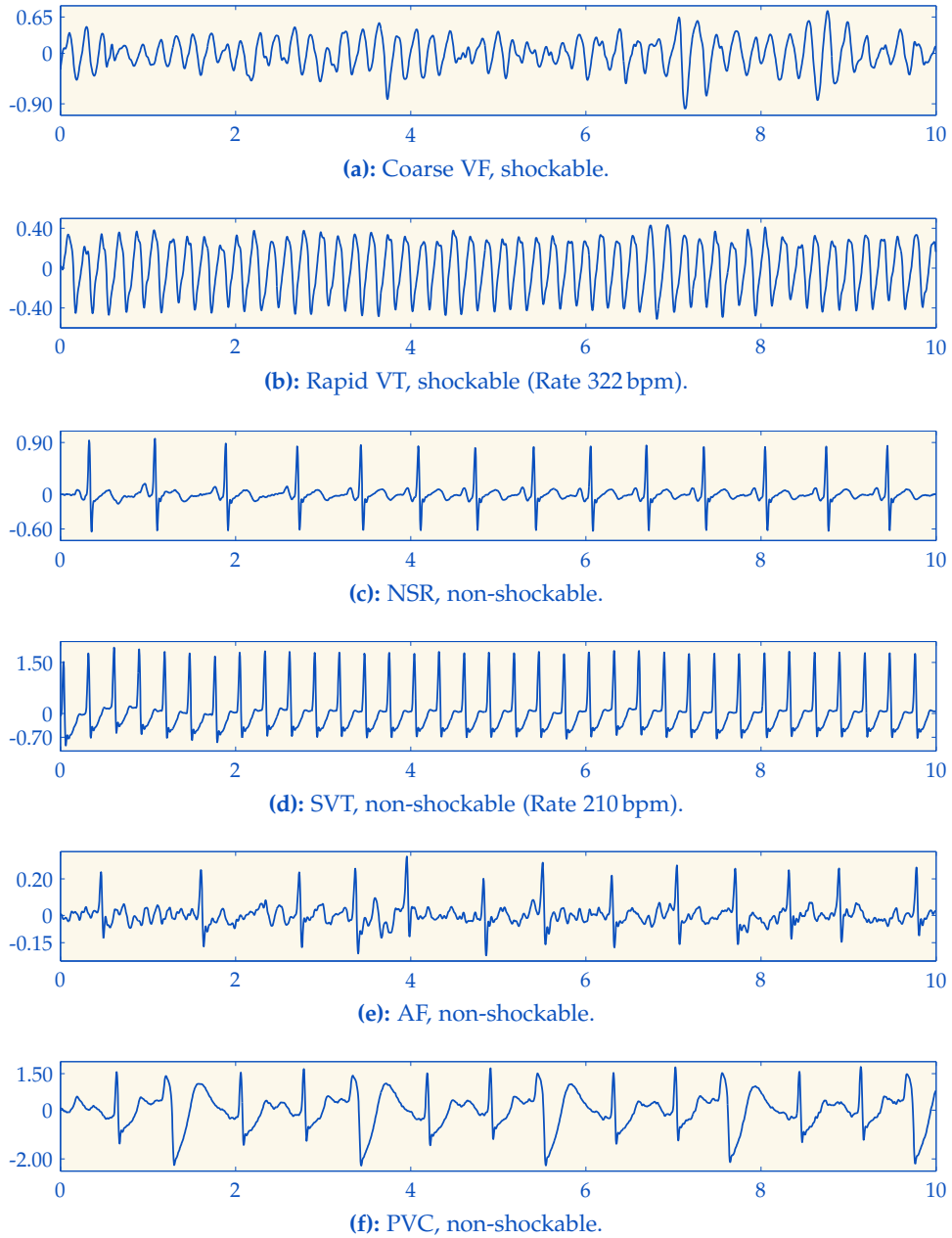


**Figure 3.1:** Examples of shockable (a–b) and non-shockable (c–f) ECG registers. The amplitude of the ECG is measured in mV.

- *In-hospital registers.* These registers were obtained as a result of the collaboration with various Spanish hospitals. The ECG registers came from retrospective and prospective electrophysiology (EP) studies and Intensive Care Units (ICU). The EP studies were available in either digital format — the Prucka Cardiolab or the EP-Tracer systems — or as ECG paper strips. All the registers from the ICUs came in printed-paper format. The available data were in the form of 3-lead and 12-lead surface ECG recordings. Lead II was used to obtain the registers.
- *Out-of-hospital registers.* Data from OHCA episodes was gathered from two Spanish EMS. Unfortunately, the storage file format of the AEDs and the manual defibrillators used by the EMS was not available to our research group, and the registers had to be printed out in paper and later digitized.

The original registers were reviewed by expert cardiologists who marked the start and end times of the registers to guarantee two aspects: a unique rhythm type during the entire register and the absence of artifacts. Only registers with durations exceeding 3.2s — the length of the analysis window of the AED shock advice algorithm described in Chapter 4 — were included in the databases. The study dates, acquisition characteristics (see Table 3.1), and patient data were annotated when available; in particular, the age of the pediatric patients.

In summary, the surface ECG data came in two different formats: digital recordings and printed-paper recordings. The digital registers came in the MIT or AHA file formats or in the propri-

Acquisition parameters	Digital registers			Paper registers
	EP-Tracer	Cardiolab	MIT/CU/AHA	
$f_s$ (Hz)	1000	1000	360/250/250	500
Resolution ( $\mu\text{V}$ )	1.25	5 <sup>a</sup>	2.4/5/2.4	5
BW (Hz)	0.05-150	0.05-100	0.1-100/0-70/ 0.05-100	0.5-40 <sup>b</sup>

<sup>a</sup> For a  $\pm 10$  mV dynamic range and 12 bit quantization.  
<sup>b</sup> Minimum acquisition bandwidth.

**Table 3.1:** Signal characteristics of the data acquisition systems: sampling frequency ( $f_s$ ), resolution and acquisition bandwidth (BW).

etary file format of the EP equipment. All registers were converted to a common format with a sampling rate of  $f_s = 250$  Hz.

The paper strips were digitized. The digitization process started by obtaining a digital image of the ECG — lead II in the case of multilead EP studies — using a flatbed scanner. Paper strips with a color grid were scanned in 24-bit color, and paper strips with black grids in 8-bit gray scale. The grid was eliminated using thresholding techniques producing a binary image of the ECG trace. The binarized ECG trace was put through a line detection and noise reduction procedure, and the digitized register was obtained. All registers were then visually inspected by superposing the original image and the digitized register. Figure 3.2 shows an extract of a digitized paper strip containing a pediatric VF rhythm. For a paper speed of 25 mm/s and a gain setting of 10 mm/mV, a scanning resolution of 508 dpi yields a  $f_s = 500$  Hz and a resolution of  $5 \mu\text{V}$ , as indicated in Table 3.1. The digitized registers were finally downsampled to  $f_s = 250$  Hz.

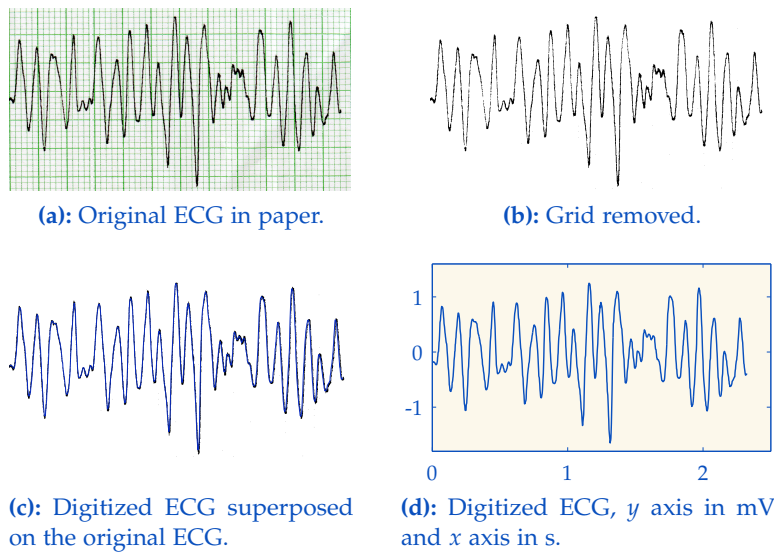


**Figure 3.2:** Example of a digitized EP study: the rhythm in the original paper strip is a pediatric VF.

### 3.1.2 The classification of the ECG registers

Following the AHA statement, the classification of the ECG registers requires agreement among three expert reviewers of cardiac arrest rhythms. Consequently, the ECG registers were printed

out and handed to three independent cardiologists, who classified them in one of the rhythm types specified in the AHA statement. Finally, each register was classified as shockable, non-shockable, or intermediate. The criteria followed to determine the shock/noshock recommendation for potentially shockable rhythms were:<sup>25</sup> the patient is unresponsive, the patient has no palpable pulse, and the age of the patient is unknown.<sup>†</sup>

The shock/noshock recommendation depends on the heart rate for VT; fast VT is considered shockable, and slow VT is classified as intermediate. The AHA statement allows the manufacturer to specify the rate threshold for fast VT because tolerance to VT varies widely among patients.<sup>80</sup> In our databases, shockable VT included polymorphic VT and fast monomorphic VT. Fast VT was defined as VT with rates above 150 bpm in adults and 20 bpm above age-matched normal rate in children; i. e., 180 bpm for children under 1 year and 150 bpm for children over 1 year.<sup>16</sup> These criteria are not universally accepted; for instance, the pediatric studies published to date have all used different criteria: 250 bpm for monomorphic VT in Cecchin et al.,<sup>25</sup> 20 bpm above age-matched normal rate in Atkinson et al.,<sup>16</sup> and 200 bpm in Atkins et al.<sup>15</sup> We adopted the criteria used by Atkinson et al. because it is the most inclusive and therefore posed a greater challenge to the design of the algorithms.

During the classification process, two types of discrepancies among the cardiologists occurred: in the determination of the rhythm type and in the shock/noshock decision. The latter are the important ones from the point of view of the design of shock advice algorithms. In fact, the AHA statement requires a consensus decision only for the shock/noshock diagnosis. All the registers with non-agreeing diagnoses were further discussed. The final consensus diagnosis was reached after the assessment of the risks of each potential recommendation.

Non-shockable fast pediatric SVT and shockable pediatric VT proved to be the most difficult rhythms to classify. In a number of cases, the reviewers could not reach a consensus decision and stated that additional information, such as other ECG leads, was needed for a diagnosis. Figure 3.3 shows some of those cases. Discrepancies were resolved by adopting the original interpretation from the rhythm source. Our hypothesis is that it may not be feasible for a cardiologist to discriminate pediatric SVT and VT accurately based on the surface ECG alone, particularly when the rate of pediatric SVT is high. A consensus decision of three independent cardiologists is the only possibility for registers obtained

<sup>†</sup> The cardiologist did know whether the patient was adult or pediatric.



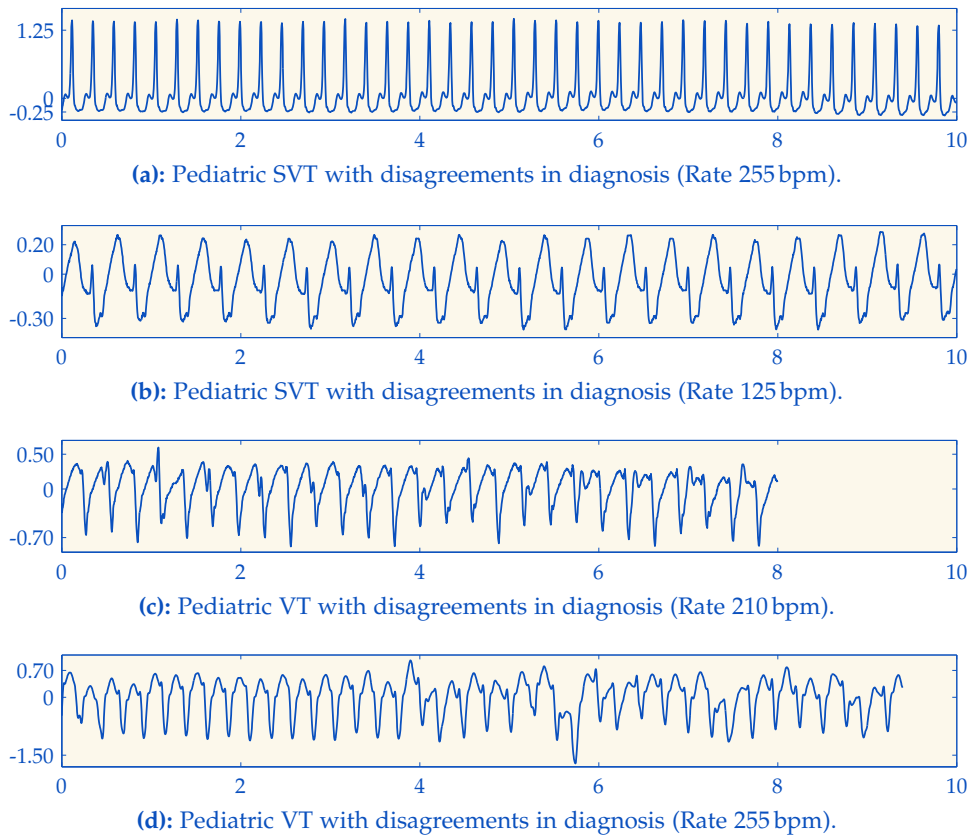


**Figure 3.3:** Examples of pediatric VT and SVT with disagreements in the cardiologist's classification. In these cases, the diagnosis from the rhythm source was adopted.

from AEDs in the field. When registers come from EP studies, the diagnosis from the physician aware of the clinical history of the patient might be more reliable. Atkins et al.,<sup>15</sup> also found difficulties in the diagnosis of pediatric rhythms using a single lead and mentioned that in a number of cases much discussion and multiple views of the registers were needed for a consensus; and Atkinson et al.,<sup>16</sup> presented an example of a pediatric SVT in which the cardiologist's classification could change depending on the ECG acquisition bandwidth. Atkins et al. defined pediatric SVT based on three criteria: the presence/absence of P waves, the heart rate, and the duration of QRS complexes.<sup>15</sup> However, criteria based on rate and QRS duration using a single lead might be insufficient because wide QRS complex tachycardia in children is likely to be of supraventricular origin.<sup>22</sup> Furthermore, infants may have a QRS duration in VT less than 90 ms.<sup>123</sup>

### 3.1.3 Databases of adult registers

#### *The Reanibex database*

This is the database of adult registers used to test and certify the shock advice algorithms of the AEDs manufactured by Osatu S. Coop., a line of products called Reanibex. The registers were collected and classified during 2000–2002, and it is the first database created by our research group. It contains registers extracted from the publicly available databases; i. e., the MIT-BIH, CU and AHA databases. More registers were added through the collaboration with the EP and ICU departments of the Basurto Hospital in Bilbao, which provided digital registers from the Cardiolab system and paper registers. The database was completed with the addition of registers from OHCA episodes obtained from the EMS of Osakidetza (the Basque Health Service) and the EMS in Madrid (SAMUR). The Philips ForeRunner and the PhysioControl LifePack AEDs recorded the OHCA registers.

As stated in the AHA statement, each register within a rhythm class belongs to a different patient. The database also met the

Rhythms	Origin			Total
	MIT/CU/AHA	Basurto	OHCA	
<b>Shockable</b>				
Coarse VF	9/28/9	64	68	178
Rapid VT	8/8/1	42	20	79
<b>Non-shockable</b>				
NSR	125/13/47	2	-	187
SVT <sup>a</sup>	39/11/16	1	-	67
AF, SB, blocks, idioventricular, PVC	92/39/56	-	-	187
Asystole	5/3/1	-	65	74
<b>Intermediate</b>				
Fine VF	1/1/-	9	20	31
Other VT	1/1/1	6	16	25

<sup>a</sup> Although SVT belongs to the other non-shockable group (AF,SB, ...) it is considered as an individual category in this work.

**Table 3.2:** Number and source of the registers in the the refined Reanibex database of adult rhythms.

requirement for minimum sample sizes specified in the AHA statement. For this thesis work, the registers in the original Re-anibex database were thoroughly reviewed, and those with low signal quality or noise were discarded. For instance, out of the 200 VF registers from the original database, only 178 were selected. Table 3.2 shows a summary of the selected registers, which total 828 registers from 590 adult patients. The mean duration of the registers is  $13.5 \pm 3.3$  s and  $11.5 \pm 4.6$  s for the 257 shockable registers and  $14.6 \pm 1.6$  s for the 515 non-shockable registers.

#### *The Donostia–Emergencias database*

The Donostia–Emergencias database is the second database of adult registers, it was compiled during 2006–2007. It contains registers from EP studies conducted at the Donostia Hospital in San Sebastian using the EP-Tracer system, as well as a second set of OHCA episodes from the EMS in the Basque Country and Madrid. The Philips ForeRunner and the PhysioControl LifePack AEDs recorded the registers.

Table 3.3 shows a summary of the collected registers; in this case, more than one register per patient and rhythm class were allowed

Rhythms	Origin		Total
	Donostia	OHCA	
<b>Shockable</b>			
Coarse VF	140 (113)	88 (83)	<b>228 (196)</b>
Rapid VT	105 (101)	22 (20)	<b>127 (121)</b>
<b>Non-shockable</b>			
NSR	105 (104)	1 (1)	<b>106 (105)</b>
SVT	21 (20)	2 (2)	<b>23 (22)</b>
AF, SB, blocks, idioventricular, PVC	31 (31)	16 (15)	<b>47 (46)</b>
Asystole	2 (2)	446 (436)	<b>448 (438)</b>
<b>Intermediate</b>			
Fine VF	3 (2)	34 (30)	<b>37 (32)</b>
Other VT	6 (6)	14 (14)	<b>20 (20)</b>

**Table 3.3:** Number and source of the registers in the Donostia–Emergencias database of adult rhythms. The number of patients is indicated in parenthesis.

but only if the morphology of the rhythm was sufficiently different. The Donostia–Emergencias database contains 1036 registers from 838 adult patients. The mean duration of the registers is  $12.9 \pm 5.7$  s and  $11.1 \pm 5.9$  s for the 355 shockable registers and  $13.9 \pm 5.4$  s for the 624 non-shockable registers.

### 3.1.4 The pediatric database

ILCOR's approval in 2003 of the use of AEDs in 1–8 year olds<sup>120</sup> triggered our need to create a database of pediatric registers. The database was created in two phases that span a period of 3 years, from early 2005 to late 2007.

During the initial phase, Dr A Bodegas and Dr E Pastor from the Cruces Hospital in Barakaldo and Dr F Benito from La Paz Hospital in Madrid provided us with retrospective EP studies from pediatric patients. These registers came either in digital format from the Cardiolab system or in paper format. Drs Benito, Bodegas and Pastor participated in the register classification process. The results from the initial phase were presented at the 2006 Computers in Cardiology conference.<sup>65</sup>

In 2006, we extended the network of cooperating hospitals to include Dr JM Porres from the Donostia Hospital, Dr JL López-Herce from the pediatric ICU at the Gregorio Marañón Hospital in Madrid, and Dr J Brugada from the San Joan de Deu Hospital in Barcelona. In this second phase, we added registers in digital format from the EP-Tracer systems of the Donostia and San Joan de Deu hospitals and digitized paper registers from the Gregorio Marañón Hospital. Drs Bodegas, Pastor, and Porres classified the registers during the second phase.

The pediatric database contains 1090 registers from 649 pediatric and adolescent patients aged between 1 day and 20 years (mean age  $7.1 \pm 4.5$  years). Table 3.4 summarizes the composition of the pediatric database. The registers had a mean duration of  $13.7 \pm 8.9$  s and  $10.9 \pm 4.9$  s for the 124 shockable registers and  $14.1 \pm 9.3$  s for the 958 non-shockable registers.

Table 3.5 summarizes the registers obtained from pediatric patients in the 1–8 years old group, the population to which the 2003 ILCOR recommendations apply. For this age group, we collected 563 registers from 378 patients, mean age  $4.7 \pm 2.2$  years. The registers had a mean duration of  $14.3 \pm 8.0$  s and  $11.6 \pm 5.1$  s for the 57 shockable registers and  $14.6 \pm 8.2$  s for the 504 non-shockable registers.

Contrary to the AHA statement, the pediatric database included several registers from the same patient and rhythm type, if the

Rhythms	Origin					Total
	Cruces	La Paz	Donostia	GM	SJD	
<b>Shockable</b>						
Coarse VF	8 (2)	43 (14)	4 (4)	– (–)	3 (2)	<b>58 (22)</b>
Rapid VT	9 (7)	34 (17)	4 (2)	5 (1)	14 (9)	<b>66 (36)</b>
<b>Non-shockable</b>						
NSR	240 (226)	33 (33)	17 (13)	– (–)	250 (182)	<b>540 (454)</b>
SVT	58 (42)	68 (50)	8 (8)	6 (5)	182 (131)	<b>322 (236)</b>
AF, SB, blocks, idioventricular, PVC	33 (30)	8 (6)	5 (4)	6 (3)	44 (39)	<b>96 (82)</b>
Asystole	– (–)	– (–)	– (–)	– (–)	– (–)	– (–)
<b>Intermediate</b>						
Fine VF	– (–)	4 (2)	– (–)	– (–)	– (–)	<b>4 (2)</b>
Other VT	– (–)	4 (3)	– (–)	– (–)	– (–)	<b>4 (3)</b>

**Table 3.4:** Number of registers and patients per origin in the pediatric database. GM stands for Gregorio Marañón, and SJD stands for San Joan de Deu.

morphology of the arrhythmias was sufficiently different. All the previous studies on AED shock advice algorithms in children<sup>25,16,15</sup> have relaxed the AHA recommendations because of the difficulty of gathering pediatric ventricular arrhythmias.

The pediatric database has two important shortcomings. First, the number of shockable registers is low, well below the minimum required by the AHA. The numbers are nevertheless comparable to those reported in the previous studies on the field (see Table 2.2). Our database contains 124 shockable registers (57 in the 1–8 year old group) while Cecchin et al.,<sup>25</sup> Atkinson et al.,<sup>16</sup> and Atkins et al.<sup>15</sup> reported 131, 76, and 120 shockable registers, respectively. These numbers reflect the low incidence of shockable rhythms in children. Second, the pediatric registers were obtained in hospital; i. e., there are no registers from pediatric OHCA, which is also a limitation of all the previous studies on the field. Pediatric OHCA registers are scarce; for instance, Rossano et al.<sup>118</sup> reviewed the interventions of three EMS from 1982 to 2002 in patients up to 18 years of age and only identified 57 victims with VF, 43 of whom had VF as the initial rhythm.

Conversely, our database contains a large number of fast pediatric SVT, both in the complete and in the 1–8 year old group. It is well known that pediatric SVT can have a very high heart rate

Rhythms	Origin					Total
	Cruces	La Paz	Donostia	GM	SJD	
<b>Shockable</b>						
Coarse VF	1 (1)	15 (8)	2 (2)	– (–)	– (–)	<b>18 (11)</b>
Rapid VT	7 (5)	24 (11)	– (–)	5 (1)	3 (2)	<b>39 (19)</b>
<b>Non-shockable</b>						
NSR	217 (206)	21 (21)	– (–)	– (–)	74 (53)	<b>312 (280)</b>
SVT	38 (27)	36 (24)	– (–)	3 (3)	70 (49)	<b>147 (103)</b>
AF, SB, blocks, idioventricular, PVC	29 (26)	5 (4)	– (–)	2 (1)	9 (7)	<b>45 (38)</b>
Asystole	– (–)	– (–)	– (–)	– (–)	– (–)	– (–)
<b>Intermediate</b>						
Fine VF	– (–)	– (–)	– (–)	– (–)	– (–)	– (–)
Other VT	– (–)	2 (2)	– (–)	– (–)	– (–)	<b>2 (2)</b>

**Table 3.5:** Number of registers and patients per origin in the pediatric database. The data refers to the subset of 1–8 year old patients.

that might produce erroneous shock recommendations when algorithms designed for adult patients are used.<sup>120,15</sup> Our database, therefore, is a useful tool to test the specificity of AED algorithms on pediatric patients.

There are no asystole registers in the pediatric database because of the lack of pediatric OHCA episodes and the difficulty in gathering asystole from children in an in-hospital setting.<sup>†</sup> During asystole, there is no cardiac electrical activity, and the ECG is close to a flat line. An accurate identification of asystole for adult patients guarantees the correct diagnosis for the pediatric case because asystole is similar for adult and pediatric patients.

### 3.1.5 Databases for the development and testing of AED shock advice algorithms

The pediatric and the two adult databases were merged to form a database of adult and pediatric registers that contains all the collected registers from the sources described in Section 3.1.1. The intermediate rhythms were removed because there are no

<sup>†</sup> Asystole is usually associated with a confirmation of death.

algorithm performance goals for these rhythms.<sup>†</sup> Several registers from the same patient in the same rhythm class were allowed in the pediatric case but not in the adult case. Consequently, some registers from the Donostia–Emergencias database were discarded.

The registers were randomly split into two similar sets regarding numbers of registers and patients. The first database, described in Table 3.6a, was used to develop the AED shock advice algorithm. The second database, shown in Table 3.6b, was used to test the algorithm. There is an important difference between the development and test databases. The development database contains a single register per patient and rhythm class. The test database contains all the pediatric registers not included in the development database; therefore, rhythm repetition was allowed. For instance, there are 58 pediatric VF from 22 patients. A single VF register was selected from half the patients for inclusion in the development database (11 VF from 11 patients); the rest (47 VF from 17 patients) were added to the test database. The independence between test and development is respected because pediatric rhythm repetition was only allowed when the morphology of the arrhythmias was different. The objective of this partition strategy is to develop the algorithm using adult and pediatric data while testing the algorithm in the largest possible pediatric database.

### 3.2 A database to test rhythm analysis during real OHCA episodes

The 1997 AHA statement establishes the framework for the development and testing of AED shock advice algorithms. Although our adult databases contain a large number of OHCA registers, most of them are either asystole or shockable rhythms. There are very few OHCA non-shockable rhythms, which may be very different from the NSR or SVT rhythms in our databases. Furthermore, during OHCA a CPR artifact frequently corrupts the ECG. No statement exists describing the composition of the databases to develop and test CPR cancellation algorithms, although the most advanced studies in this field<sup>46,39,67</sup> used data from OHCA episodes. One of the most comprehensive datasets of OHCA episodes was gathered in the prospective study led by Dr Lars Wik, aimed at measuring the quality of out-of-hospital CPR.<sup>146,84</sup>

<sup>†</sup> The benefits of defibrillation are uncertain for intermediate rhythms; consequently, the AHA statement mentions that results should simply be reported.

Rhythms	Original database			Total
	Reanibex	Don.-Emerg.	Paediatric	
<b>Shockable</b>				
Coarse VF	89 (89)	98 (98)	11 (11)	<b>198 (198)</b>
Rapid VT	40 (40)	61 (61)	18 (18)	<b>119 (119)</b>
<b>Non-shockable</b>				
NSR	94 (94)	53 (53)	227 (227)	<b>374 (374)</b>
SVT	34 (34)	11 (11)	118 (118)	<b>163 (163)</b>
AF, SB, blocks, idioventricular, PVC	94 (84)	24 (24)	42 (42)	<b>160 (150)</b>
Asystole	37 (37)	219 (219)	–	<b>256 (256)</b>

**(a):** Development database for AED shock advice algorithms. All the patients within a rhythm type are different.

Rhythms	Original database			Total
	Reanibex	Don.-Emerg.	Paediatric	
<b>Shockable</b>				
Coarse VF	89 (89)	98 (98)	47 (17)	<b>234 (204)</b>
Rapid VT	39 (39)	60 (60)	48 (24)	<b>147 (123)</b>
<b>Non-shockable</b>				
NSR	93 (93)	52 (52)	313 (266)	<b>458 (411)</b>
SVT	33 (33)	11 (11)	204 (155)	<b>248 (199)</b>
AF, SB, blocks, idioventricular, PVC	93 (84)	22 (22)	54 (47)	<b>169 (153)</b>
Asystole	37 (37)	219 (219)	–	<b>256 (256)</b>

**(b):** Test database for AED shock advice algorithms. All the patients within a rhythm type are different, except in the paediatric case. Paediatric rhythm repetition is only allowed for rhythms with different morphology.

**Table 3.6:** Number of registers and patients per origin in the development and test databases used in Chapter 4 to design the universal AED shock advice algorithm.



Our research group gained access to these data through the collaboration with Prof. Trygve Eftestøl, who leads the Norwegian research group that has produced the most important advances in the field of CPR artifact cancellation algorithms.

The OHCA episodes were recorded between March 2002 and September 2004 in three locations: Akershus in Norway, Stockholm in Sweden, and London in the UK. The study, which the regional ethics committees approved, consisted of two phases. During phase I,<sup>146</sup> the paramedics were instructed to follow the 2000 guidelines for CPR and ECC;<sup>2</sup> in phase II,<sup>84</sup> feedback on CPR quality via the defibrillators was activated. The data were recorded at  $f_s = 500$  Hz with a 16-bit resolution using the Laerdal HeartStart 4000SP, a modified version of the HeartStart 4000 that allowed the recording of additional reference signals. The ECG channel was recorded with a resolution of  $1.031 \mu\text{V}$  per least significant bit and a bandwidth of 0.9–50 Hz. For each OHCA case, the initial rhythm and each subsequent change in rhythm were annotated, and the rhythms were grouped in five classes: VF and non-perfusing fast VT (rate > 150 bpm) in the shockable category, and asystole, PEA, and Pulse-giving Rhythms (PR)<sup>†</sup> in the non-shockable category.

The ECG registers extracted from the prospective study were composed of two consecutive 15.5 s intervals: CPR artifacts corrupted the first interval and were immediately followed by a second interval without CPR artifact. The rhythm annotations in the original databases were used to certify that the underlying heart rhythm was the same in both intervals. Therefore, these registers can be used to assess the effect of the CPR artifact on the diagnosis of the shock advice algorithm, as well as how much the diagnosis improves after the CPR artifact is suppressed. Figure 3.4 shows three examples of the extracted registers.

Chapter 5 analyzes the performance of the universal AED algorithm presented in Chapter 4 for OHCA episodes, in both the presence and the absence of CPR artifacts. During chest compressions, the artifact is suppressed using the LMS algorithm described in Irusta et al.<sup>67</sup> The CPR artifact suppression method is based on the instantaneous frequency of the chest compressions. This information was not directly recorded by the HeartStart 4000SP, although it can be deduced from the compression depth signal following the procedure described in Section 5.3.2. The compression depth and the ECG registers were extracted and

<sup>†</sup> Wik et al.<sup>146</sup> defined PEA as QRS complexes without blood flow, indicated either by a clinically detected pulse or blood-flow-induced changes in thoracic impedance. PR was defined as QRS complexes with blood flow as indicated by the same factors.

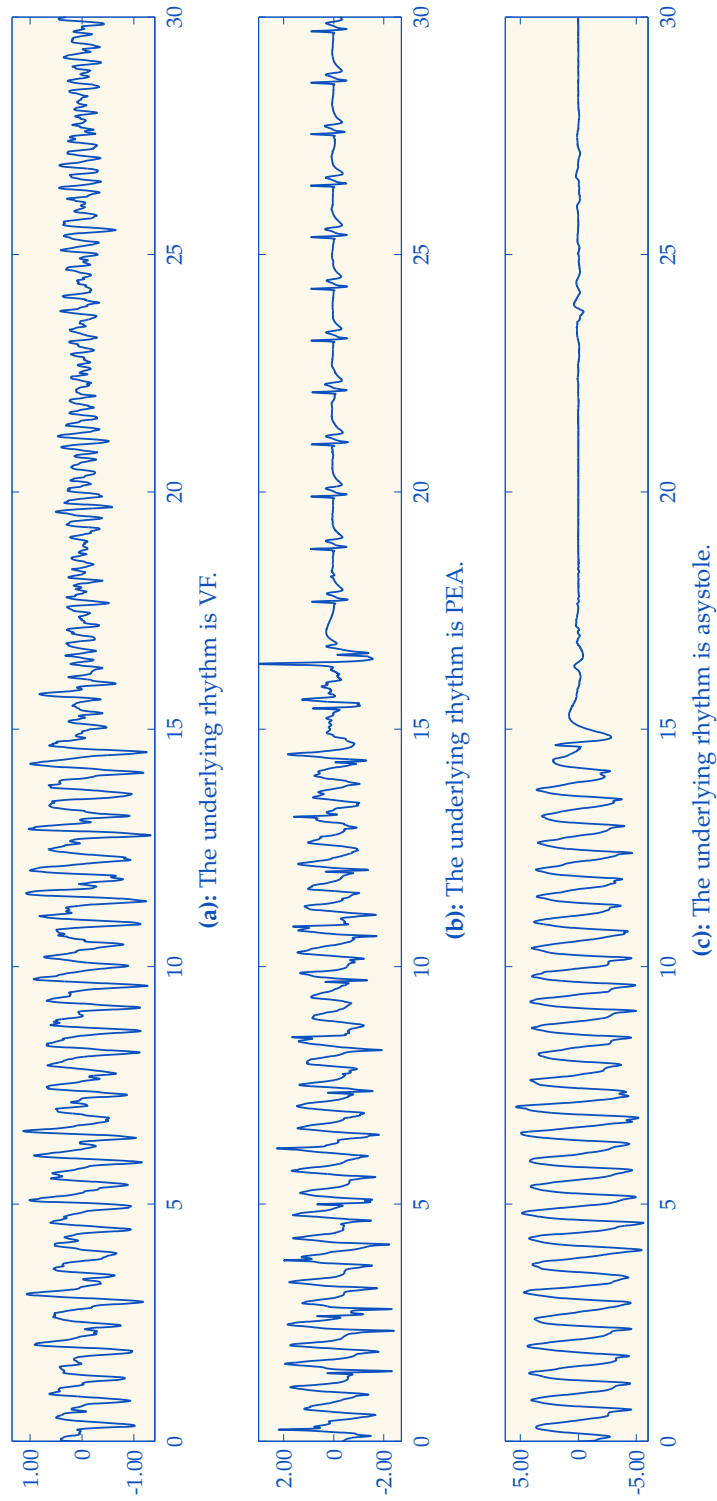


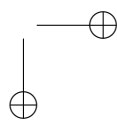
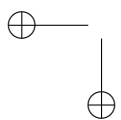
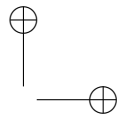
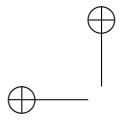
**Figure 3.4:** ECG registers extracted from the prospective study on CPR quality. A CPR artifact corrupts the ECG in the initial 15 s interval. In the second 15 s interval, chest compressions were stopped, and the ECG shows the underlying rhythm. The  $y$  axis shows the ECG in mV.

downsampled to  $f_s = 250$  Hz, and the ECG registers were preprocessed with an order-four Butterworth bandpass filter (0.7–30 Hz).

Table 3.7 shows a summary of the extracted episodes, the extraction contains 381 ECG registers from 299 patients. According to the annotations of the underlying rhythm, 89 are shockable (84 VF and 5 VT) and 292 are non-shockable (88 ASY, 166 PEA, and 38 PR) cases. All the registers within the same rhythm class belong to a different patient except two VF instances. The low incidence of VT in OHCA explains the low number of VT registers. In fact, it is estimated that patients in OHCA with VT as the first recorded rhythm are 1% of those found in VF and are customarily all grouped under VF.<sup>35</sup>

Rhythms	Registers
<b>Shockable</b>	
Coarse VF	84 (82)
Rapid VT	5 (5)
<b>Non-shockable</b>	
PEA	166 (166)
PR	38 (38)
Asystole	88 (88)
<b>Total</b>	<b>381 (299)</b>

**Table 3.7:** Number of registers in the database of OHCA episodes corrupted by CPR. The number of patients is indicated in parenthesis. This database is used to test the CPR suppression algorithm described in Chapter 5 in combination with the AED shock advice algorithm described in Chapter 4.





# 4 | SHOCK ADVICE ALGORITHM

This chapter presents a new shock advice algorithm designed and validated for adult and pediatric patients together. To date, two different strategies have been proposed to adapt the rhythm analysis algorithms of AEDs for their use in children. Initially, two AED rhythm analysis algorithms designed for adult patients were tested on comprehensive databases of pediatric arrhythmias.<sup>25,16</sup> In both studies, the specificities for non-shockable pediatric arrhythmias and the sensitivity for pediatric VF were above the AHA specifications. However, the sensitivity for pediatric VT was either too low<sup>25</sup> or inconclusive due to the low number of pediatric VT registers in their databases.<sup>16</sup> More recently, Atkins et al. showed that the specificity of an adult algorithm fell below the AHA performance goal for pediatric SVT.<sup>15</sup> Pediatric rhythms have faster heart rates and lower QRS durations<sup>25,15</sup> that might produce lower SVT specificities and lower VT sensitivities in children.<sup>15</sup> To solve this problem, Atkins et al. defined pediatric specific thresholds to be used when the pediatric defibrillation pads are attached to the AED.

The algorithm described in this chapter is based on a new design strategy: a universal algorithm designed and validated using adult and pediatric arrhythmias together.

## 4.1 Overview of the shock advice algorithm

### 4.1.1 Basic design principles

Two have been the guiding principles for the design of the new shock advice algorithm:

1. *Universal algorithm.* A single algorithm valid for adult and pediatric patients. To this aim, the design of the algorithm is based on a set of new features that, regardless of age, quantify the distinctive characteristics of shockable and non-shockable rhythms. It is particularly important that those features are independent of the heart rate, which is significantly higher for pediatric arrhythmias. The complete algorithm and its constituent blocks are designed and validated in the

framework of the AHA statement on the assessment of the performance of AED arrhythmia analysis algorithms.<sup>80</sup> The datasets used for development and testing are composed of a large number of both adult and pediatric arrhythmias. This design methodology guarantees that the algorithm will be valid for the two patient groups.

2. *Minimize the hands-off intervals.* The algorithm must diagnose the rhythm in less than 10 s to shorten the hands-off intervals for rhythm analysis. For this purpose, the discrimination features are computed in non-overlapping 3.2 s ECG segments. The algorithm assigns a shock/noshock decision to each segment and a register is classified as shockable or non-shockable using a majority criterion on three consecutive segments; i. e., the algorithm diagnoses a register in either 6.4 s or 9.6 s.

#### 4.1.2 Block diagram of the decision algorithm

The decision algorithm analyzes the digitized ECG,

$$x_{ecg}(n) = x_{ecg}(t)|_{t=nT_s} \quad \text{with} \quad f_s = \frac{1}{T_s} = 250 \text{ Hz}, \quad (4.1)$$

and classifies each 3.2 s segment in one of the categories described in Table 4.1 and assigns the corresponding shock/noshock decision to the segment. The block diagram of the processing flow is described in Figure 4.1. Each segment is processed sequentially by a set of sub-algorithms and when one of the categories established in Table 4.1 is decided the analysis ends.

The decision algorithm starts by identifying the absence of cardiac electrical activity (*asystole algorithm*). If no cardiac electrical activity is detected the segment is classified as ASY and the analysis concludes. Segments with cardiac electrical activity are further processed in the second sub-algorithm, *QRS algorithm*, where the decision algorithm tests if narrow-QRS complexes are present. Narrow-QRS complexes, which are a strong indication of a pulsed rhythm, are not found in fatal ventricular arrhythmias; consequently, if narrow-QRS complexes are detected the analysis ends and the segment is classified as PR. Otherwise, the segment is classified as nPR, a ventricular origin is suspected and the analysis continues.

Fast ventricular arrhythmias are further processed to discriminate VT from VF. Whereas VF is always shockable, VT is classified

as shockable if the ventricular rate exceeds the  $Th_R$  threshold.<sup>†</sup> The *Regularity algorithm* discriminates regular (VT) from irregular (VF) ventricular arrhythmias; irregular ventricular segments are classified as VF and the analysis finishes. Suspected VT is further analyzed by the *SVT/VT algorithm*. This algorithm is included to identify fast pediatric SVT with wide-QRS complexes, which might be classified as nPR by the *QRS algorithm*. These are fast and regular non-shockable rhythms likely to be misclassified as shockable VT.<sup>15</sup> When SVT is detected the algorithm stops. Otherwise, the ventricular rate is calculated and VT is classified as shockable rapid VT (rVT) for rates above  $Th_R$  or as non-shockable slow VT (sVT) for rates below  $Th_R$ .

Each sub-algorithm was adjusted by maximizing the sensitivity and the specificity for the subclass of rhythms it identifies. The sub-algorithms and the decision algorithm were designed using the rhythms in the development database (Table 3.6a) and the complete design was tested on the test database (Table 3.6b).

However, we do not report in the manuscript the final results for either the coefficients of the decision algorithms or the detection thresholds, because this algorithm is used in a commercial AED and is protected by company rights.

Segment types	AHA types	Characteristics
<b>Non-shockable</b>		
<b>ASY</b> Asystole	Asystole	Absence of cardiac electrical activity.
<b>PR</b> Pulsed Rhythm	AF, SB, blocks, PVC, SVT, NSR	Rhythms with well defined QRS complexes.
<b>SVT</b> Supraventricular tachycardia	SVT	Supraventricular tachycardias not identified as pulsed rhythms, i. e. with either very fast rates or wide QRS complexes.
<b>sVT</b> slow VT	Other VT	Ventricular Tachycardia with rates below the threshold for shockable VT.
<b>Shockable</b>		
<b>rVT</b> rapid VT	rapid VT	Ventricular Tachycardia with rates above the threshold for shockable VT.
<b>VF</b> coarse VF	coarse VF	Ventricular Fibrillation, the algorithm does not check coarseness (amplitude > 200 $\mu$ V).

**Table 4.1:** Description of the categories assigned to the 3.2 s ECG segments.

<sup>†</sup> The AHA statement indicates that the rate criteria is specified by the AED manufacturer.<sup>80</sup>

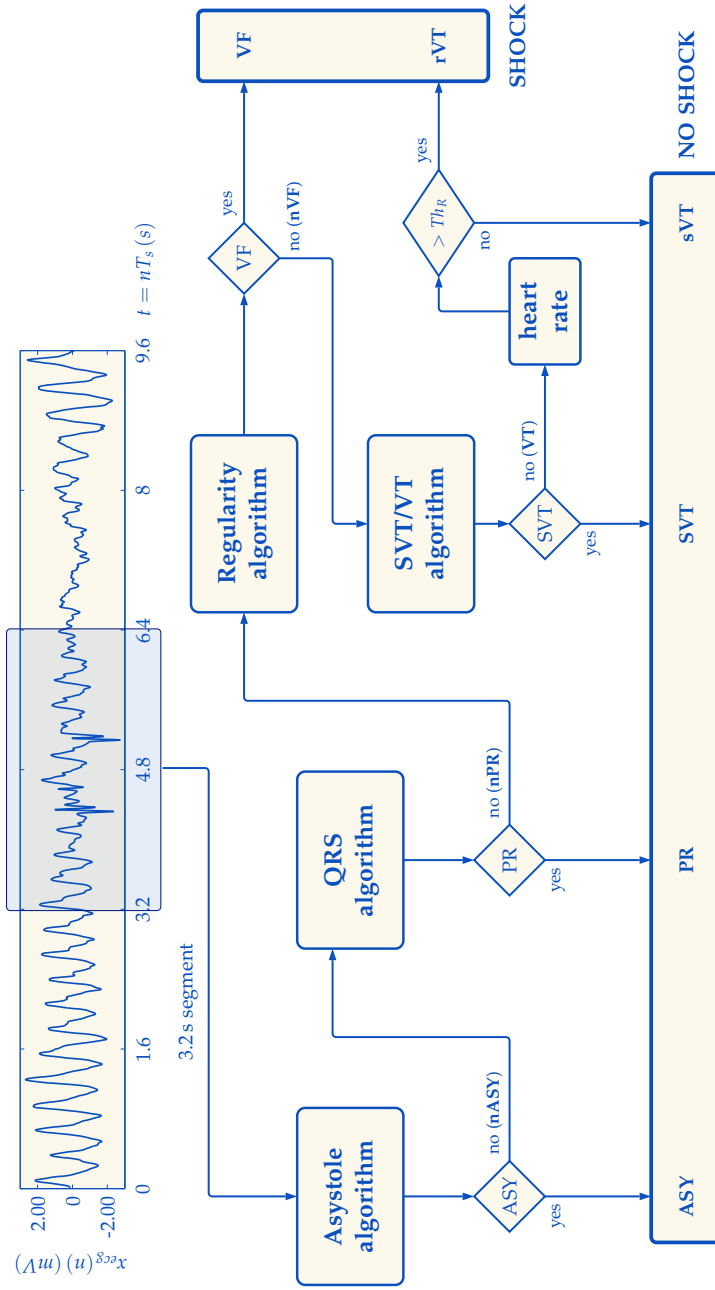


**Figure 4.1:** Block diagram of the shock advice algorithm. If one of the sub-algorithms classifies the 3.2 s segment in one of the rhythm types compiled in Table 4.1 the analysis concludes, and the segment is classified either as shockable or non-shockable. Otherwise (nASY, nPR or nVF classifications) the segment is further analyzed by the next sub-algorithm.



## 4.2 Asystole algorithm

The objective of the *Asystole algorithm* is to identify segments with either very low or no cardiac electrical activity at all. For such segments the ECG is a low power signal because all the electrical activity is concentrated around the baseline. This characteristic of asystolic rhythms is parametrized by the process described in Figure 4.2, the block diagram of the *Asystole algorithm*.

First the ECG segment,  $x_{ecg}(n)$ , is preprocessed by a band-pass filter (BPF) to suppress baseline wander and low frequency noise.<sup>†</sup> The preprocessed ECG segment,  $\hat{x}_{ecg}(n)$ , is divided into two non-overlapping subsegments of 1.6 s, and the power of each subsegment is calculated as:

$$P_i = 10^3 \times \frac{1}{N/2} \sum_{(i-1) \cdot N/2}^{i \cdot N/2 - 1} \hat{x}_{ecg}^2(n) \quad i = 1, 2 \quad (4.2)$$

where  $N = 3.2 \cdot f_s = 800$  is the number of samples in the 3.2 s segment, and  $10^3$  is a scaling factor.

The segment is classified as an asystole if the lowest of the two power values obtained is below the  $Th_p$  threshold; i. e., a 1.6 s interval of very low cardiac activity is enough to suspect asystole. This is a broad criterion because bradycardias or IV rhythms with rates below 40 bpm present low activity periods of larger duration. However all these arrhythmias should be classified as non-shockable, and including a broader class of non-shockable rhythms is acceptable from the shock/noshock point of view.

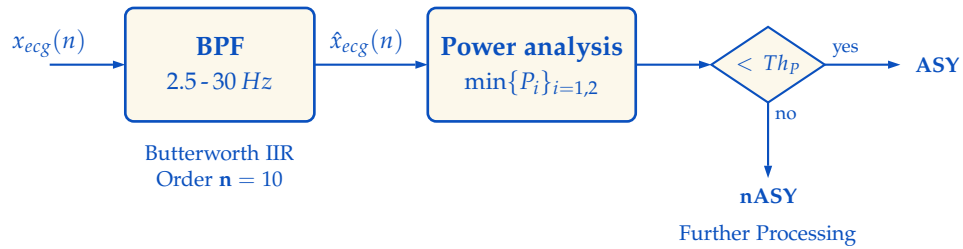


Figure 4.2: Block diagram of the *Asystole algorithm*.

<sup>†</sup> The low cutoff frequency of the filter is unusually high (2.5 Hz), however we are not interested in preserving the ECG waveform but rather in suppressing low frequency artifacts that produce large errors in the calculation of the power of the underlying asystolic rhythm. Power calculations for regular pulsed rhythms (well defined QRS complexes) or for fast ventricular arrhythmias (dominant frequencies above 2.5 Hz) are only marginally affected by the preprocessing filter.

Rhythm type	Records <sup>a</sup>	P				
		min	$P_{0.5}$	$P_{50}$	$P_{99.5}$	max
<b>Shockable</b>						
Coarse VF	198 (565)	0.95	1.52	23.74	1087.21	1494.70
Rapid VT	119 (347)	2.14	2.74	128.21	1465.51	1494.97
<b>Non-shockable</b>						
NSR	374 (1333)	1.43	1.80	22.10	351.23	551.24
SVT	163 (586)	2.48	3.11	46.98	710.14	778.20
AF, SB, blocks, idioventricular, PVC	160 (596)	$< 10^{-3}$	0.01	42.05	576.31	700.77
<b>Asystole</b>	256 (867)	$< 10^{-3}$	$< 10^{-3}$	0.02	0.79	2.82

<sup>a</sup> The number of 3.2 s segments is indicated in parenthesis.

**Table 4.2:** Values of the  $P$  parameter for the ECG segments of the development database. The statistical distribution is characterized in terms of percentiles,  $P_x$  means percentile  $x$  of the distribution.

Rhythm type	Records <sup>a</sup>	No Shock	Undecided
		ASY	nASY
<b>Shockable</b>			
Coarse VF	198 (565)	0	565
Rapid VT	119 (347)	0	347
<b>Non-shockable</b>			
NSR	374 (1333)	0	1333
SVT	163 (586)	0	586
AF, SB, blocks, idioventricular, PVC	160 (596)	23	573
Asystole	256 (867)	862	5

<sup>a</sup> The number of 3.2 s segments is indicated in parenthesis.

**Table 4.3:** Partial classification of the *Asystole algorithm* for the development database. At this stage a segment is either classified as ASY, or needs to be further processed. The 23 segments from non-shockable rhythms classified as ASY correspond to either IV rhythms (22) or SB (1).

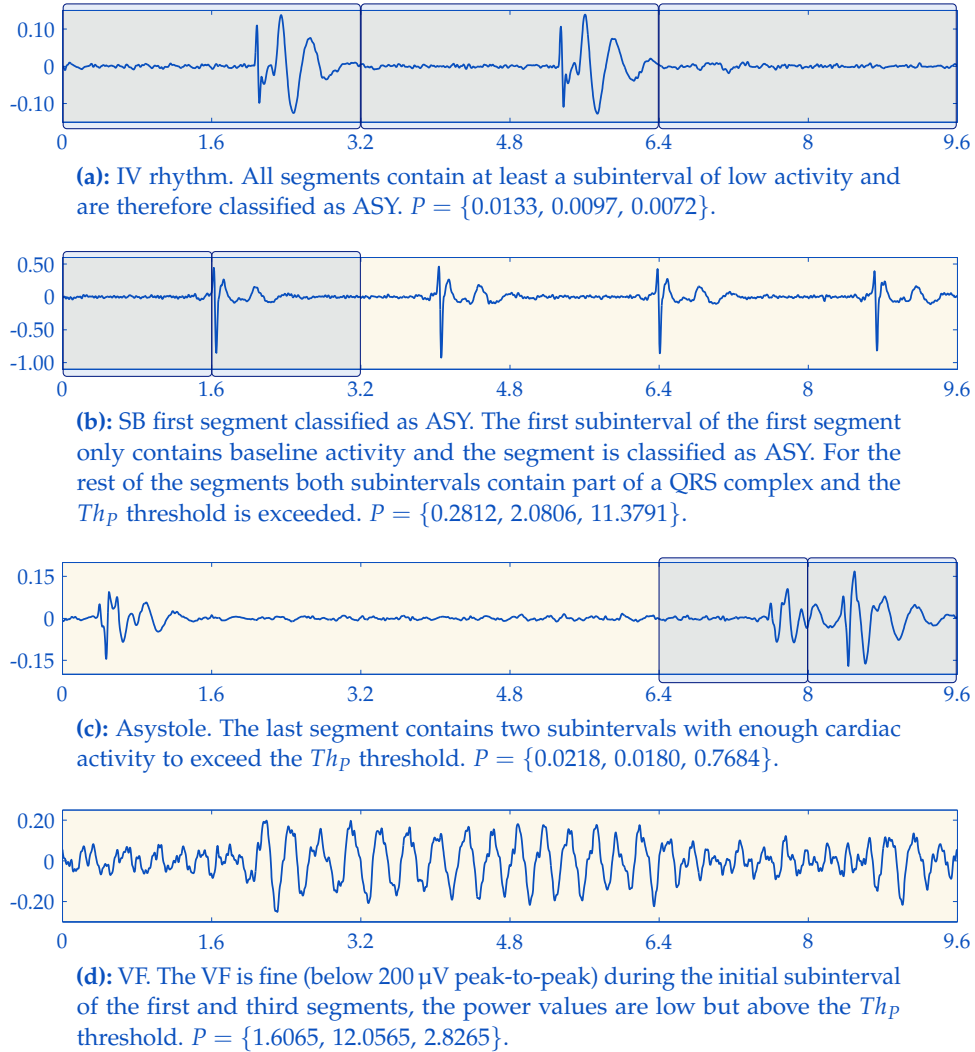


**Figure 4.3:** Examples of borderline rhythms for the *Asystole algorithm*. The figures show  $\hat{x}_{ecg}(n)$  in mV as a function of  $t = nT_s$  in s. The tick marks in the time axis mark the limits between the 1.6 s subintervals.

Table 4.2 shows the values of  $P$  power parameter obtained in the development database. Asystole is well separated from the shockable rhythms (the  $P_{99.5}$  percentile for asystole is smaller than the  $P_{0.5}$  percentile for rapid VT or coarse VF), although there is a slight overlap with a few non-shockable rhythms (slow bradycardias or IV rhythms). Table 4.3 shows the partial classification of the *Asystole algorithm*. It is possible to identify 99.4% (862/867)

of the segments from the asystolic rhythms while avoiding misclassifying a single segment of the shockable rhythms. The 23 non-shockable segments identified as ASY either correspond to IV rhythms (22/23) or to slow bradychardias (1/23). A discussion of some borderline rhythms or segments of rhythms for the *Asystole algorithm* is shown in Figure 4.3.

### 4.3 QRS algorithm

The objective of the *QRS algorithm* is to identify the presence of QRS complexes in the ECG segment. The algorithm is designed to be more accurate for narrow QRS complexes because they are usually associated with pulsed rhythms. In any case, and although there exists no way to certify the presence of pulse from a single lead ECG, lethal ventricular arrhythmias do not present narrow QRS complexes. Identifying such complexes serves to discard many rhythm types from being shockable.

Figure 4.4 shows the block diagram of the *QRS algorithm*. The algorithm consists of two phases: a feature extraction phase from three different signal analysis domains and a decision algorithm

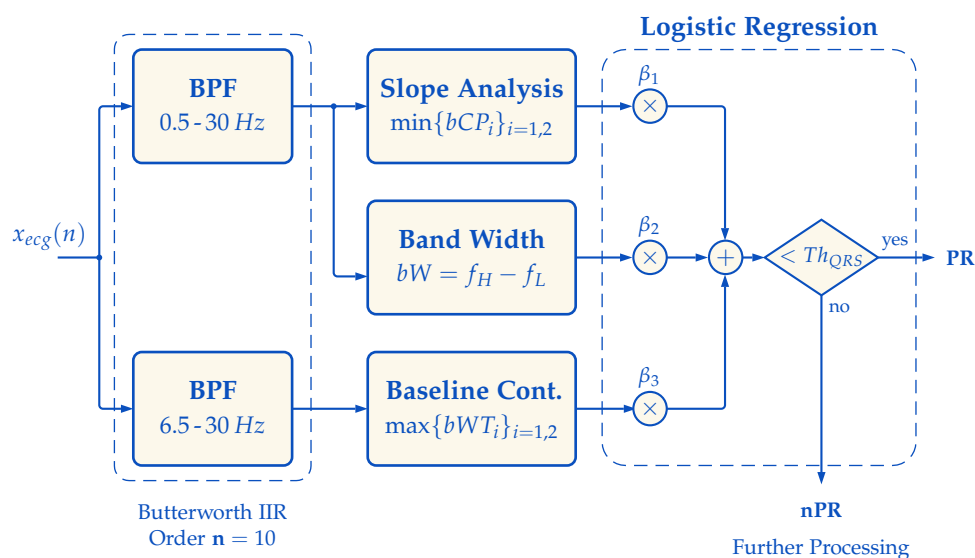


**Figure 4.4:** Block diagram of the *QRS algorithm*. The algorithm starts by calculating three features:  $bCP$  in the slope domain,  $bW$  in the frequency domain and  $bWT$  in the time domain. These features are then optimally combined to detect pulsed rhythms, using a logistic regression classifier.

based on an optimal combination of those features to detect pulsed rhythms.

The *QRS algorithm* analyzes the ECG segment in three different domains: slope, frequency and time. For each domain, the analysis starts with a preprocessing BPF to obtain  $\hat{x}_{ecg}(n)$ , the preprocessed ECG segment. The low cutoff frequency of the filters was independently adjusted to maximize the discriminative power of each feature. In the following subsections we describe the analysis domain and the basic principles behind each of the discrimination features.

#### 4.3.1 Slope domain: *bCP* parameter

In a normal sinus rhythm the ECG varies slowly most of the time, during QRS complexes however the ECG changes very rapidly. These differences in the rate of variation of the ECG have been extensively exploited to identify QRS complexes in the normal ECG.<sup>89</sup> In our analysis we are not interested in locating QRS complexes within the normal ECG but rather in quantifying the differences between non-shockable rhythms with QRS complexes and rhythms without QRS complexes, an indication of a possible shockable rhythm. We have defined a new parameter to discriminate these two broad classes of rhythms, based on the analysis of the ECG in the slope domain.

The analysis starts by estimating the slope of the ECG as the first difference of the preprocessed ECG. Since we are only interested in the magnitude of the variation, the first difference is squared to obtain  $x_d(n)$ :

$$x_d(n) = (\hat{x}_{ecg}(n+1) - \hat{x}_{ecg}(n))^2 \quad n = 1, \dots, N-1. \quad (4.3)$$

Then,  $x_d(n)$  is normalized to amplitude one,

$$\bar{x}_d(n) = \frac{x_d(n)}{\max\{x_d\}}. \quad (4.4)$$

The differences in the amplitudes of  $\bar{x}_d(n)$  are large for ECG segments with QRS complexes, with peaks during QRS complexes and valleys for the slow varying intervals of the ECG. Conversely, shockable rhythms with no QRS complexes present more evenly distributed values of  $\bar{x}_d(n)$ . Figure 4.5 shows the characteristic  $\bar{x}_d(n)$  waveforms for ECG segments with and without QRS complexes.

An adequate way to quantify the differences in slope between rhythms with and without QRS complexes is to evaluate the

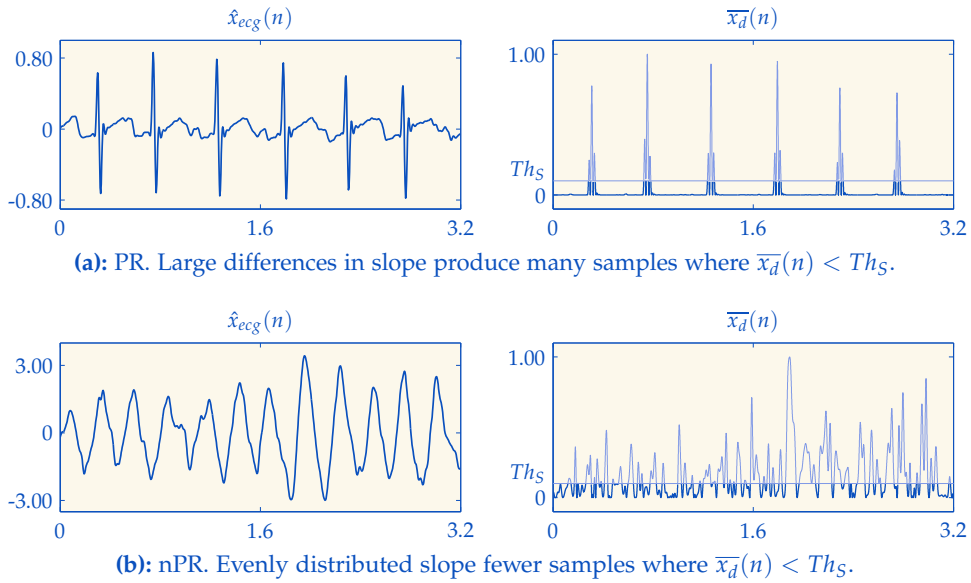


**Figure 4.5:** Differences in the distribution of the slope,  $\bar{x}_d(n)$ , between PR and nPR ECG segments.

proportion of time  $\bar{x}_d(n)$  is below a threshold  $Th_S$ , or equivalently the proportion of samples below the threshold,

$$bCP = P(\bar{x}_d(n) < Th_S) \quad (4.5)$$

Following the procedure described in Section 4.2 for the *Asystole algorithm*, the 3.2 s ECG segment is divided in two 1.6 s subintervals, and  $bCP$  is evaluated for both subintervals. The ECG segment is assigned the smallest of the two values. In this way both subintervals must contain at least a QRS complex to suspect a PR, as shown in Figure 4.6. Slow pulsed rhythms such as bradycardias might not meet this criterion, however these segments are classified as ASY (non-shockable) by the *Asystole algorithm* and do not pose a problem for the shock/noshock diagnosis. Furthermore, at this stage a non-shockable segment misclassified as nPR is not yet assigned a shock diagnosis, while a shockable segment classified as PR is assigned an erroneous non-shockable diagnosis (see Figure 4.1).

#### 4.3.2 Frequency domain: $bW$ parameter

The frequency domain has been frequently proposed to identify ventricular arrhythmias, either as an standalone domain<sup>88,19</sup> or in combination with features extracted from other domains,<sup>71</sup> for

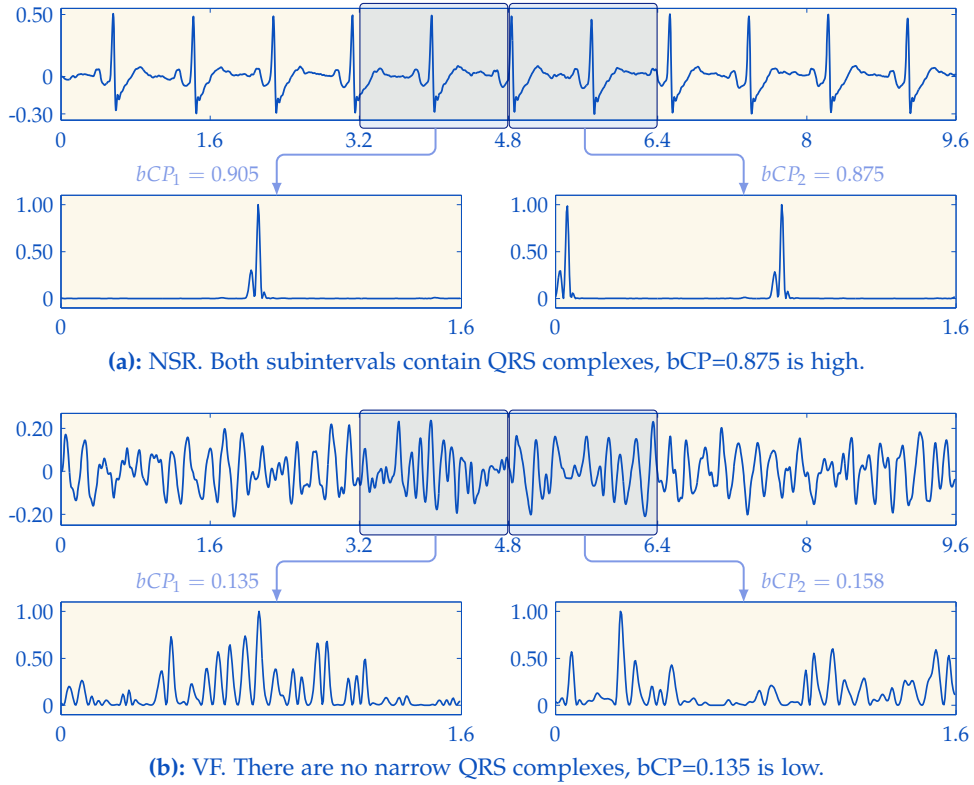


**Figure 4.6:** Analysis in the slope domain. The parameter  $bCP$  parameter is evaluated in subwindows of 1.6s duration, the ECG segment is then assigned the smallest of both values; i. e., both subintervals must contain QRS complexes to suspect a PR.

a thorough account see Section 2.1.1. In particular, features like the VF leakage<sup>88</sup> or  $A_2$ <sup>19</sup> have been shown to partially discriminate ventricular rhythms on pediatric and adult arrhythmias.<sup>70,12</sup> Both these features measure the concentration of the ECG power around the dominant frequency (DF)<sup>†</sup> using two very different approaches. Our frequency domain analysis is based on the work by Barro et al.,<sup>19</sup> although we parametrize the information in a physically more meaningful way by assigning a bandwidth to each ECG segment.

The analysis in the frequency domain starts by computing an estimate of  $P_{\hat{x}\hat{x}}(f)$ , the power spectral density of the ECG segment. The preprocessed ECG segment is first Hamming windowed and then  $\hat{X}_{ecg}(f)$  is computed, as its FFT zero-padded to 4096 points.

<sup>†</sup> The frequency at which the power spectral density is at its maximum.

$P_{\hat{x}\hat{x}}(f)$  is estimated as the square of the amplitude of the FFT, normalized to a unit area under the curve:

$$P_{\hat{x}\hat{x}}(f) = \frac{|\hat{X}_{ecg}(f)|^2}{\sum_{f=0}^{f_s/2} |\hat{X}_{ecg}(f)|^2}. \quad (4.6)$$

We then define the high and low frequencies ( $f_H$  and  $f_L$ ) which delimit the center frequency band that contains a proportion  $\alpha$  of the power of the ECG segment:

$$\frac{1 + \alpha}{2} = \sum_{f=0}^{f_H} P_{\hat{x}\hat{x}}(f) \quad \text{and} \quad \frac{1 - \alpha}{2} = \sum_{f=0}^{f_L} P_{\hat{x}\hat{x}}(f), \quad (4.7)$$

a simple definition of the bandwidth follows:

$$bW = f_H - f_L. \quad (4.8)$$

These frequencies and the  $bW$  they delimit are shown in Figure 4.7 for a segment with QRS complexes and for a shockable segment.

The second feature of the *QRS algorithm* is  $bW$ . ECG segments with quasiperiodic and fast changing QRS complexes concentrate their frequency components around the harmonics of the cardiac frequency with major components up to 25 Hz. Ventricular arrhythmias are more sinus like narrow band signals, the energy is concentrated around the DF and most components are

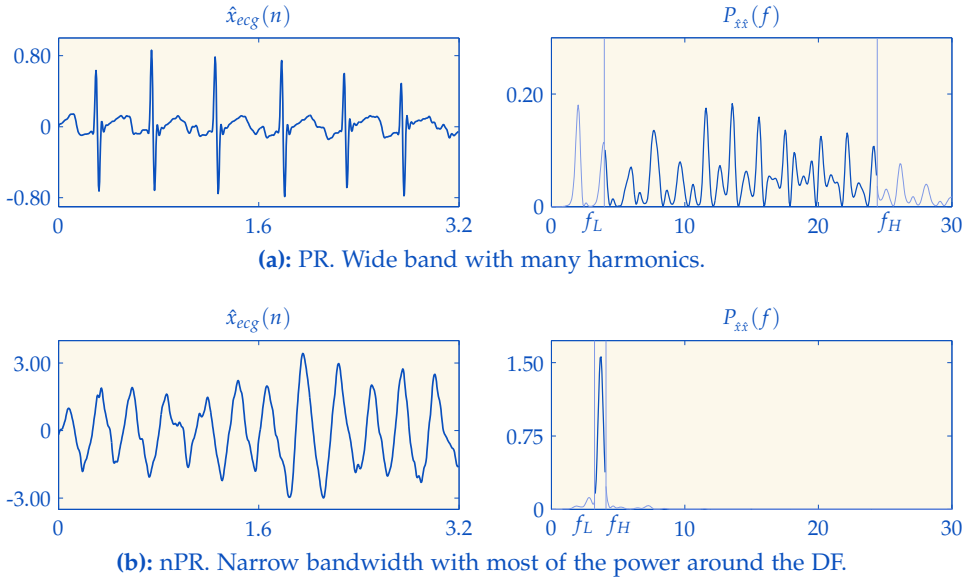
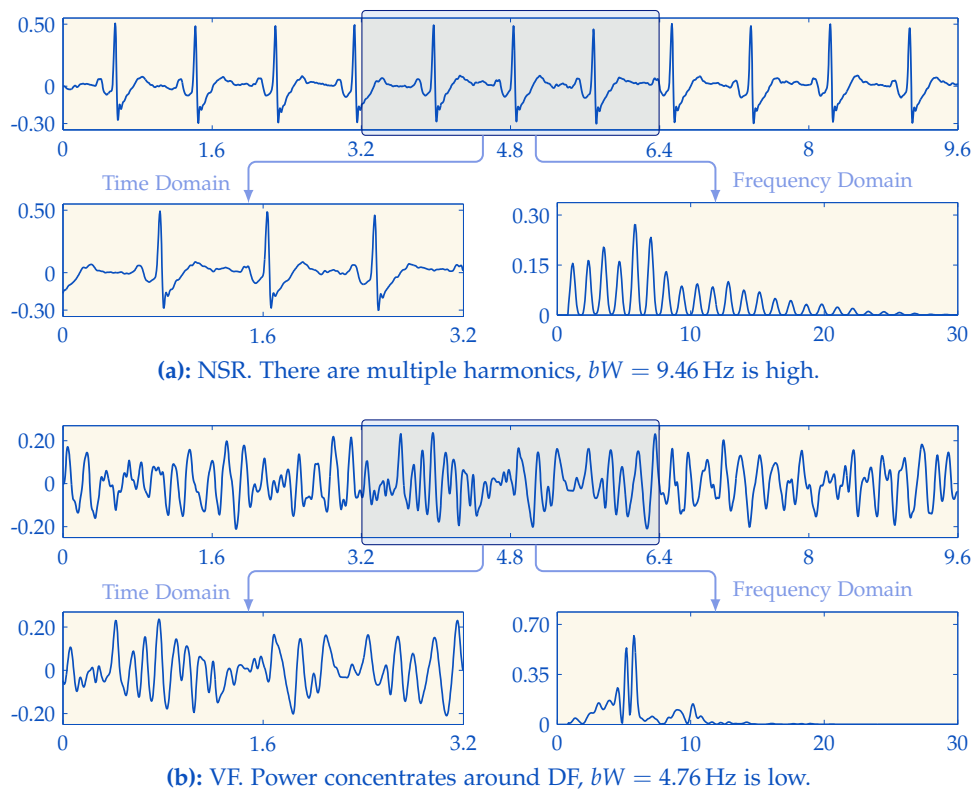


Figure 4.7: Differences in bandwidth between PR and nPR ECG segments.





**Figure 4.8:** Analysis in the frequency domain. The parameter  $bW$  is calculated for the whole 3.2 s segment.

under 10 Hz. Figure 4.8 graphically illustrates these differences and shows that this parameter, unlike those from the slope and time domains, is calculated for the whole 3.2 s segment.

### 4.3.3 Time domain: $bWT$ parameter

An ECG with well defined QRS complexes normally has large ECG intervals around the baseline or isoelectric line. These intervals shorten as the heart rate increases. Conversely, the proportion of time spent by the ECG around the baseline is low for shockable rhythms because of the fast ventricular activity. This difference between shockable and non-shockable rhythms is related to the presence of QRS complexes and has been previously quantified in terms of the probability density function of the amplitudes of the ECG.<sup>91,113</sup>

The time domain analysis of the ECG described in this section proposes a new feature related to the isoelectric content of the ECG. We are nevertheless not interested in an accurate estimation of the isoelectric content but rather in a feature that discriminates shockable from non-shockable rhythms.

First the ECG is preprocessed using a BPF between 6.5–30 Hz. The unusually large low cutoff frequency was selected to eliminate P and T waves, highlighting the presence of the QRS complex and maximizing the baseline effect. Such a high low cutoff frequency will degrade the waveform of shockable segments because it either exceeds or is close to the DF of shockable arrhythmias. However, suppressing the dominant component produces a noisier signal with a smaller baseline content, thus increasing the discriminative power of the parameter. The effect of the preprocessing filter on the ECG is shown Figure 4.9, for both a PR and a nPR ECG segment.

The preprocessed ECG is then normalized so that the maximum absolute value of the amplitude of  $\hat{x}_{ecg}(n)$  is one,

$$\overline{\hat{x}_{ecg}}(n) = \frac{\hat{x}_{ecg}(n)}{\max\{|\hat{x}_{ecg}|\}}. \quad (4.9)$$

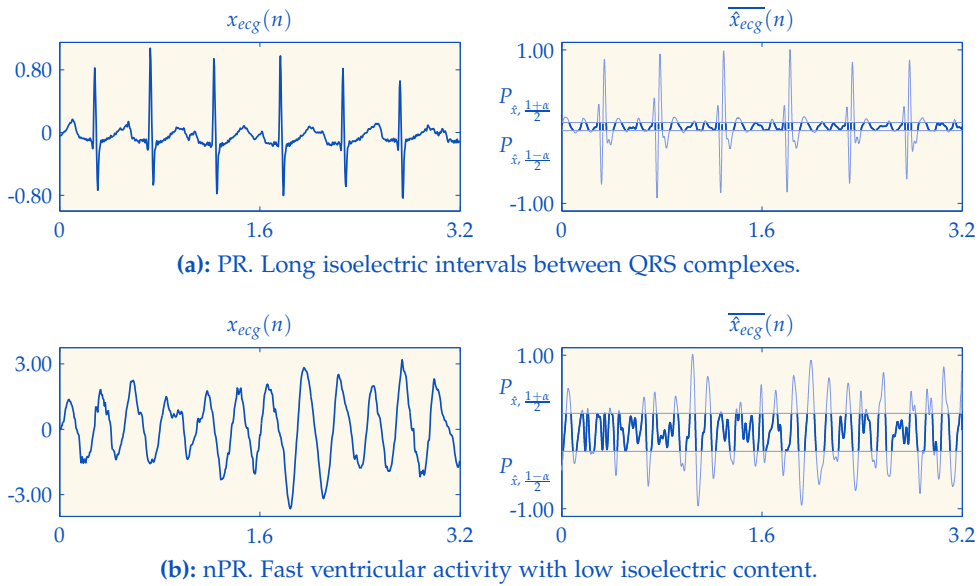


**Figure 4.9:** Differences in the baseline content for PR and nPR segments. The waveform of the normalized preprocessed ECG,  $\overline{\hat{x}_{ecg}}(n)$ , is very distorted because of the large low cutoff frequency of the preprocessing filter.

The time domain parameter  $bWT$  is defined as the center amplitude range that contains a percent  $\alpha$  of the samples of  $\overline{\hat{x}_{ecg}}(n)$ :

$$bWT = P_{\overline{\hat{x}}, 50+\alpha/2} - P_{\overline{\hat{x}}, 50-\alpha/2} \quad (4.10)$$

where  $P_{\overline{\hat{x}}, k}$  is the percentile  $k$  of the distribution of the amplitudes of  $\overline{\hat{x}_{ecg}}(n)$ . These percentiles are shown in Figure 4.9 for a PR and a nPR segment. When the segment has QRS complexes a small amplitude interval contains a large proportion of samples, and  $bWT$  is small. On the other hand, for fast ventricular arrhythmias a large amplitude interval is needed to include a similar proportion of samples and  $bWT$  is large.

The time domain analysis is also performed in 1.6 s subintervals. Following the principle described in the slope domain, a QRS complex needs to be detected in both subintervals, the value of

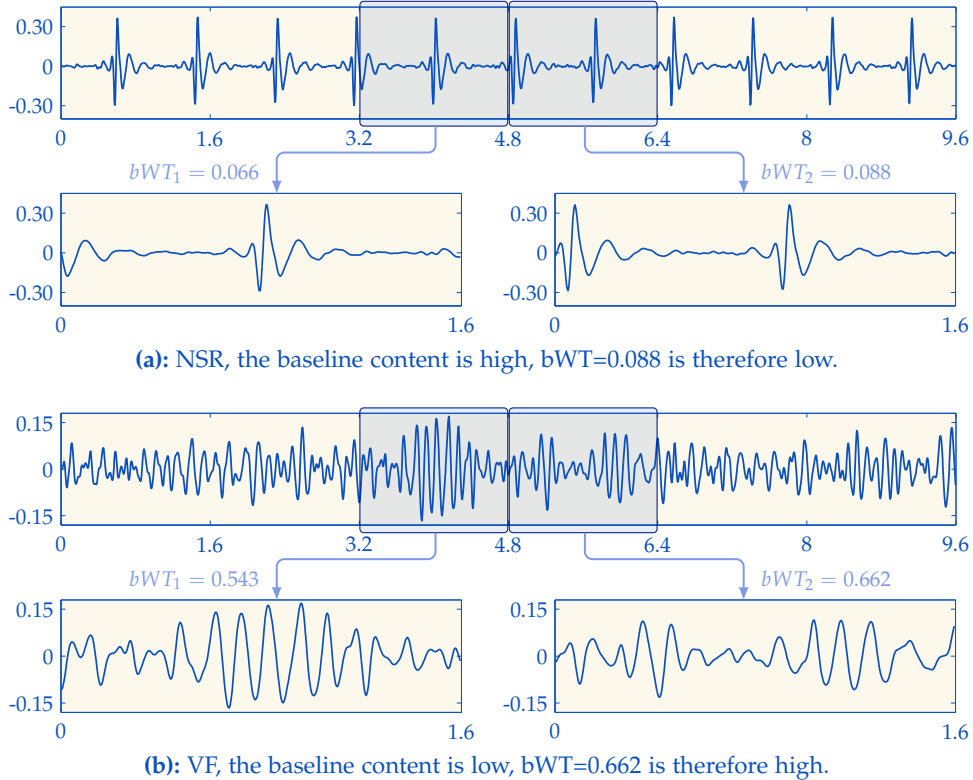


**Figure 4.10:** Analysis in the time domain. The  $bWT$  parameter is evaluated in subwindows of 1.6 s duration, the ECG segment is then assigned the largest of both values; i. e., both subintervals must contain QRS complexes to suspect a PR. The rhythms shown in this figure are those shown in Figure 4.6, the differences in waveform are explained by the different preprocessing filters.

$bWT$  assigned to the segment is therefore the largest of the two values obtained for the subintervals, as indicated in Figure 4.10.

#### 4.3.4 Decision algorithm

The discrimination features derived from the slope ( $bCP$ ), frequency ( $bW$ ) and time ( $bWT$ ) domains were calculated for all the segments in the development database after the rhythms labeled as asystole were excluded. The distribution of the values of the features for the shockable and non-shockable rhythms are shown in Figure 4.11. There is a clear separation between shockable and non-shockable ECG segments for all three features, the overlap of the distributions is therefore low.

The *QRS algorithm* is a binary classifier that discriminates between ECG segments with QRS complexes (PR) and segments without QRS complexes (nPR). The segments from registers classified as non-shockable should be classified as PR and segments from shockable registers as nPR, although at this stage the AED algorithm does not yet decide if a segment is shockable (see Figure 4.1). The discriminative power of each feature and of the combination of features was evaluated using the Bhattacharyya distance.<sup>51</sup> For multivariate gaussian distributions with mean value  $\mu$  and covariance matrix  $\Sigma$ , Bhattacharyya's distance between classes 1 and 2 is:

$$D_B = \frac{1}{8}(\mu_2 - \mu_1)^T \left\{ \frac{\Sigma_1 + \Sigma_2}{2} \right\} (\mu_2 - \mu_1) + \frac{1}{2} \ln \frac{\left| \frac{\Sigma_1 + \Sigma_2}{2} \right|}{\sqrt{|\Sigma_1| |\Sigma_2|}}. \quad (4.11)$$

The  $D_B$  values between the shockable and non-shockable segments of the development database are shown in Table 4.4, which shows that combining the information from the three domains yields the best discriminative power.

The features were linearly combined to fit a multiple logistic regression model.<sup>†</sup> For each segment we defined the following feature vector:

$$\mathbf{x} = \{1, bCP, bW, bWT\}. \quad (4.12)$$

<sup>†</sup> Indirect classification methods such as the k-NN algorithm require longer computation times and additional storage and do not improve the detection results on our databases.

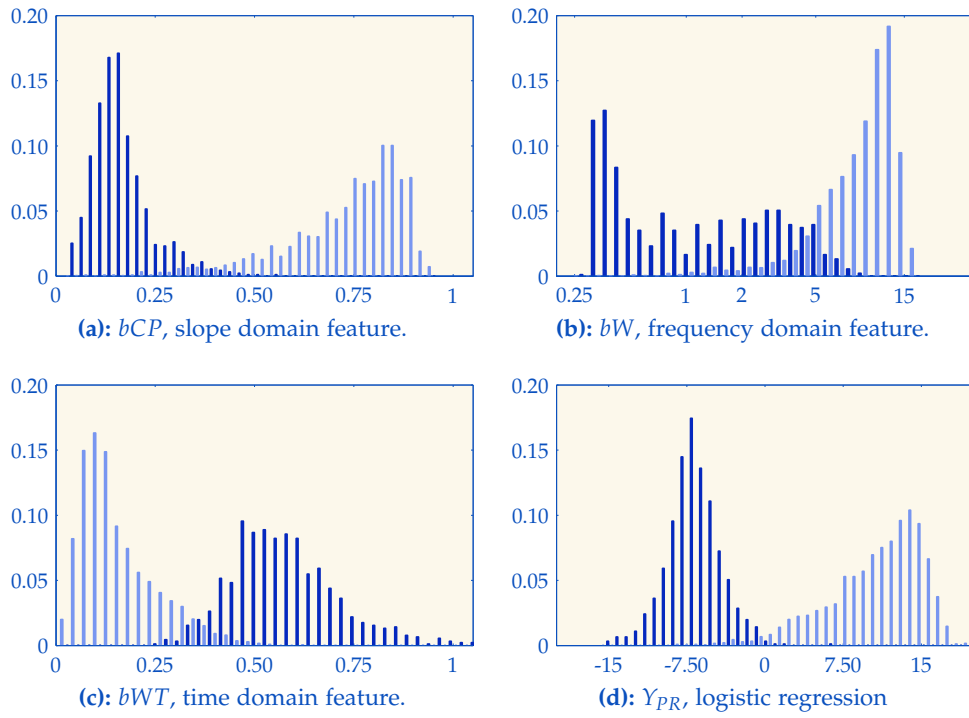


**Figure 4.11:** Normalized histograms of the features that intervene in the *QRS algorithm* for the shockable (■) and non-shockable (▒) segments in the development database. Note that the  $x$  axis for the  $bW$  parameter is in logarithmic scale.

FEATURES	$D_B(\text{PR}, \text{nPR})$
{ $bW$ }	1.232
{ $bWT$ }	1.510
{ $bCP$ }	3.172
{ $bWT, bW$ }	2.303
{ $bCP, bW$ }	2.580
{ $bCP, bWT$ }	3.480
{ $bCP, bWT, bW$ }	3.690

**Table 4.4:** Discriminative power of the features for the *QRS algorithm*. A larger value of  $D_B$  corresponds to a better discriminative power.

Then, the logistic regression model assigns the following probability of being PR to the segment:

$$P_{PR} = \frac{1}{1 + e^{-\beta \mathbf{x}^T}}, \quad (4.13)$$

$$\beta \mathbf{x}^T = \beta_0 + \beta_1 bCP + \beta_2 bW + \beta_3 bWT. \quad (4.14)$$

The decision threshold was set at  $P_{PR} = 0.5$ ; i. e., the segment was classified as PR for  $P_{PR} > 0.5$  or as nPR for  $P_{PR} \leq 0.5$ .<sup>†</sup>

Before the  $\beta$  regression coefficients were determined two sources of bias were eliminated. First, longer registers have more 3.2 s segments and contribute with more feature vectors to the optimization process. Second, the number of non-shockable registers is much larger than the number of shockable registers. These sources of bias were eliminated by assigning the following weights to a register with  $k$  feature vectors:

$$\omega_{PR,k} = \frac{1}{N_{NS} \cdot k} \quad \text{and} \quad \omega_{nPR,k} = \frac{5}{N_S \cdot k}, \quad (4.15)$$

where  $N_{NS}$  and  $N_S$  are the number of non-shockable (excluding asystole) and shockable registers of the development database.

In this manner all registers contribute with the same total weight within their class. The total weights are 1 for the non-shockable class and 5 for shockable class; i. e., the penalty for missing shockable registers is five times higher than for non-shockable registers. A non-shockable segment classified as nPR at this stage can be recovered later but a shockable segment classified as PR is misclassified by the AED algorithm. The weighted instances from the development database were used to determine the regression coefficients in the Waikato Environment for Knowledge Analysis (WEKA) software.<sup>54</sup> The detection threshold depicted in Figure 4.4 is the  $Th_{QRS} = -\beta_0$  regression coefficient.

The histogram for  $Y_{PR} = \beta \mathbf{x}^T$  is shown in Figure 4.11d, and the classification results for the development database are the ones shown in Table 4.5. The proportion of misclassified non-shockable segments excluding asystole ( $31/2515$ ) is larger than the proportion of misclassified shockable segments ( $3/912$ ) because of the strategy adopted for the weights of shockable and non-shockable registers.

Figure 4.12 shows some of the segments misclassified by the *QRS algorithm*. As shown by the two examples of misclassified shockable segments, the algorithm is sensitive to the presence of intervals where the ECG varies rapidly, spiky noise can be interpreted as QRS complexes and the segment is diagnosed as

<sup>†</sup> This is equivalent to PR for  $\beta \mathbf{x}^T > 0$  and nPR for  $\beta \mathbf{x}^T \leq 0$ .

PR. Non-shockable rhythms with very wide QRS complexes might also be misclassified as nPR because both the baseline content and the differences in slope are small. Furthermore, misclassifications are more probable as the heart rate increases because although the bandwidth increases, both the baseline content and bCP decrease. Pediatric SVT frequently presents very high heart rates. These rhythms, which are very regular, will be discriminated from VT by the *SVT/VT algorithm* described in Section 4.5.

Rhythm type	Records <sup>a</sup>	No Shock		Undecided
		ASY	PR	nPR
<b>Shockable</b>				
Coarse VF	198 (565)	0	2	563
Rapid VT	119 (347)	0	1	346
<b>Non-shockable</b>				
NSR	374 (1333)	0	1322	11
SVT	163 (586)	0	574	12
AF, SB, blocks, idioventricular, PVC	160 (596)	23	565	8
Asystole	256 (867)	862	4	1

<sup>a</sup> The number of 3.2 s segments is indicated in parenthesis.

**Table 4.5:** Partial classification of the QRS algorithm for the development database. After the detection of asystole, at this stage a segment can only be identified as PR, otherwise the segment needs to be further processed for a final classification.

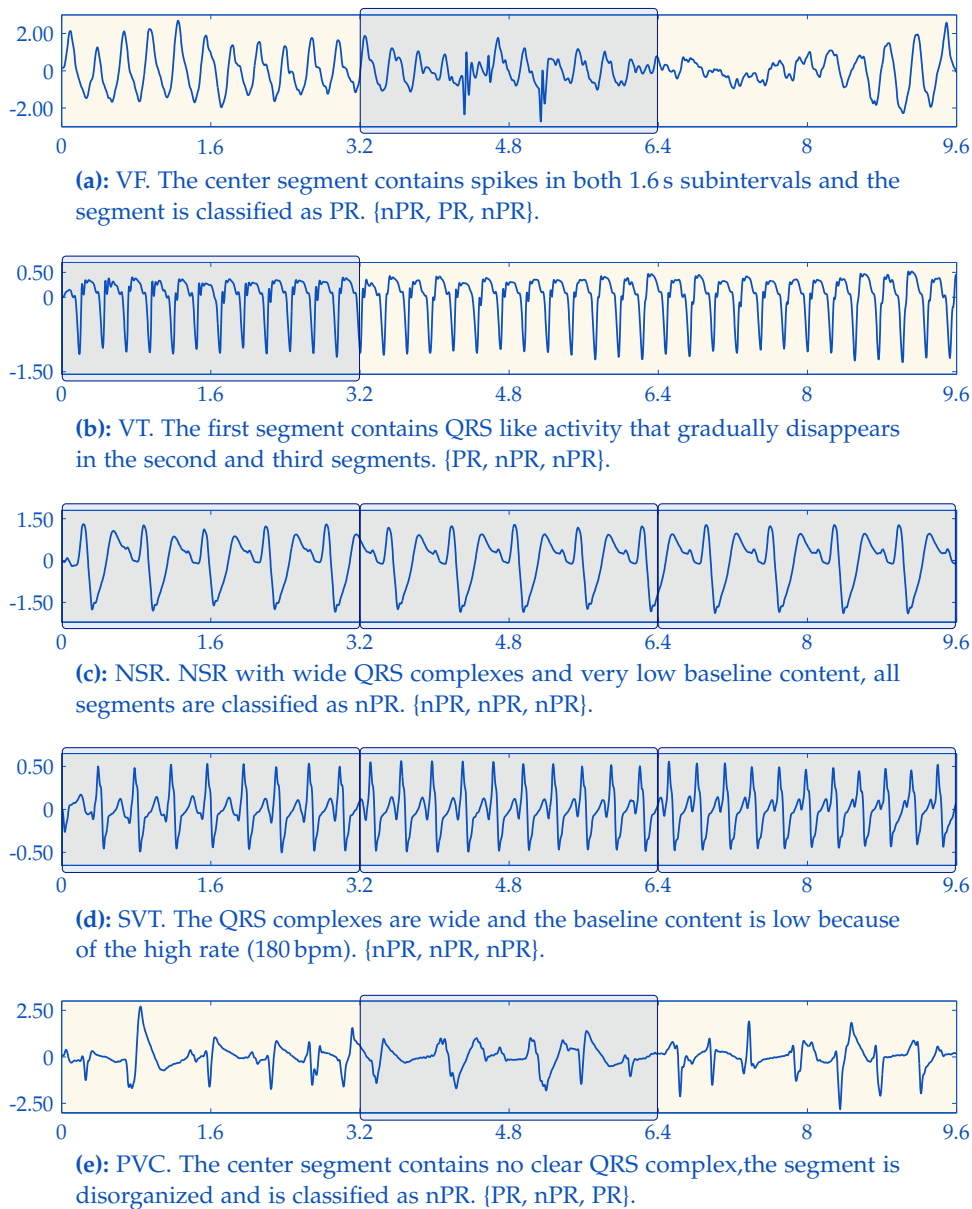


**Figure 4.12:** Examples of registers and segments misclassified by the *QRS algorithm*. The figures show  $\hat{x}_{ecg}(n)$  in mV as a function of  $t = nT_s$  in s for a BPF: 0.5–30 Hz.



## 4.4 Regularity algorithm

The objective of the *Regularity algorithm* is to discriminate between regular and irregular ECG segments within fast ventricular arrhythmias; i. e., to discriminate VT from VF. Although at first glance both segment types correspond to shockable rhythms, VT should only be shocked when its rate is above a threshold.<sup>†</sup> VT must therefore be discriminated from VF and its rate must be calculated before deciding whether or not VT is shockable.

The differences in the ECG waveform between VF and VT are shown in Figure 4.13. Monomorphic VT presents an almost periodic waveform with a very regular ventricular activation sequence.<sup>‡</sup> On the contrary, VF is a disorganized arrhythmia and the electrical ventricular activity varies both in frequency and waveform. The autocorrelation function (ACF) of the ECG has been applied to discriminate VT from VF<sup>57,17,27</sup> precisely because the ACF stresses the underlying organization, the periodicities, of the signal.

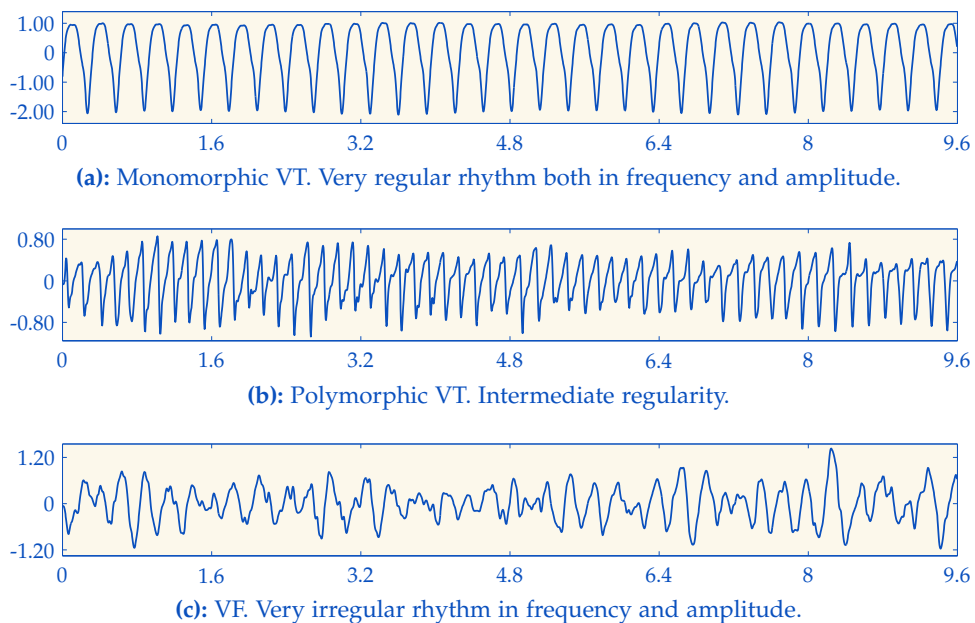


**Figure 4.13:** Examples of shockable rhythms ranging from the very regular monomorphic VT to the most irregular VF.

<sup>†</sup> Although the rate threshold is decided by the AED manufacturer, in an OHCA episode with a pulseless unresponsive patient in VT a shock is a sensible treatment.

<sup>‡</sup> Polymorphic VT occurs when the ventricular activation sequence varies, consequently the surface ECG is less regular.

Figure 4.14 shows the block diagram of the *Regularity algorithm*. The regularity of the ECG segment is assessed through the analysis of the positive peaks of the ACF. For this purpose three new features have been derived, each related to a stronger regularity condition. These features are sequentially tested in a heuristic decision tree to determine when a segment is regular. If any of the regularity conditions fails the ECG segment is classified as VF. When all the conditions are met the segment is regular, although it is not yet classified as VT. Regular segments are further processed by the *SVT/VT algorithm* described in Section 4.5 to recover part of the supraventricular segments misclassified as nPR by the *QRS algorithm*. However, only the segments from the VF and VT registers in the development database were used to optimize the performance of the *Regularity algorithm*.

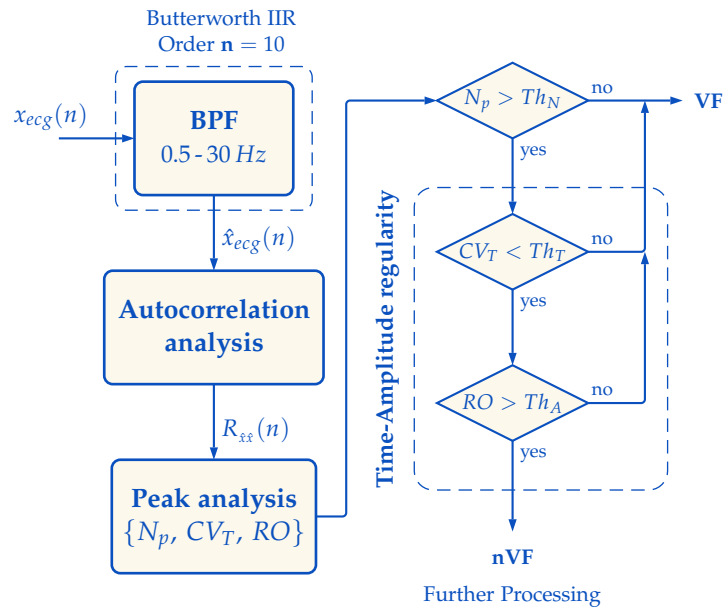


**Figure 4.14:** Block diagram of the *Regularity algorithm*. The regularity of the ECG segment is determined by analyzing three features derived from the analysis of the peaks of the autocorrelation function, the number of peaks ( $N_p$ ) and their variability in time ( $CV_T$ ) and amplitude ( $RO$ ).

#### 4.4.1 Signal analysis using the ACF

Our *Regularity algorithm* based on the ACF was inspired by the work of Chen et al.<sup>27</sup> We have, however, introduced a new set of parameters derived from the analysis of the positive peaks of

the ACF to quantify the differences in regularity between VT and VF more accurately. The analysis starts by computing the biased estimate of the ACF of the preprocessed segment,

$$R_{\hat{x}\hat{x}}(n) = \frac{1}{N} \sum_{m=0}^{N-n-1} \hat{x}_{ecg}(m+n)\hat{x}_{ecg}(m), \quad (4.16)$$

which measures the similarity of  $\hat{x}_{ecg}(m)$  to its lagged copy as a function of the lag. For a periodic signal the ACF has positive peaks separated by the period, because the similarity is maximum when the signal is lagged by an integer number of periods.

First we compute the ACF of the 3.2 s segment for a 0-2.7 s time interval. Then, we determine the positive peaks<sup>†</sup> of the ACF, to analyze the underlying periodicities of the ECG segment. The lag in seconds of the peaks located at lags  $n_k$  are:

$$t_k = T_s \cdot n_k \quad k = 0, \dots, N_p - 1, \quad (4.17)$$

where  $N_p$ <sup>‡</sup> is the number of peaks of the ACF.

$N_p$  is the first discrimination feature of the *Regularity algorithm*. A fast regular rhythm such as VT contains a large number of peaks, for a ventricular frequency of 90 bpm there are at least four periods ( $N_p = 5$ ) in a 2.7 s interval. Consequently when the number of peaks is small the segment is classified as VF, Figure 4.15a shows an example.

#### *Regularity of the periodicity: peak location*

When the number of peaks is large, it is possible to study the regularity of the intervals between consecutive peaks, which are calculated as:

$$T_k = t_{k+1} - t_k \quad k = 0, \dots, N_p - 2. \quad (4.18)$$

For a purely periodic signal all  $T_k$  are equal to the period. An irregular signal with no dominant frequency components has irregularly distributed peaks. To measure the dispersion of the periodicities of the signal we calculate a normalized measure of the dispersion, the coefficient of variation of the  $T_k$ ,

$$CV_T = \frac{\sigma(T_k)}{\mu(T_k)}, \quad (4.19)$$

<sup>†</sup>  $R_{\hat{x}\hat{x}}(n)$  must be above a positive threshold to detect a peak.

<sup>‡</sup>  $N_p \geq 1$  because there is always a peak at the origin

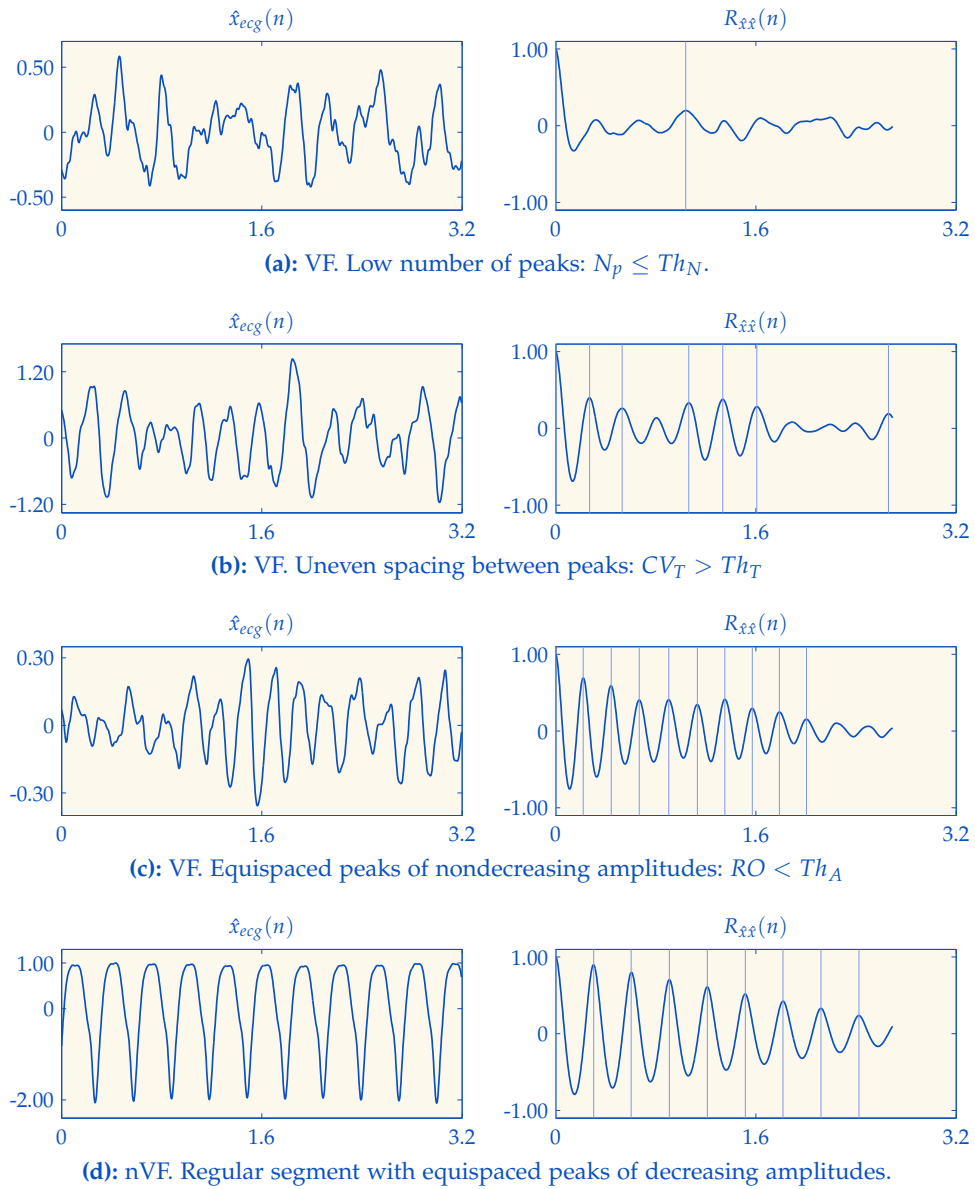


**Figure 4.15:** Possible cases for the analysis of the regularity of the positive peaks of the autocorrelation function.

where  $\mu$  and  $\sigma$  stand for the mean value and the standard deviation respectively. Segments with an irregular peak separation have large values of  $CV_T$  and are classified as VF, Figure 4.15b shows an example. Conversely, segments with low values of  $CV_T$  have a strong underlying periodicity which corresponds to the dominant ventricular rate, which can be estimated as the inverse of the mean value of the period (the dispersion is low):

$$f_c(\text{bpm}) = \frac{60}{\mu(T_k)}. \quad (4.20)$$

*Waveform regularity: amplitude of the peaks*

Finally, we discriminate the subclass of irregular segments that show a strong temporal regularity caused by a dominant underlying frequency component. One such case is shown in Figure 4.15c, where the dominant frequency component results in equispaced peaks of the autocorrelation function although the waveform varies from cycle to cycle. In this case we continue by analyzing the amplitudes of the detected peaks:

$$A_k = R_{\hat{x}\hat{x}}(n_k) \quad k = 0, \dots, N_p - 1. \quad (4.21)$$

For a periodic signal these amplitudes decrease<sup>†</sup> according to the following expression:<sup>27</sup>

$$A_k = \frac{N - n_k}{N} \quad k = 0, \dots, N_p - 1. \quad (4.22)$$

Rather than evaluating how well the amplitudes of the peaks fit Equation 4.22 we test how well the peak ordering follows the expected decreasing order, as suggested by Chen et al.<sup>27</sup> Let  $A_{ok}$  denote the  $A_k$  amplitudes ordered by decreasing value, then

$$A_{ok} = R_{\hat{x}\hat{x}}(n_{ok}) \quad k = 0, \dots, N_p - 1, \quad (4.23)$$

$n_{ok}$  are the lags of the positive peaks ordered by decreasing amplitudes. The sequence of time lags  $t_{ok} = T_s \cdot n_{ok}$  as a function of the index number  $k = 0, \dots, N_p - 1$  is linear for a periodic signal, and the slope of the linear fit is the period.<sup>‡</sup> Conversely, if the cycle duration is constant because of a dominant underlying frequency component, but the waveform varies from cycle to cycle, the amplitudes of the peaks are not necessarily monotonically decreasing, as shown in Figure 4.15c.

<sup>†</sup> The amplitude decreases as the lag increases for the biased estimate of the ACF, see Equation 4.16.

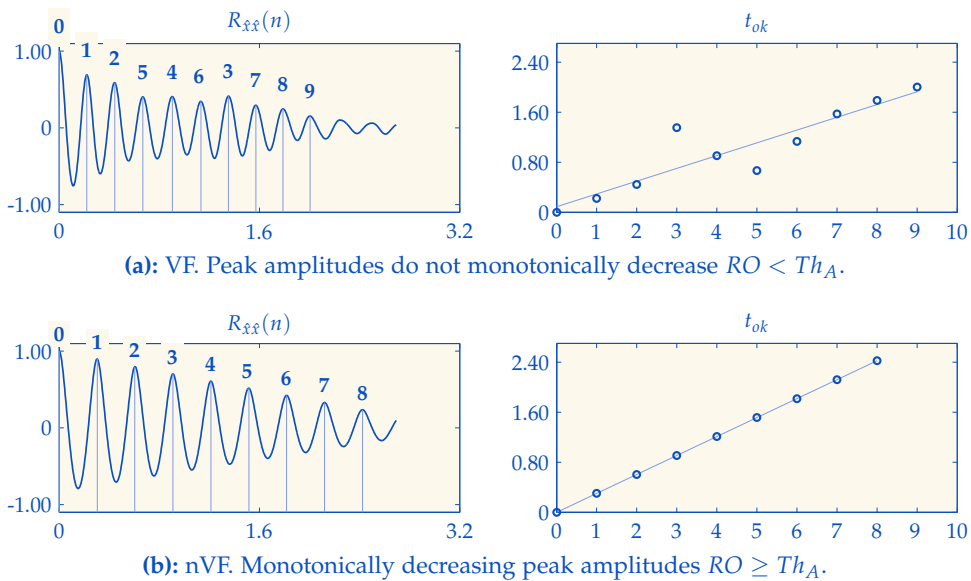
<sup>‡</sup> The interval between consecutive peaks is the period and the amplitude of the peaks decreases according to Equation 4.22.

The last discrimination parameter ( $RO$ ) is the square of the correlation coefficient for the least square linear fit of the independent variable  $y_k = t_{ok}$  to the independent variable  $x_k = k$ . Its value is 1 when the relation is linear and 0 when the variables are independent,

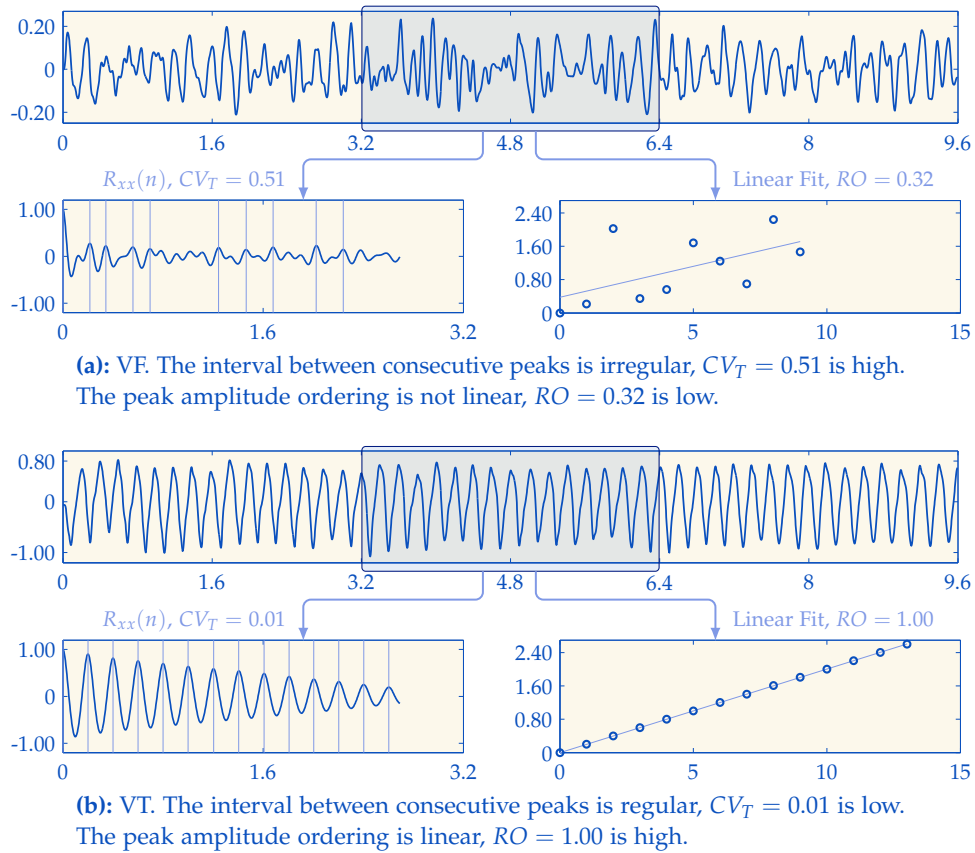
$$RO = r^2 = \frac{[\sum_k (x_k - \mu_x)(y_k - \mu_y)]^2}{\sum_k (x_k - \mu_x)^2 \sum_k (y_k - \mu_y)^2}. \quad (4.24)$$

Figure 4.16 shows the process for the examples of Figure 4.15c and Figure 4.15d. Segments that do not present peaks with monotonically decreasing amplitudes have small values of  $RO$  and are classified as VF, Figure 4.16a shows an example. A segment with a large value of  $RO$ , like the one shown in Figure 4.16b, meets the three regularity conditions of the algorithm, it is assigned a nVF label and it is further processed by the *SVT/VT algorithm*.

Figure 4.17 shows a graphical summary of the analysis process in the autocorrelation domain. Consecutive segments of the rhythm are analyzed to evaluate the regularity of the periodicity (interval between consecutive peaks of the ACF) and waveform (linear fit).



**Figure 4.16:** Least squares fit of  $t_{ok}$  as a function of  $k$  for the segments shown in Figure 4.15c and Figure 4.15d. Both cases have a dominant underlying frequency component ( $CV_T \leq Th_T$ ), the ordering of the amplitudes of the peaks reveals the more irregular nature of VF.



**Figure 4.17:** Analysis in the autocorrelation domain. The ACF is computed for a 0-2.7 s time interval, and the regularity of the peaks is determined both in time ( $CV_T$ ) and waveform ( $RO$ ).

#### 4.4.2 Classification results

The classification results for the development database are shown in Table 4.6. The proportion of misclassified VF and VT segments is large, 17.1% of the VF segments are classified as nVF ( $96/563$ ) and 11.3% of the VT segments are classified as VF ( $39/346$ ). This striking large proportion of misclassification is caused by two reasons: the *Regularity algorithm* is designed to identify clearly irregular segments as VF, and the differences in the approach to rhythm classification between the cardiologists and the AED algorithm.

Long intervals of regular ventricular activity are not rare during VF, these intervals might be sufficiently regular both in periodicity and waveform to produce a nVF diagnosis. The accurate classifi-

Rhythm type	Records <sup>a</sup>	No Shock		Shock	Undecided
		ASY	PR	VF	nVF
<b>Shockable</b>					
Coarse VF	198 (565)	0	2	467	96
Rapid VT	119 (347)	0	1	39	307
<b>Non-shockable</b>					
NSR	374 (1333)	0	1322	0	11
SVT	163 (586)	0	574	0	12
AF, SB, blocks, idioventricular, PVC	160 (596)	23	565	4	4
Asystole	256 (867)	862	4	1	0

<sup>a</sup> The number of 3.2 s segments is indicated in parenthesis.

**Table 4.6:** Partial classification of the *Regularity algorithm* for the development database. At this stage the algorithm analyzes the segments classified as nPR, and classifies as VF those segments that present irregular ventricular activity in either periodicity or waveform. Regular segments are assigned a nVF label and are further processed.

cation of VT segments is also difficult because VT is not always regular in waveform, particularly polymorphic VT. In both cases the shock/noshock decision of the AED algorithm is not jeopardized, fast regular intervals of ventricular activity during VF will later be classified as shockable rapid VT and polymorphic VT is already assigned a shockable VF diagnosis. Figure 4.18 shows several examples of borderline cases for the *Regularity algorithm* that illustrate the difficulties for an accurate VT/VF discrimination when only a 3.2 s segment of a single surface lead is observed.

The large number of misclassified segments is thus explained by the differences in the approach to rhythm classification by the cardiologists and the AED algorithm. The cardiologists observe the full length of the register to classify it as VT or VF, as described in Section 3.1.2. Small intervals of regularity during VF or irregularity during polymorphic VT do not alter the diagnosis for the full register. The AED algorithm, on the contrary, classifies each 3.2 s segment of the register and is therefore much affected by these variations in regularity. This difference is most evident during lethal ventricular arrhythmias because the dynamics of the arrhythmia are more variable.



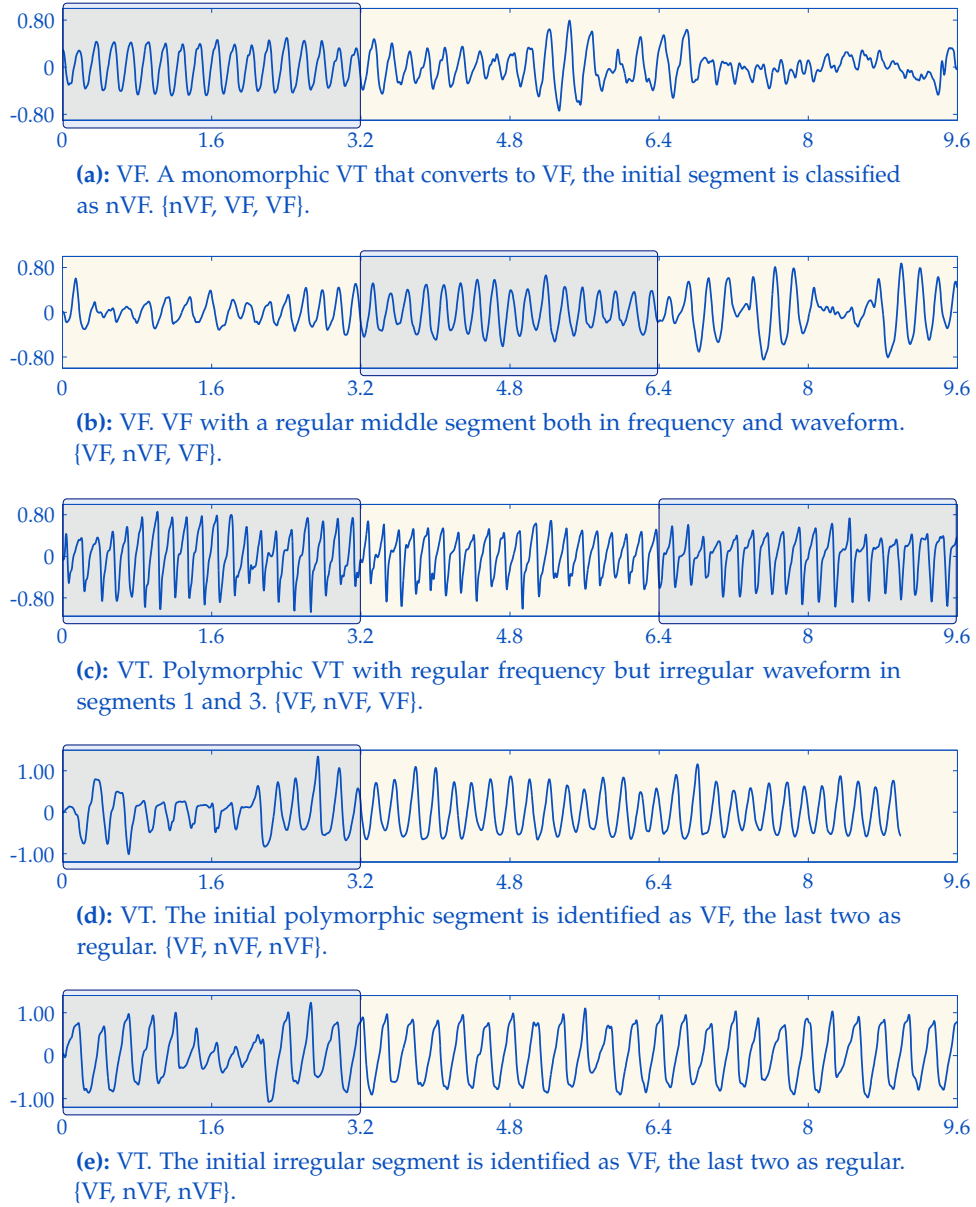


**Figure 4.18:** Examples of borderline cases for the *Regularity algorithm*. Although all the examples are shockable (VF or VT), the regularity of the rhythm might change over time, producing differences in the classification of its segments. Fast regular segments will be classified as rVT (shockable) by the *SVT/VT algorithm*. The figures show  $\hat{x}_{ecg}(n)$  in mV as a function of  $t = nT_s$  in s for a BPF: 0.5–30 Hz.

## 4.5 SVT/VT algorithm

The objective of the *SVT/VT algorithm* is to identify those supraventricular segments for which no QRS complexes were found. Most of these segments are regular, as shown in Table 4.6, and must therefore be discriminated from VT. The highest proportion occurs for SVT, but it is only a 2% (12/586). However, fast pediatric SVT has been shown produce many errors in the shock/noshock diagnosis of AED algorithms,<sup>15</sup> which justifies the protective addition of an algorithm to discriminate SVT from VT. In fact, we have already proposed using a SVT/VT discrimination algorithm to adapt adult AED algorithms for pediatric use,<sup>66,68</sup> the algorithm described in this section is based on that work. Naturally, an adult algorithm adapted for adult and pediatric use is less robust than our shock advice algorithm which was designed for both patient groups together.

Figure 4.19 shows the block diagram of the *SVT/VT algorithm*. The algorithm analyzes the ECG segment in the frequency domain to compute two features that parametrize its spectral power distribution. These features are then optimally combined using a logistic regression classifier to discriminate SVT from VT. As shown in Figure 4.1, the *SVT/VT algorithm* is the final stage of

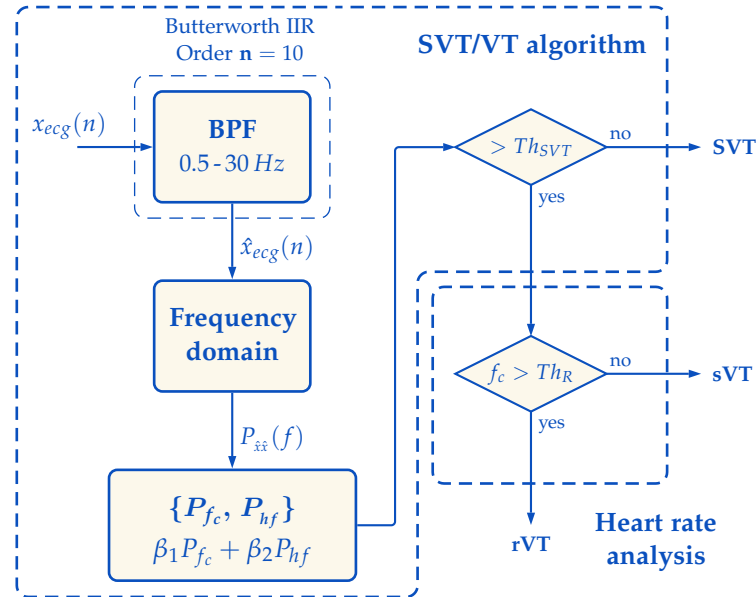


**Figure 4.19:** Block diagram of the *SVT/VT algorithm* followed by the analysis of the heart rate.

the shock advice algorithm. All the segments processed by the algorithm are therefore assigned a diagnosis. Segments classified as SVT are non-shockable. The shock/noshock decision for VT segments depends on the ventricular rate given by Equation 4.20. When the ventricular rate is above  $Th_R$ , the threshold for fast VT, the segment is classified as shockable rapid VT (rVT), otherwise the segment is classified as slow non-shockable VT (sVT).

To optimize the performance of the algorithm, we first selected the segments from the VT and SVT registers in the development database. Then we only considered those identified as regular by the *Regularity algorithm*, 286 SVT and 307 VT segments. This excludes some VT but includes many SVT segments that would be correctly classified as PR by the *QRS algorithm*. By adding these SVT segments we obtain a more robust classifier, otherwise, as shown in Table 4.6, we would only consider 12 SVT segments.

#### 4.5.1 Discrimination features in the frequency domain

Monomorphic VT presents regular ventricular beats that frequently appear as a sinus-like waveform; its power spectral distribution is therefore concentrated around the frequency of the ventricular rate. SVT is also very regular, however its waveform is a more complex combination of a QRS complex, P and T waves, and its power is distributed among the harmonics of the heart rate. Figure 4.20 shows the power spectral distributions for VT and SVT segments, and the graphical description of the two parameters used to quantify the spectral differences between SVT and VT.

The first parameter,  $P_{f_c}$ , measures the relative power content around the cardiac frequency,  $f_c$ . The cardiac frequency in bpm is given by Equation 4.20 because the *SVT/VT algorithm* is applied to temporally regular segments,  $f_c$  (Hz) is then

$$f_c \text{ (Hz)} = \frac{1}{\mu(T_k)}. \quad (4.25)$$

Although we intuitively expect that  $f_c$  will coincide with the DF, this may not be the case when the energy is distributed in many harmonics as shown for the SVT segment of Figure 4.20c.

The relative power content around  $f_c$  is computed for a  $2\Delta f$  bandwidth symmetrically distributed around  $f_c$ ,

$$P_{f_c} = \sum_{f=f_c-\Delta f}^{f_c+\Delta f} P_{\hat{x}\hat{x}}(f), \quad (4.26)$$

where  $P_{\hat{x}\hat{x}}(f)$  is given by Equation 4.6.

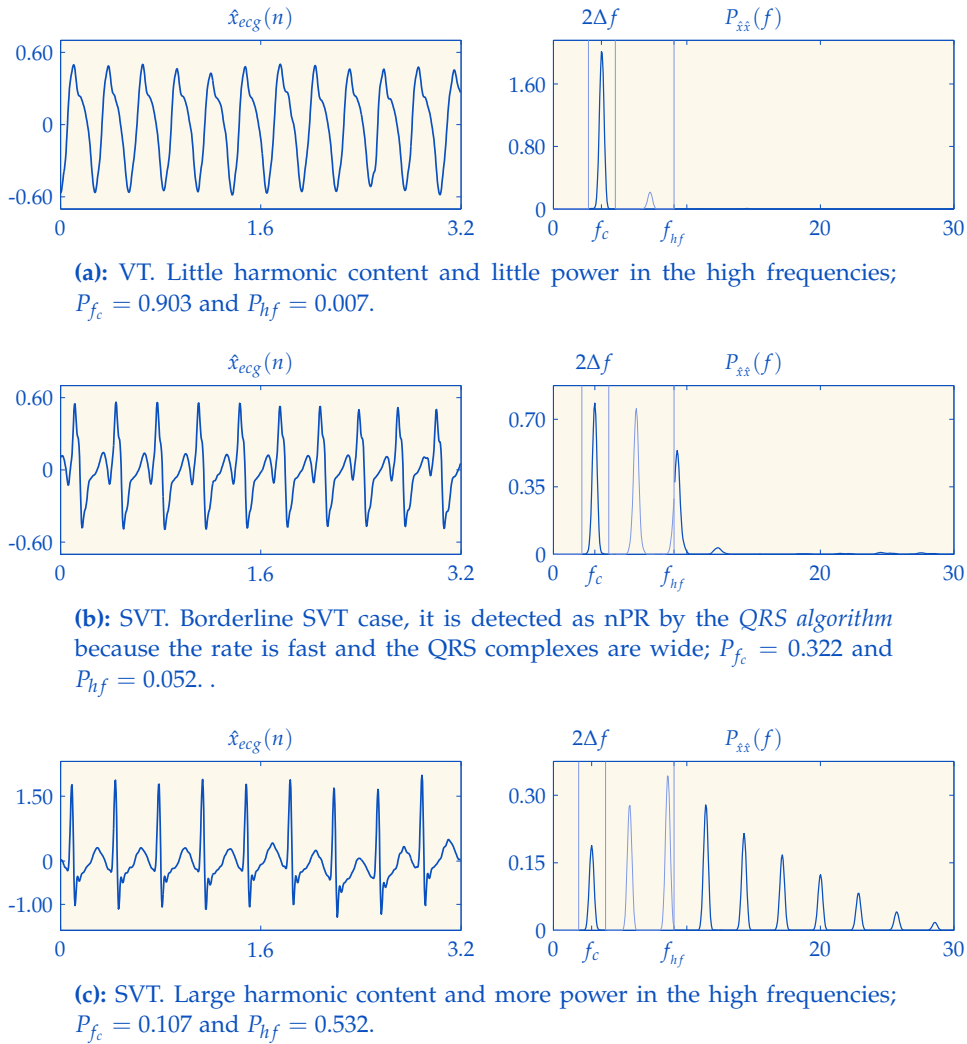


Figure 4.20: Differences in the power spectral density between SVT and VT segments.

The second parameter measures the relative power content of the higher harmonics. For a cutoff frequency  $f_{hf}$  that separates the high and low frequencies, the relative power content of the higher harmonics is:

$$P_{hf} = \sum_{f=f_{hf}}^{30} P_{\hat{x}\hat{x}}(f). \quad (4.27)$$

Figure 4.20a shows how VT segments concentrate most of the power around  $f_c$ , consequently  $P_{f_c}$  is large and  $P_{hf}$  is small. Conversely, Figure 4.20c shows how SVT segments distribute their

power among several harmonics of  $f_c$ ,  $P_{f_c}$  is smaller and  $P_{hf}$  larger. However, discriminating SVT from VT using a single lead becomes more difficult for fast SVT with wide QRS complexes, as shown in Figure 4.20b.

#### 4.5.2 Decision algorithm

The spectral parameters  $\{P_{f_c}, P_{hf}\}$  were computed for all regular SVT and VT segments, the distribution of their values are shown in Figure 4.21. Combining the parameters increases the discriminative power, as demonstrated in Table 4.7a. We therefore repeated the procedure described in Section 4.3.4 to design the following logistic regression classifier:

$$P_{SVT} = \frac{1}{1 + e^{-\beta \mathbf{x}^T}}, \quad (4.28)$$

$$\beta \mathbf{x}^T = Y_{SVT} = \beta_0 + \beta_1 P_{f_c} + \beta_2 P_{hf}. \quad (4.29)$$

The decision threshold was set at  $P_{SVT} = 0.5$ ; i. e., the segment was classified as SVT for  $P_{SVT} > 0.5$  or as VT for  $P_{SVT} \leq 0.5$ .<sup>†</sup>

Again, bias due to the differences in numbers of registers and number of segments per register were avoided by assigning the following weights to a register with  $k$  segments:

$$\omega_{SVT,k} = \frac{1}{N_{SVT} \cdot k} \quad \omega_{VT,k} = \frac{10}{N_{VT} \cdot k} \quad (4.30)$$

where  $N_{SVT}$  and  $N_{VT}$  are the number of SVT and VT registers that have at least a regular segment; i. e., that participate in the design

FEATURES	$D_B(SVT, VT)$	SVT/VT algorithm	
$\{P_{f_c}\}$	2.383	Segments	
$\{P_{hf}\}$	1.826		
$\{P_{f_c}, P_{hf}\}$	2.737		
		SVT	VT
		SVT	277
		VT	1
			306

(a): Feature selection.                      (b): Classification results.

**Table 4.7:** Feature selection and classification results for the SVT/VT algorithm. The number of segments is smaller than the total number of SVT and VT segments in the development database because only regular SVT and VT segments were used to optimize the performance of the algorithm.

<sup>†</sup> this equivalent to SVT for  $Y_{SVT} > 0$  and VT for  $Y_{SVT} \leq 0$ .

of the algorithm. The total weight assigned to the VT segments is 10 times larger than that of the SVT segments because the proportion of SVT segments that the *SVT/VT algorithm* classifies is low (see Table 4.6). The detection threshold for the algorithm is again  $Th_{SVT} = -\beta_0$ .

Figure 4.21a shows the histogram for  $Y_{SVT}$ . The classification results for the development database are shown in Table 4.7b. The number of segments reported in Table 4.7b is smaller than the total number of SVT and VT segments in the development database because the performance of the algorithm was optimized for the subset of regular SVT and VT segments. The proportion of misclassified SVT segments ( $9/286$ ) is larger than the proportion of misclassified VT segments ( $1/307$ ) because of the strategy adopted for the weights of the SVT and VT registers. However, the *SVT/VT algorithm* will only classify a small fraction of the SVT segments shown in Table 4.7b as most SVT segments are correctly identified by the *QRS algorithm*.

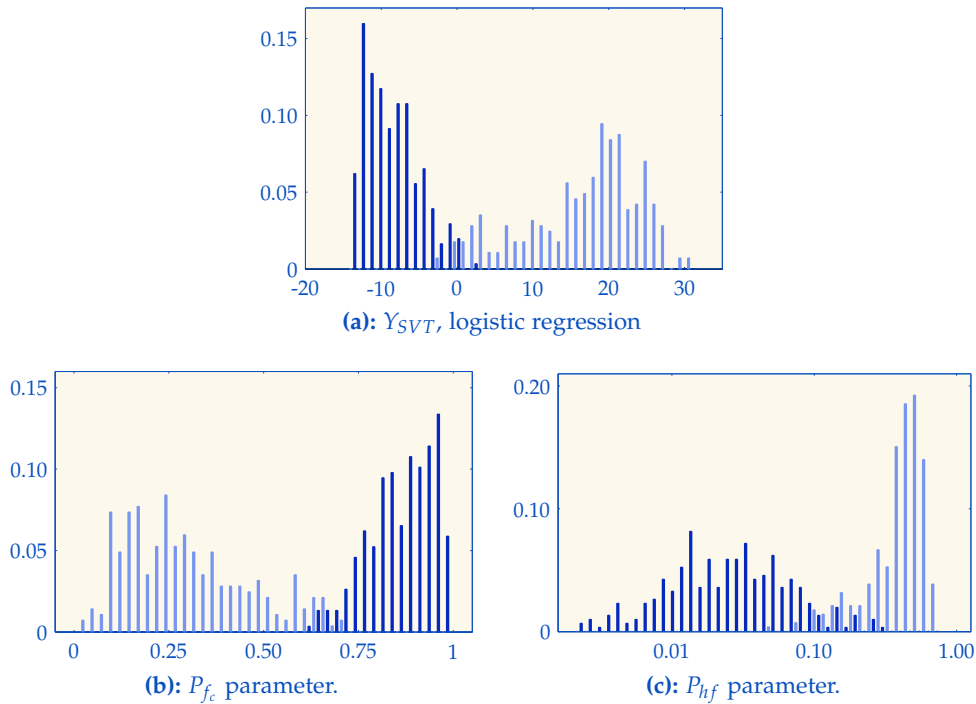


**Figure 4.21:** Normalized histograms of the features that intervene in the *SVT/VT algorithm* for the regular VT (■) and SVT (■) segments of the development database. Note that the  $x$  axis for the  $P_{hf}$  parameter is in logarithmic scale.

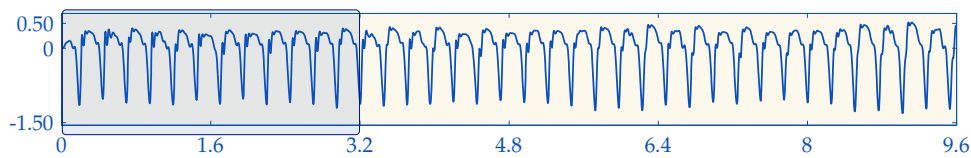
There are borderline cases and incorrectly classified SVT and VT segments, like the ones shown in Figure 4.22. As described in Section 3.1.2, the accurate discrimination between SVT and VT based on a single lead is very troublesome, particularly for high rate pediatric SVT which frequently presents wide QRS complexes.

The final classification results for the development database are shown in Table 4.8. Adding the *SVT/VT algorithm* and checking the ventricular rate for VT segments completes the shock advice algorithm. All segments are classified, both in one of the segment types described in Table 4.1 and as either shockable or non-shockable. The shock/noshock decision for the VT segments depends on the heart rate given by Equation 4.20, consequently the 13 non-shockable segments classified as sVT by the algorithm have a correct no shock diagnosis although they are wrongly identified as VT. A thorough discussion of the classification results for the test database is done in Section 4.6, however the results shown in Table 4.8 for the development database are well above AHA criteria. The shock advice algorithm incorrectly classifies only  $8/912 = 0.9\%$  shockable,  $4/2515 = 0.2\%$  non-shockable and  $1/867 = 0.1\%$  asystole segments.

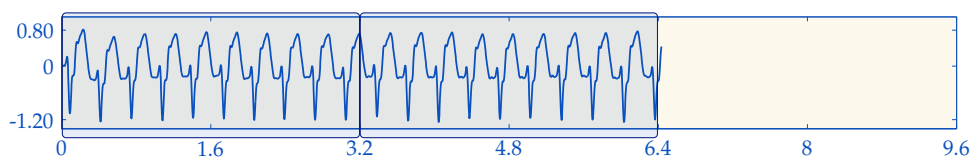
Rhythm type	Records <sup>a</sup>	No Shock				Shock	
		ASY	PR	SVT	sVT	rVT	VF
<b>Shockable</b>							
Coarse VF	198 (565)	0	2	1	3	92	467
Rapid VT	119 (347)	0	1	0	1	306	39
<b>Non-shockable</b>							
NSR	374 (1333)	0	1322	6	5	0	0
SVT	163 (586)	0	574	8	4	0	0
AF, SB, blocks, idioventricular, PVC	160 (596)	23	565	0	4	0	4
Asystole	256 (867)	862	4	0	0	0	1

<sup>a</sup> The number of 3.2 s segments is indicated in parenthesis.

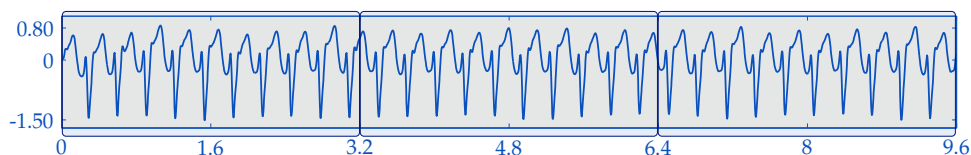
**Table 4.8:** Final classification results of the segments in the development database. The highlighted segments are those classified by the *SVT/VT algorithm*, the last block of the shock advice algorithm.



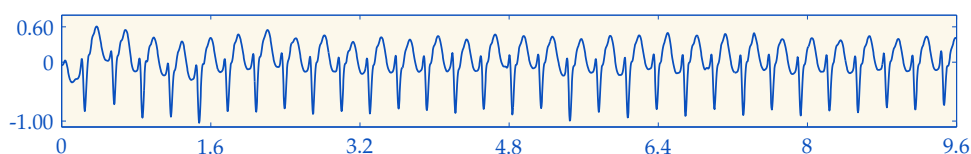
**(a): VT.** The first segment is misclassified as SVT, the first segment contains high frequency components that gradually disappear. This segment however is classified as PR (see Figure 4.12b).  $Y_{SVT} = \{0.65, -0.50, -1.44\}$ .



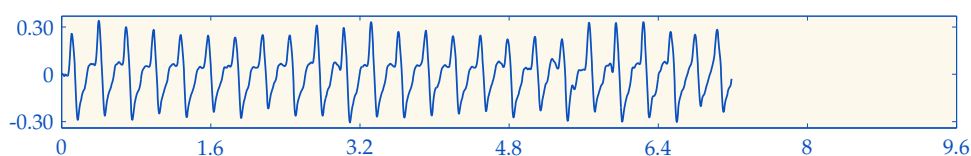
**(b): SVT.** All segments are misclassified as VT because most of the signal power is in the large sinusoidal T waves; i.e., the harmonic content is low.  $Y_{SVT} = \{-1.92, -1.95\}$ .



**(c): SVT.** All segments are misclassified as VT, again most of the signal power is in the large sinusoidal T waves.  $Y_{SVT} = \{-0.39, -0.57, -0.54\}$ .



**(d): SVT.** Large T waves, although their power content gradually decreases. All segments are correctly identified.  $Y_{SVT} = \{0.13, 0.81, 1.36\}$ .



**(e): SVT.** Wide QRS complex tachycardia, most of the power is in the low frequencies. All segments are correctly identified.  $Y_{SVT} = \{0.15, 0.89\}$ .

**Figure 4.22:** Examples of misclassified (a-c) and borderline (d-e) segments for the SVT/VT algorithm. The figures show  $\hat{x}_{ecg}(n)$  in mV as a function of  $t = nT_s$  in s for a BPF: 0.5–30 Hz.



## 4.6 Classification results

This section presents and discusses the classification results for the AED shock advice algorithm on the development and test databases described in Section 3.1.5. It starts analyzing the classification of the segments in the different categories assigned by the algorithm. Then, the shock/noshock classification results are presented for the segments and the registers, and compared with the AHA specifications compiled in Table 1.3. Finally, the shock/noshock decision results are broken down into pediatric and adult patients. The section concludes with a graphical analysis of some examples of misclassified segments and registers.

### 4.6.1 Segment type classification

The AED shock advice algorithm classifies each 3.2s segment in one of the categories described in Table 4.1. The classification follows the steps shown in Figure 4.1, the flow diagram of the algorithm. We can trace the classification process for a segment once we know the category the algorithm assigns to that segment. These data are important to identify the strengths and weaknesses of the shock advice algorithm and its sub-algorithms. The categories assigned by the algorithm to the segments of the development database are compiled in Table 4.9a<sup>†</sup> and to the segments of the test databases in Table 4.9b.

The results for the test database show that most of the errors for the non-shockable segments occur for SVT classified as rVT, and for other non-shockable rhythms (particularly PVC and IV rhythms) classified as VF. The *QRS algorithm* fails to identify these segments as PR when they present wide QRS complexes, furthermore the misclassifications are more frequent for rhythms with higher heart rates like SVT. These wrongly classified segments are suspected to be ventricular, and are not recovered by the *SVT/VT algorithm*. Additionally, there are 21 non-shockable segments classified as non-shockable VT (sVT).

Most errors for the shockable segments are caused by narrow complex VT identified as PR by the *QRS algorithm* and to borderline cases of the *SVT/VT algorithm*.

<sup>†</sup> In the preceding sections we have unfolded the results for the development database in steps as each sub-algorithm was added to the shock advice algorithm.

Rhythm type	Records <sup>a</sup>	No Shock				Shock	
		ASY	PR	SVT	sVT	rVT	VF
<b>Shockable</b>							
Coarse VF	198 (565)	0	2	1	3	92	467
Rapid VT	119 (347)	0	1	0	1	306	39
<b>Non-shockable</b>							
NSR	374 (1333)	0	1322	6	5	0	0
SVT	163 (586)	0	574	8	4	0	0
AF, SB, blocks, idioventricular, PVC	160 (596)	23	565	0	4	0	4
Asystole	256 (867)	862	4	0	0	0	1

<sup>a</sup> The number of 3.2s segments is indicated in parenthesis.

(a): Classification of the segments in the development database.

Rhythm type	Records <sup>a</sup>	No Shock				Shock	
		ASY	PR	SVT	sVT	rVT	VF
<b>Shockable</b>							
Coarse VF	234 (646)	0	1	2	1	95	547
Rapid VT	147 (445)	0	7	2	0	389	47
<b>Non-shockable</b>							
NSR	458 (1620)	0	1613	2	3	0	2
SVT	248 (843)	0	794	27	14	7	1
AF, SB, blocks, idioventricular, PVC	169 (635)	24	593	5	3	0	10
Asystole	256 (860)	856	3	0	1	0	0

<sup>a</sup> The number of 3.2s segments is indicated in parenthesis.

(b): Classification of the segments in the test database.

**Table 4.9:** Detailed classification of the ECG segments of the development and test databases. The definition of the types of classification is given in Table 4.1, and the flow diagram of the algorithm with the possible classification outputs is shown in Figure 4.1.

### 4.6.2 Shock/Noshock classification

Although the internal classification process is useful to assess and understand how the algorithm works, the only relevant diagnosis of an AED shock advice algorithm is the shock/noshock decision. The algorithm classifies each segment in a category which, as stated in Table 4.1, is linked to a shock/noshock diagnosis. The registers are composed of several 3.2 s segments. Registers were assigned a shock/noshock diagnosis using a majority criterion on the individual shock/noshock classification of three consecutive ECG segments, when available. Shorter registers with two segments were classified as non-shockable if either of the segments was classified as non-shockable.

The performance of a shock advice algorithm is assessed in terms of the contingency table and the performance metrics described in Table 1.2. Each metric measures an important aspect of the algorithm performance. The AHA statement on AED shock advice algorithms, however, only establishes performance goals for two of the metrics defined in Table 1.2: the sensitivity (Se), the proportion of correctly identified shockable events; and the specificity (Sp), the proportion of correctly identified non-shockable events.<sup>80</sup>

The sensitivity and specificity results for the development and test databases are compiled in Table 4.10 for the segments and in Table 4.11 for the registers. The 90% confidence intervals (CI) are computed using the adjusted Wald interval for binomial proportions.<sup>6</sup> The algorithm exceeds the AHA performance goals for all rhythm categories in the test database, in fact the 90% low CI is above the AHA performance goal for all rhythm categories, both for the segments and the registers.

The complete set of performance metrics for the registers in the test and development databases are given in Table 4.12. The metrics include: the sensitivity and specificity for all shockable and non-shockable registers; the accuracy (Acc), the proportion of correctly identified registers; the positive predictive value (PPV), the proportion of correct shock diagnoses; and the negative predictive value (NPV), the proportion of correct no shock diagnoses.

Rhythm type	Segments			AHA goals <sup>80</sup>
	S	NS	Se/Sp (%) <sup>a</sup>	
<b>Shockable</b>				
Coarse VF	559	6	98.9 (97.9-99.5)	> 90 %
Rapid VT	345	2	99.4 (98.2-99.9)	> 75 %
<b>Non-shockable</b>				
NSR	0	1333	100 (99.8-100)	> 99 %
SVT	0	586	100 (99.5-100)	> 95 %
AF, SB, blocks, idioventricular, PVC	4	592	99.3 (98.5-99.7)	> 95 %
Asystole	1	866	99.9 (99.4-100)	> 95 %

<sup>a</sup> 90% CI indicated in parenthesis.

(a): Sensitivity and specificity for the segments of the development database.

Rhythm type	Segments			AHA goals <sup>80</sup>
	S	NS	Se/Sp (%) <sup>a</sup>	
<b>Shockable</b>				
Coarse VF	642	4	99.4 (98.6-99.8)	> 90 %
Rapid VT	436	9	98.0 (96.5-98.9)	> 75 %
<b>Non-shockable</b>				
NSR	2	1618	99.9 (99.6-100)	> 99 %
SVT	8	835	99.1 (98.3-99.5)	> 95 %
AF, SB, blocks, idioventricular, PVC	10	625	98.4 (97.4-99.1)	> 95 %
Asystole	0	860	100 (99.6-100)	> 95 %

<sup>a</sup> 90% CI indicated in parenthesis.

(b): Sensitivity and specificity for the segments of the test database.

**Table 4.10:** Sensitivity and specificity of the shock advice algorithm for the 3.2s segments of the development and test databases. All the low 90% CI exceed the AHA performance goals for all rhythm categories.

Rhythm type	Records			AHA goals <sup>80</sup>
	S	NS	Se/Sp (%) <sup>a</sup>	
<b>Shockable</b>				
Coarse VF	197	1	99.5 (97.6-100)	> 90 %
Rapid VT	118	1	99.2 (96.0-100)	> 75 %
<b>Non-shockable</b>				
NSR	0	374	100 (99.1-100)	> 99 %
SVT	0	163	100 (98.0-100)	> 95 %
AF, SB, blocks, idioventricular, PVC	0	160	100 (98.0-100)	> 95 %
Asystole	0	256	100 (98.7-100)	> 95 %

<sup>a</sup> 90% CI indicated in parenthesis.

(a): Sensitivity and specificity for the registers in the development database.

Rhythm type	Records			AHA goals <sup>80</sup>
	S	NS	Se/Sp (%) <sup>a</sup>	
<b>Shockable</b>				
Coarse VF	233	1	99.6 (97.9-100)	> 90 %
Rapid VT	146	1	99.3 (96.8-100)	> 75 %
<b>Non-shockable</b>				
NSR	0	458	100 (99.3-100)	> 99 %
SVT	2	246	99.2 (97.5-100)	> 95 %
AF, SB, blocks, idioventricular, PVC	1	168	99.4 (97.2-100)	> 95 %
Asystole	0	256	100 (98.7-100)	> 95 %

<sup>a</sup> 90% CI indicated in parenthesis.

(b): Sensitivity and specificity for the registers in the test database.

**Table 4.11:** Sensitivity and specificity of the shock advice algorithm for the registers in the development and test databases. All the low 90% CI exceed the AHA performance goals for all rhythm categories.

Metric	Database <sup>a</sup>		
	Development	Test	Total
<b>Se</b> (%)	99.4 (98.8-99.4)	99.5 (98.8-99.8)	99.7 (99.3-99.9)
<b>Sp</b> (%)	100 (99.8-100)	99.7 (99.5-99.8)	99.9 (99.7-99.9)
<b>Acc</b> (%)	99.8 (99.6-99.8)	99.7 (99.3-99.8)	99.6 (99.2-99.7)
<b>PPV</b> (%)	100 (99.4-100)	99.2 (98.5-99.5)	99.9 (99.8-100)
<b>NPV</b> (%)	99.8 (99.6-99.8)	99.8 (99.6-99.9)	99.8 (99.6-99.9)

<sup>a</sup> 90% CI indicated in parenthesis.

**Table 4.12:** Additional performance metrics for the registers in the test and the development databases. The results are derived from the data in Table 4.11a and Table 4.11b. For a definition of the metrics see Table 1.2.

### 4.6.3 Results for the adult and pediatric patients

One of the design principles of the AED shock advice algorithm is that it is universal; i. e., valid for adult and pediatric patients. To this end, we propose a new design strategy that combines adult and pediatric registers for the development and test phases of the algorithm.

The classification results for the adult and pediatric cases are shown in Table 4.13 for the segments and Table 4.14 for the registers in the test database. All the sensitivities and specificities are above the AHA performance goals for the adult and pediatric patients. However, when the results for the adult and pediatric patients are separately analyzed, the sample sizes are smaller and consequently some of the the low 90% CI are below the AHA performance goals. For instance, there are 145 adult NSR registers in the test database. Although they are all correctly identified as non-shockable, the low 90% CI for the specificity is under 99%, the AHA performance goal for NSR specificity.

Finally, Table 4.15 shows the additional performance metrics for the pediatric and adult registers in the test database.

Rhythm type	Segments			AHA goals <sup>80</sup>
	S	NS	Se/Sp (%) <sup>a</sup>	
Coarse VF	522	3	99.4 (98.5-99.8)	> 90 %
Rapid VT	294	1	99.7 (98.4-100)	> 75 %
<b>Non-shockable</b>				
NSR	2	566	99.6 (98.9-99.9)	> 99 %
SVT	0	185	100 (98.3-100)	> 95 %
AF, SB, blocks, idioventricular, PVC	10	443	97.8 (96.4-98.7)	> 95 %
Asystole	0	860	99.9 (99.7-100)	> 95 %

<sup>a</sup> 90% CI indicated in parenthesis.

**(a):** Sensitivity and specificity for the segments of the adult database.

Rhythm type	Segments			AHA goals <sup>80</sup>
	S	NS	Se/Sp (%) <sup>a</sup>	
<b>Shockable</b>				
Coarse VF	120	1	99.2 (96.1-100)	> 90 %
Rapid VT	142	8	94.7 (90.7-97.1)	> 75 %
<b>Non-shockable</b>				
NSR	0	1052	100 (99.7-100)	> 99 %
SVT	8	650	98.8 (97.8-99.3)	> 95 %
AF, SB, blocks, idioventricular, PVC	0	182	100 (98.2-100)	> 95 %
Asystole	-	-	-	> 95 %

<sup>a</sup> 90% CI indicated in parenthesis.

**(b):** Sensitivity and specificity for the segments of the pediatric database.

**Table 4.13:** Sensitivity and specificity results for the segments of the adult and pediatric patients in the test database. All the low 90% CI exceed the AHA performance goals for all rhythm categories except for adult NSR.

Rhythm type	Records			AHA goals <sup>80</sup>
	S	NS	Se/Sp (%) <sup>a</sup>	
Coarse VF	187	0	100 (98.3-100)	> 90%
Rapid VT	99	0	100 (96.8-100)	> 75%
<b>Non-shockable</b>				
NSR	0	145	100 (97.8-100)	> 99%
SVT	0	44	100 (93.1-100)	> 95%
AF, SB, blocks, idioventricular, PVC	1	114	99.1 (95.9-100)	> 95%
Asystole	0	256	100 (98.7-100)	> 95%

<sup>a</sup> 90% CI indicated in parenthesis.

**(a):** Sensitivity and specificity for the registers in the adult database.

Rhythm type	Records			AHA goals <sup>80</sup>
	S	NS	Se/Sp (%) <sup>a</sup>	
<b>Shockable</b>				
Coarse VF	46	1	97.9 (90.3-99.3)	> 90%
Rapid VT	47	1	97.9 (90.5-99.4)	> 75%
<b>Non-shockable</b>				
NSR	0	313	100 (99.0-100)	> 99%
SVT	2	202	99.0 (96.9-99.8)	> 95%
AF, SB, blocks, idioventricular, PVC	0	54	100 (94.3-100)	> 95%
Asystole	-	-	-	> 95%

<sup>a</sup> 90% CI indicated in parenthesis.

**(b):** Sensitivity and specificity for the registers in the pediatric database.

**Table 4.14:** Sensitivity and specificity results for the registers of the adult and pediatric patients in the test database.



Metric	Test database <sup>a</sup>		
	Adult	Pediatric	Total
Se (%)	100 (99.4-100)	97.9 (95.4-99.1)	99.5 (98.8-99.8)
Sp (%)	99.8 (99.5-99.8)	99.7 (99.2-99.8)	99.7 (99.5-99.8)
Acc (%)	99.9 (99.5-99.9)	99.4 (98.7-99.7)	99.7 (99.3-99.8)
PPV (%)	99.7 (99.1-99.7)	97.9 (95.4-99.1)	99.2 (98.5-99.5)
NPV (%)	100 (99.7-100)	99.7 (99.2-99.8)	99.8 (99.6-99.9)

<sup>a</sup> 90% CI indicated in parenthesis.

**Table 4.15:** Additional performance metrics for the adult and pediatric registers of the test database. The results are derived from the data in Table 4.14a and Table 4.14b.

#### 4.6.4 Graphical examples of classification errors

There are two important causes of classification errors for VF (Figure 4.23): slow but regular intervals of ventricular activity during VF which are misclassified as slow VT (Figure 4.23a) and QRS like activity during VF due to rapid ventricular contractions or spiky noise (Figure 4.23d). Furthermore, for short registers with only one or two 3.2 s segments a single error will result in a misclassified register (Figure 4.23a and Figure 4.23c).

The accurate discrimination between VT and fast SVT with wide QRS complexes using a single lead is very troublesome, particularly for the pediatric case. Most errors are caused by borderline cases of the *QRS algorithm* (only VT) and *SVT/VT algorithm* (SVT and VT), see Figure 4.24 and Figure 4.25. Additionally, correctly identified VT segments with slow ventricular rates are classified as non-shockable slow VT (Figure 4.24a). The converse — SVT segments classified as slow VT — also occurs, although the no shock diagnosis is correct the classification is incorrect (Figure 4.25c).

There are some classification errors for other non-shockable registers with intervals of clear ventricular activity, see Figure 4.26c and Figure 4.26e. Occasionally, PVC segments can be incorrectly classified as shockable if the ventricular contractions form a sufficiently irregular pattern and the QRS complexes are not well defined (Figure 4.26d). The ECG shown in Figure 4.26a was classified as NSR by the cardiologists, although it is quite irregular with large P and T waves and a double hump QRS probably caused by the delayed activation of one of the ventricles.

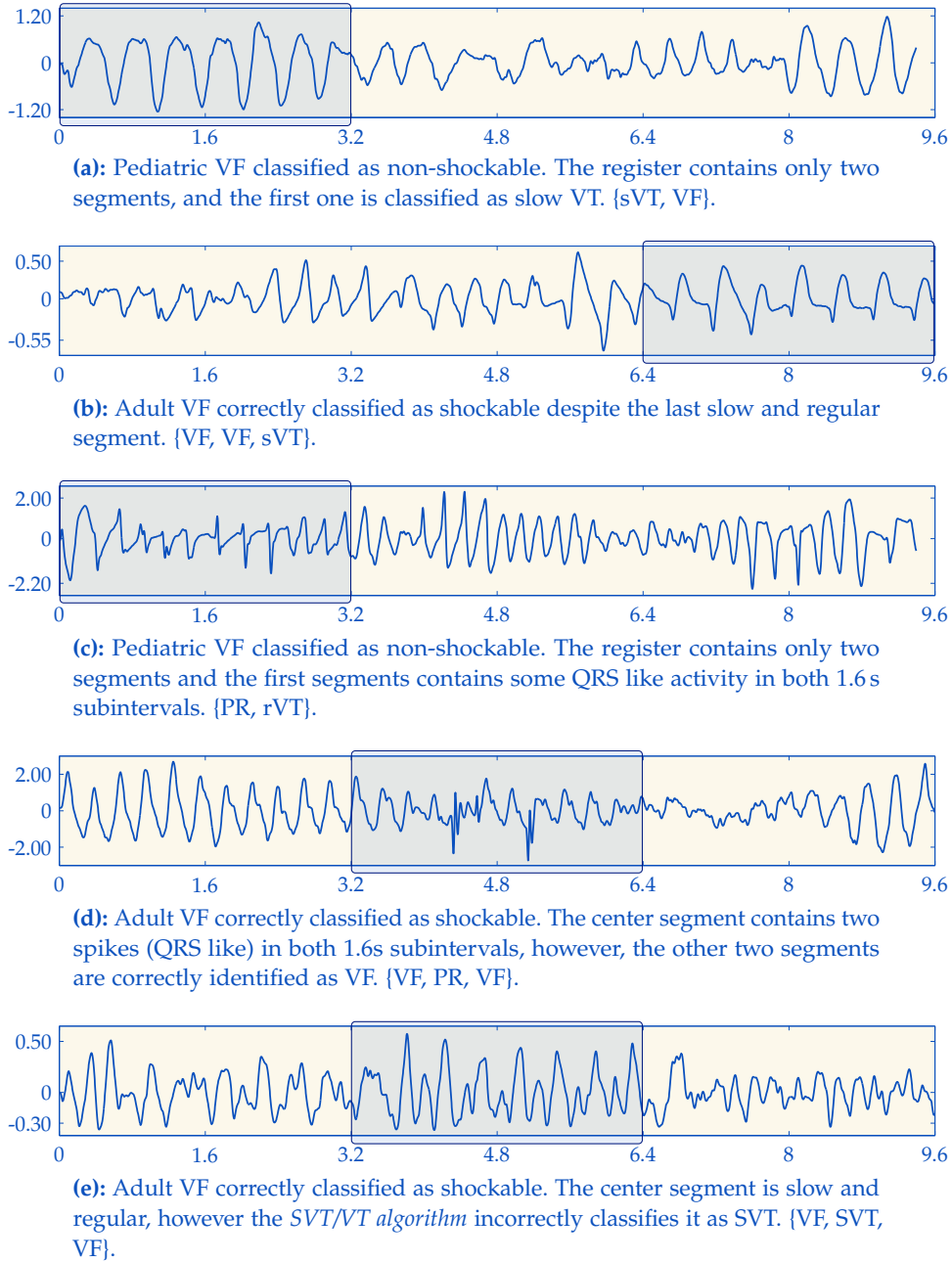
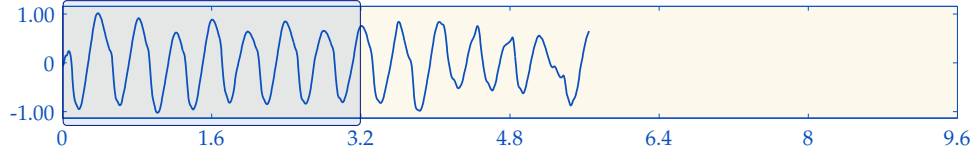
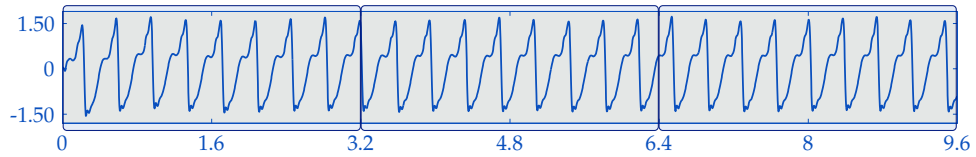


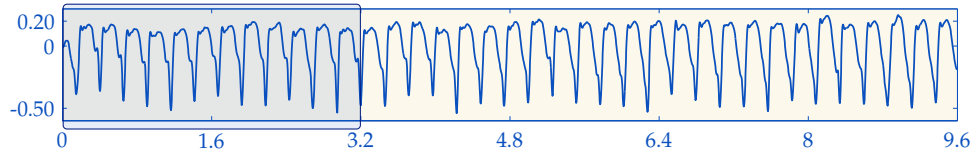
**Figure 4.23:** Examples of misclassified VF segments and registers. The figures show  $\hat{x}_{ecg}(n)$  in mV as a function of  $t = nT_s$  in s.



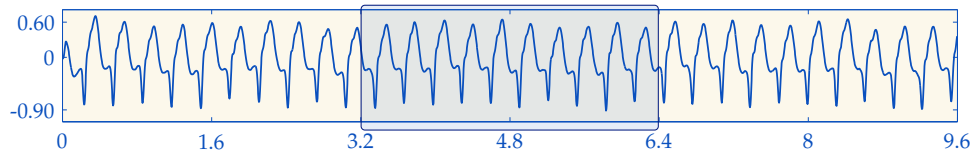
**(a):** Pediatric VT classified as non-shockable. The register contains only one slow segment that does not exceed the rate threshold for shockable VT ( $f_c = 149$  bpm). {SVT}.



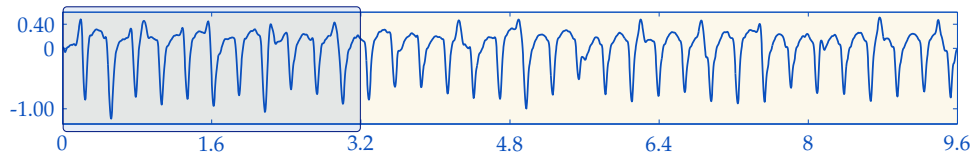
**(b):** Pediatric VT classified as non-shockable. The abrupt descents produce high frequency components and large slopes. All segments are identified as PR. {PR, PR, PR}.



**(c):** Pediatric VT. The first segment is a borderline case for the *QRS algorithm*, the following two are correctly identified ( $f_c = 235$  bpm). {PR, rVT, rVT}.



**(d):** Pediatric VT. The center segment is a borderline case for the *SVT/VT algorithm*, the other two are correctly identified ( $f_c = 190$  bpm). {rVT, SVT, rVT}.



**(e):** Pediatric VT. The first segment is a borderline case for the *SVT/VT algorithm*, the following two are correctly identified ( $f_c = 215$  bpm). {SVT, rVT, rVT}.

**Figure 4.24:** Examples of misclassified pediatric VT segments and registers. The figures show  $\hat{x}_{ecg}(n)$  in mV as a function of  $t = nT_s$  in (s).

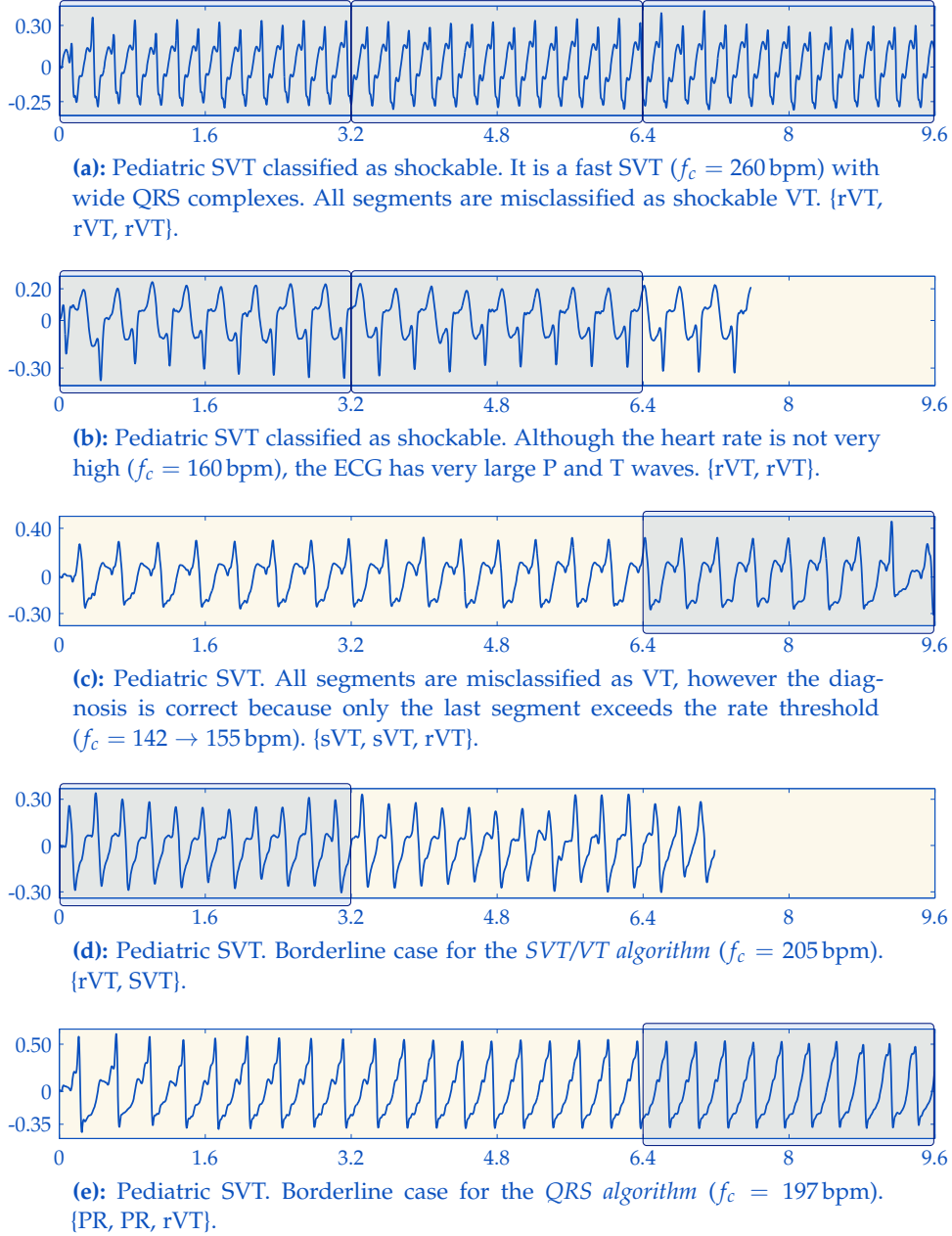
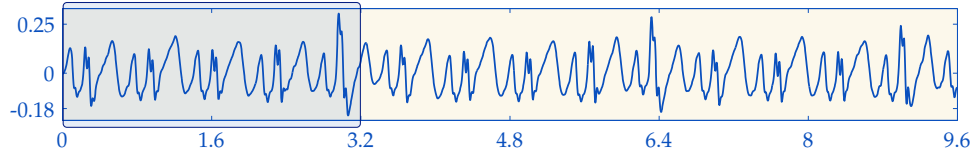
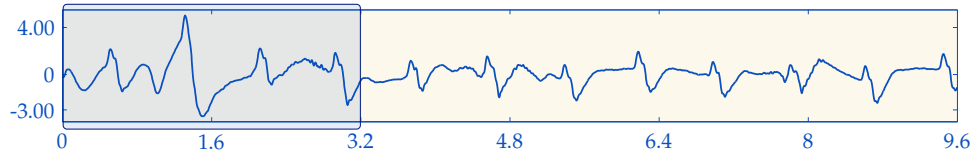


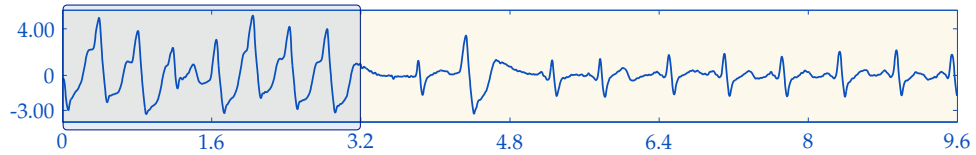
**Figure 4.25:** Examples of misclassified SVT segments and registers. The figures show  $\hat{x}_{ecg}(n)$  in mV as a function of  $t = nT_s$  in s.



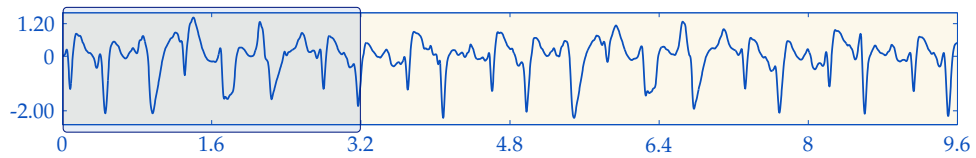
**(a):** Adult NSR. The first segment is a borderline case for the *QRS algorithm*, it is classified as nPR and as irregular. {VF, PR, PR}.



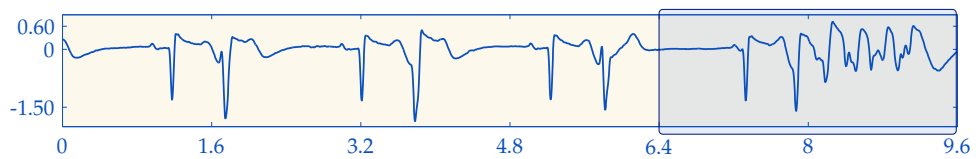
**(b):** Adult IV. The first 1.6s subinterval of the first segment has no QRS complexes, it is classified as nPR and as irregular. {VF, PR, PR}.



**(c):** Adult PVC. The initial segment contains clear ventricular activity which is correctly identified as VF. {VF, PR, PR}.

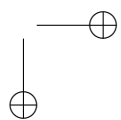
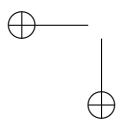
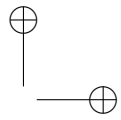
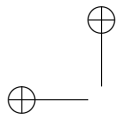


**(d):** Adult PVC. The QRS complexes are not as clear in the initial segment, which is then classified as VF because it is irregular. {VF, PR, PR}.



**(e):** Adult PVC. The last 1.6s interval of the last segment contains fast ventricular activity. {PR, PR, VF}.

**Figure 4.26:** Examples of misclassified non-shockable segments and registers. The figures show  $\hat{x}_{ecg}(n)$  in mV as a function of  $t = nT_s$  in s.





# 5 | OHCA RHYTHM ANALYSIS

This chapter presents the analysis of the performance of the AED shock advice algorithm for real OHCA episodes. First, the algorithm is tested on OHCA rhythms free of artifacts. In this way its performance is assessed for the rhythm types found in the field, which may differ from those covered in the AHA statement. Then, the algorithm is used to diagnose the rhythms during chest compressions both before and after filtering the CPR artifact. The filtering method to suppress the CPR artifact was developed as part of this thesis work.

## 5.1 Structure of the OHCA episodes

The database described in Section 3.2 serves to assess the performance of the universal shock advice algorithm in an OHCA scenario. The OHCA registers contain two distinct intervals. During the initial 15.5 s<sup>†</sup> CPR was performed, and an artifact caused by the chest compressions corrupted the underlying rhythm. In the following 15.5 s CPR was stopped, and the underlying OHCA rhythm was revealed free of CPR artifacts. Figure 5.1 describes these two intervals,<sup>‡</sup> which were used to assess the performance of the AED algorithm in the following two ways.

1. *Evaluation of the shock advice algorithm for clean OHCA registers.*  
The universal AED algorithm described in Chapter 4 was developed in the framework of the AHA statement.<sup>80</sup> Its specificity was assessed using registers obtained in hospital, with a large proportion of NSR and SVT. However,

---

<sup>†</sup> This database was created in the process of developing the dual-channel method for the suppression of the CPR artifact described in Irusta et al.<sup>67</sup> In that work, the filter performance was assessed using the AED algorithm from the Reanibex 200, which analyzes three consecutive 4.8 s ECG segments. This is the reason for the 15.5 s interval duration, which includes the interval needed for the diagnosis and an additional 1.1 s for the convergence of the filter.

<sup>‡</sup> The figure shows two consecutive 15 s intervals, for esthetic reasons the initial and final 0.5 s of the original episodes are not shown in this chapter's figures.

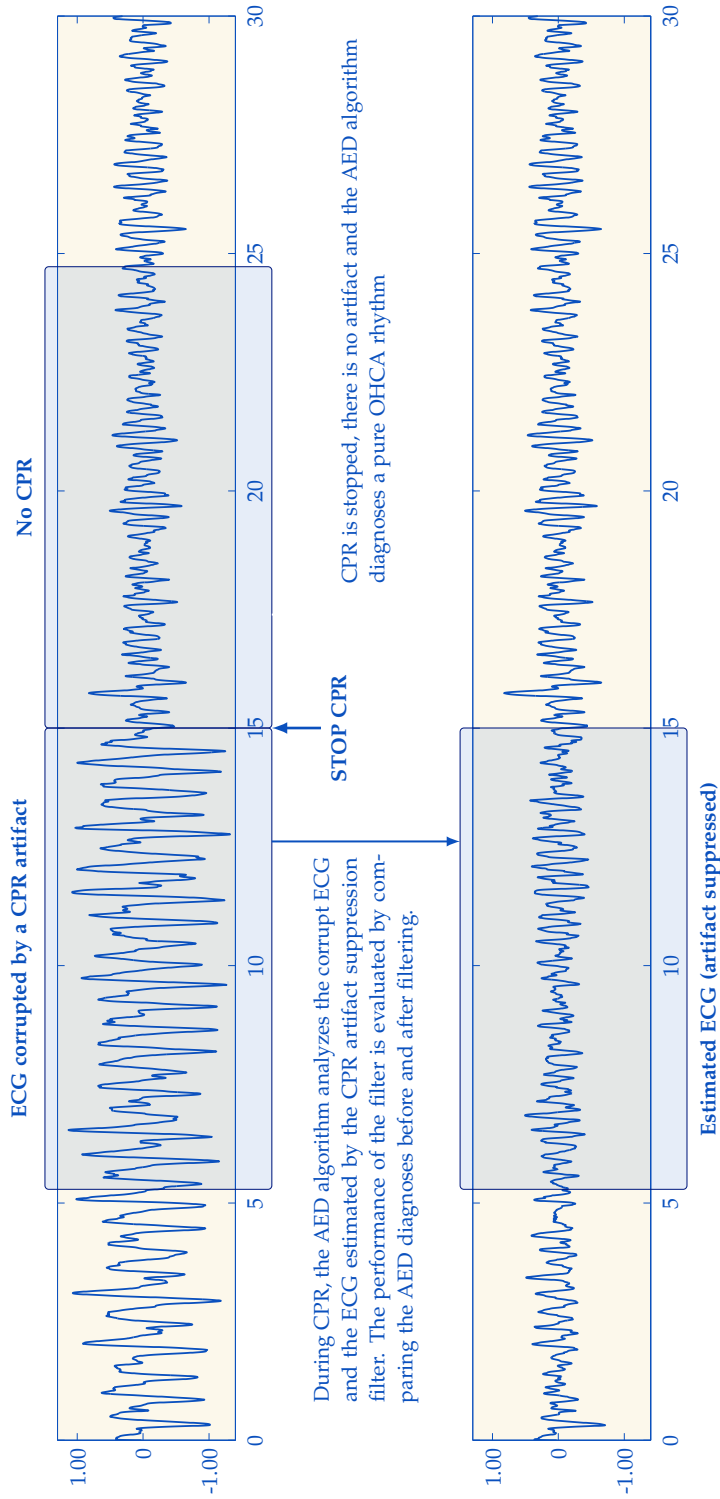


**Figure 5.1:** The analysis intervals of the OHCA episodes. During the initial 15 s CPR is administered, during the last 15 s CPR was stopped. The first interval is used to assess the goodness of the CPR artifact cancellation filter in terms of the diagnosis of the shock advice algorithm. The second interval is used to assess the performance of the shock advice algorithm on artifact-free OHCA registers. The AED algorithm analyzes the 9.6 s intervals highlighted in the figure. The figures show the ECG in mV as a function of time in s.



the non-shockable rhythms found in OHCA could be very different from NSR or SVT. In Section 5.2, we assess the performance of the algorithm for clean OHCA rhythms; i. e., on the second interval of the OHCA registers.

2. *Rhythm analysis during CPR.* The diagnosis of current AEDs is not reliable during CPR because the mechanical activity from the chest compressions introduces artifacts in the ECG. However, stopping CPR for a reliable diagnosis adversely affects the probability of ROSC after the delivery of the shock,<sup>45,149,44</sup> in fact pauses in chest compressions compromise circulation.<sup>20</sup> In Section 5.3, we assess the performance of the universal AED algorithm before and after filtering the CPR artifact. The artifact is suppressed from the first interval of the OHCA registers using the dual-channel filtering strategy introduced by Irusta et al.<sup>67</sup>

## 5.2 Diagnosing clean OHCA rhythms

The AHA statement emphasizes safety; i. e., it tries to minimize the risk of injury to the patient and the rescuer, who may be a first-time user with minimal training. Consequently, the AED must avoid inadvertent (in a conscious and breathing patient) or deliberate misuse. This is the reason why the statement requires a high specificity for rhythms accompanied by a palpable pulse and/or rhythms in a conscious patient.

However, non-shockable rhythms in OHCA are frequently found in patients without a pulse. For example, during PEA the electrical activity of the heart is not accompanied by a palpable pulse. Furthermore, the prevalence of PEA in an OHCA scenario is high both for adult and pediatric patients.<sup>101,30</sup> As shown in Figure 5.2, the heart rate and morphology of these rhythms may be very different from those found in the non-shockable rhythms of databases compliant with the AHA statement.

The classification results of the new algorithm for free-of-artifact OHCA rhythms are compiled in Table 5.1, both for the registers and their segments. The sensitivity and specificity are above AHA specification for all the rhythm categories, although the figures are below those reported in Table 4.11b for the test database. For instance, VF sensitivity drops 4 points, from 99.6 % to 95.5 %; the specificity for PEA is 97 %, 2.4 points lower than the 99.4 % obtained for the other non-shockable registers in the AHA compliant test database; and finally there is a 1 point drop in the detection of asystole.

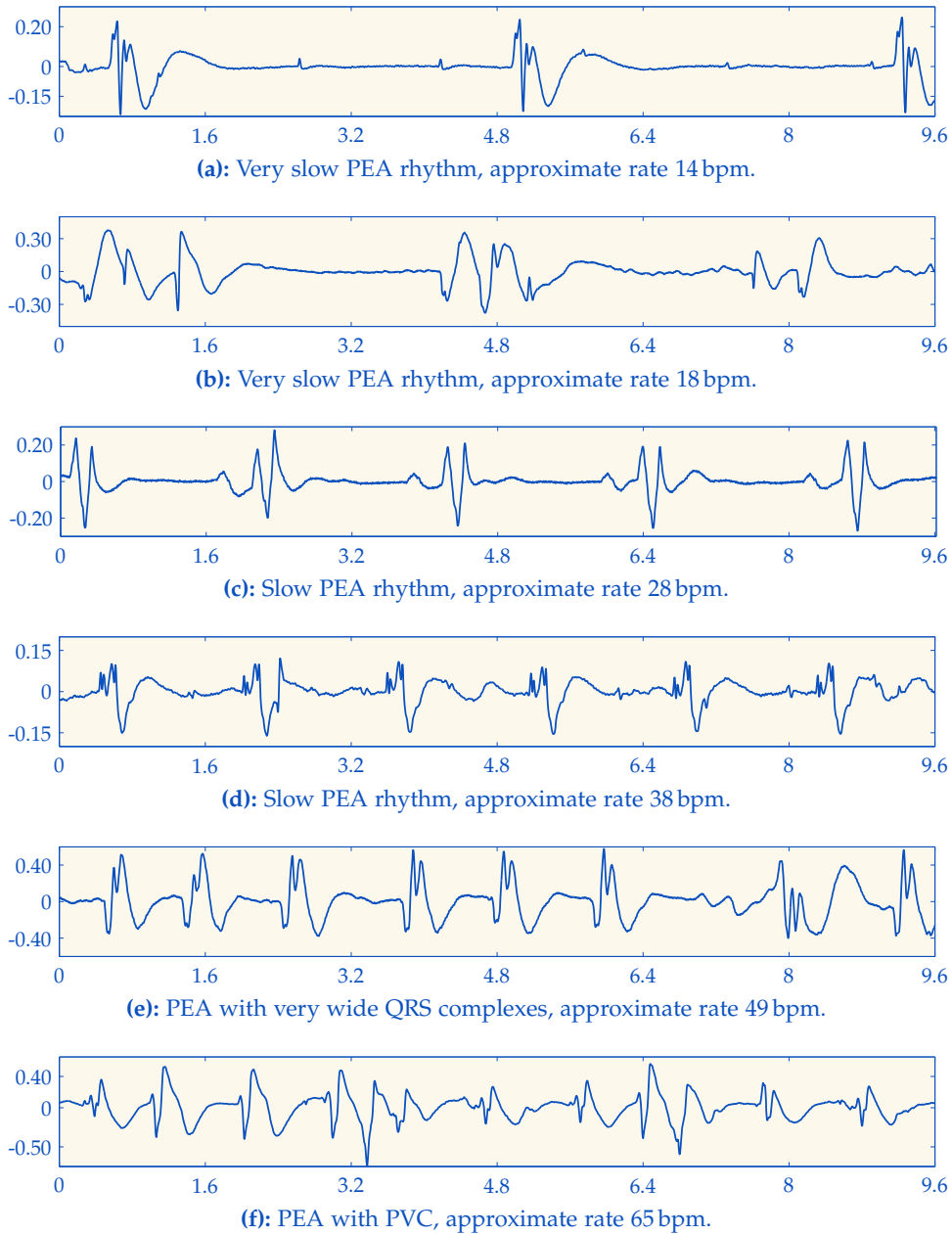


**Figure 5.2:** Six examples of PEA recorded from OHCA victims. All of the examples present very wide QRS complexes of very different morphology, the examples are ordered by increasing heart rate. The figures show the ECG in mV as a function of time in s.

The largest performance drop is found for the shockable registers, with 4/89 classified as non-shockable. Three cases are shown in Figure 5.3, a VT with a ventricular rate below the threshold for fast VT (Figure 5.3c), a VF with a very low peak-to-peak amplitude of  $\sim 100 \mu\text{V}$  (Figure 5.3b) and VF with QRS like activity caused by rapid ventricular contractions or spiky noise (Figure 5.3a). The

Rhythm type	Segments			AHA goals (%)
	S	NS	Se/Sp (%) <sup>a</sup>	
<b>Shockable</b>				
VF and VT	336	19	94.7 (92.3-96.3)	> 90 <sup>b</sup>
<b>Non-shockable</b>				
PEA	28	637	95.8 (94.3-96.9)	> 95
PR	4	148	97.4 (94.1-99.0)	> 95
Asystole	8	344	97.7 (96.0-98.8)	> 95
<b>Total</b>	40	1129	96.6 (95.6-97.4)	> 95

<sup>a</sup> 90% CI indicated in parenthesis.  
<sup>b</sup> Performance goal for VF.

(a): Sensitivity and specificity for the 3.2 s segments.

Rhythm type	Records			AHA goals (%)
	S	NS	Se/Sp (%) <sup>a</sup>	
<b>Shockable</b>				
VF and VT	85	4	95.5 (90.1-98.2)	> 90 <sup>b</sup>
<b>Non-shockable</b>				
PEA	5	161	97.0 (93.8-98.6)	> 95
PR	0	38	100 (92.1-100)	> 95
Asystole	1	87	98.9 (94.7-100)	> 95
<b>Total</b>	6	286	98.0 (96.0-99.0)	> 95

<sup>a</sup> 90% CI indicated in parenthesis.  
<sup>b</sup> Performance goal for VF.

(b): Sensitivity and specificity for the registers.

**Table 5.1:** Sensitivity and specificity of the universal AED algorithm for artifact-free OHCA rhythms.

first two examples are not found in the test database because only VT exceeding the rate threshold for fast VT and coarse VF (peak-to-peak amplitude  $>200 \mu\text{V}$ ) were included in the group of shockable rhythms.

The differences in the nature of the non-shockable rhythms between the test database and the OHCA database are not reflected in a significant drop in specificity. PEA is diagnosed accurately, only  $5/166$  are classified as shockable, and most of them are borderline PEA-VF cases like the ones shown in Figure 5.3e and Figure 5.3f. The misclassified asystole register is shown in Figure 5.3d, and is caused by the very large amplitude ( $>0.5 \text{ mV}$ ) and its irregularity. The classification results and the graphical display of the misclassified registers show that although the non-shockable registers in the development and test databases were not obtained from OHCA victims, these databases are diverse enough to design a robust AED shock advice algorithm that correctly diagnoses OHCA rhythms.

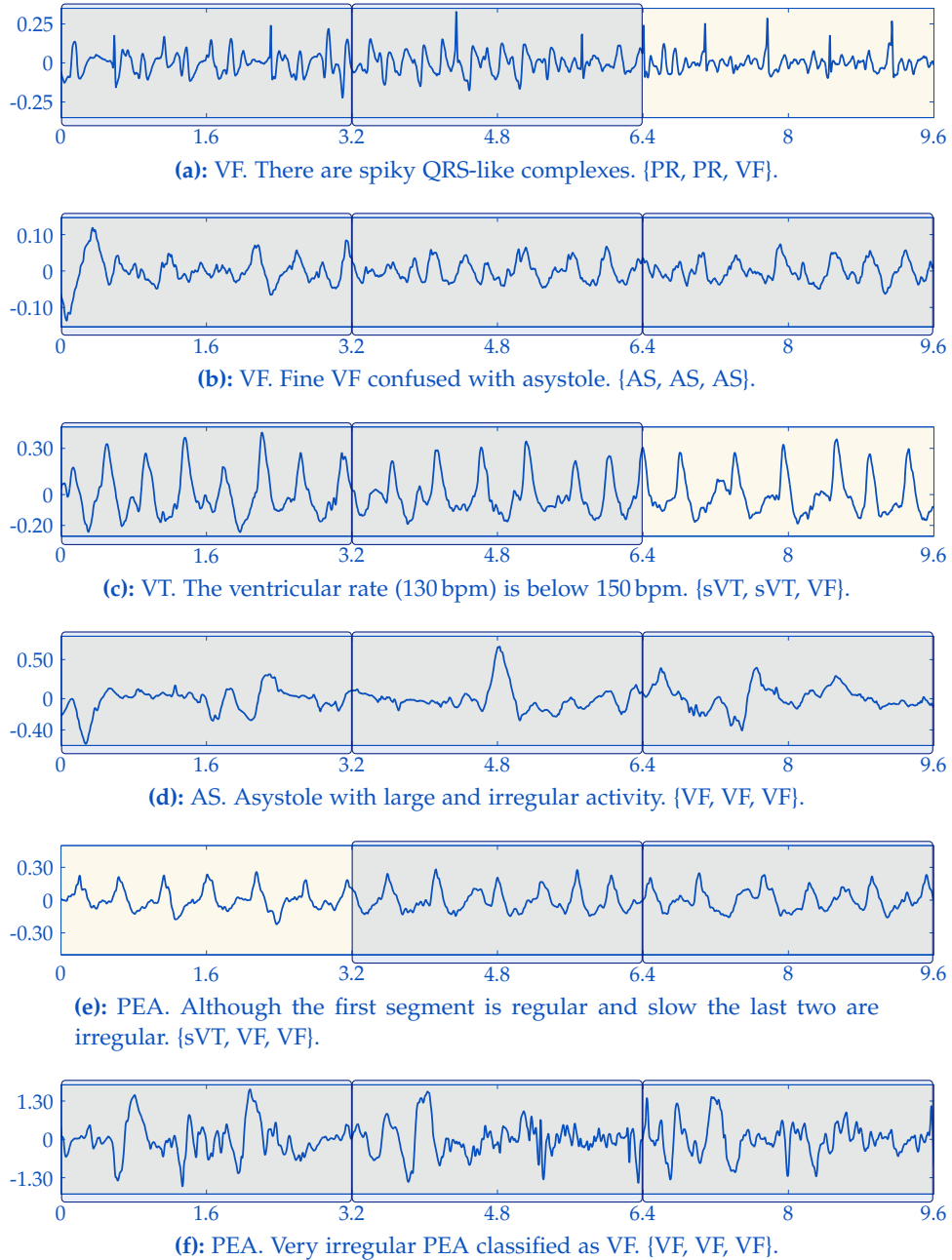


**Figure 5.3:** Examples of misclassified OHCA registers free of CPR artifacts. The figures show the ECG in mV as a function of time in s for a BPF: 0.7–30 Hz.

## 5.3 Rhythm analysis during CPR

### 5.3.1 Characteristics of the CPR artifact

The CPR artifact is generated by the mechanical activity necessary for the delivery of chest compressions. When CPR is performed manually,<sup>†</sup> the characteristics of the artifact are very variable. They depend on many factors such as: how CPR is administered, the characteristics of the patient and the recording system.

The nature of the CPR artifact is best analyzed when CPR is performed on patients in asystole; i. e., there is no underlying heart rhythm and consequently the recorded signal only reflects the presence of the artifact. Figure 5.4 shows two examples of a CPR

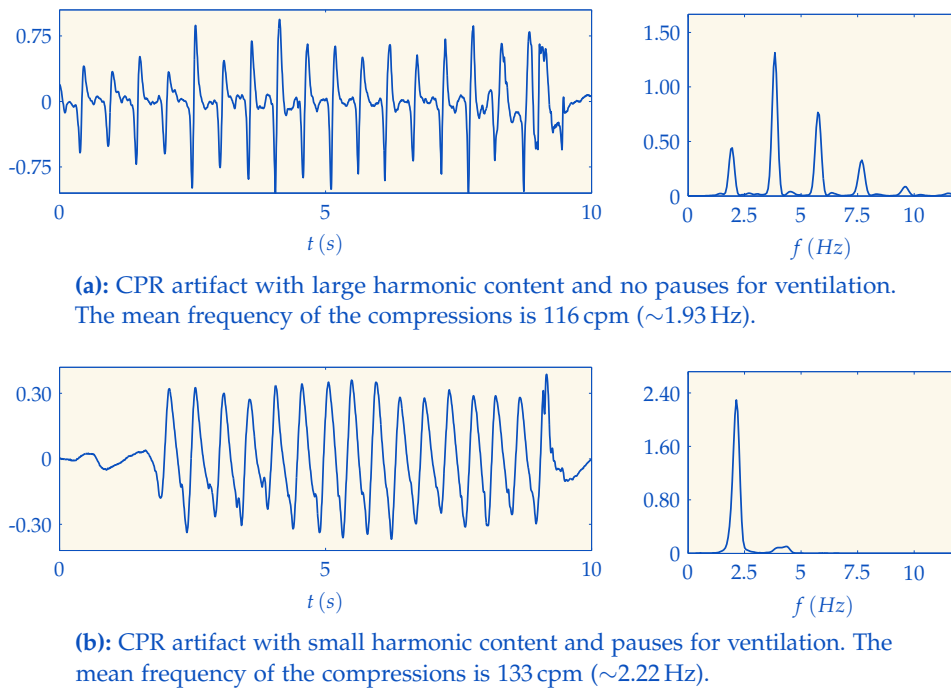


**Figure 5.4:** Two examples, in the time and frequency domain, of a CPR artifact recorded on a patient in asystole. The figures show the ECG in mV in the time domain and the normalized PSD in the frequency domain. The PSD was calculated using Welch's method with 5 s Hamming windows and 50% overlap.

<sup>†</sup> For automatic chest compression devices like the Zoll AutoPulse or the Jolife LUCAS the characteristics of the artifact are less variable. Both the frequency of the chest compressions and the waveform of the induced artifact are more predictable because CPR is delivered under the same conditions in a repetitive automatic way by the device.<sup>21</sup>

artifact recorded on a patient in asystole. There are large differences in the time and frequency domain between the two artifacts. Figure 5.4a shows an artifact with rapid waveform variations that produce large harmonic components. The chest compression rate was 116 cpm and there are no pauses for respiration in the interval shown in the figure. Conversely, Figure 5.4b shows an artifact with slower waveform variations, and consequently a lower harmonic content. The chest compression rate was 133 cpm and there are pauses in the interval shown in the figure.

The initial 15.5 s interval of the 88 asystole registers was used to analyze the characteristics of the CPR artifact in the database of OHCA episodes. The average chest compression rate was 121 cpm (range: 73–170 cpm). Although this rate is well above the 100 cpm recommended by the current guidelines,<sup>56</sup> it matches the one reported by the authors that conducted the study that originated our database of OHCA registers.<sup>146</sup> From a CPR artifact suppression standpoint, higher compression rates increase the spectral overlap with OHCA rhythms and filtering the CPR artifact becomes more difficult.

The spectral analysis of the CPR artifacts is shown in Figure 5.5. The power is distributed among the harmonics of the fundamental

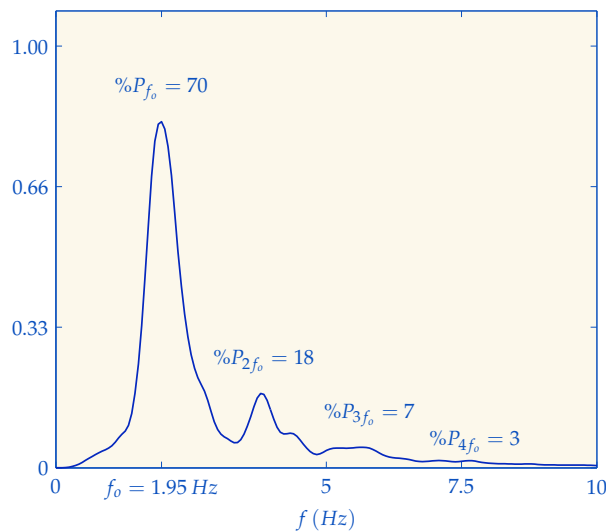


**Figure 5.5:** Normalized PSD for the CPR artifact recorded in patients in asystole. The PSD was calculated using Welch’s method with 5 s Hamming windows and 50% overlap, and then averaged with equal weight for all the registers. The value  $\%P_{\ell f_0}$  indicates the percent power content in a frequency band of bandwidth  $f_0$  and centered in  $\ell f_0$ ; i. e., it measures the contribution of the  $\ell$ -th harmonic to the total power.

component, as expected for an almost-periodic artifact. The fundamental component —  $f_0=1.95$  Hz — corresponds to the mean chest compression rate. The first three harmonics account for 95% of the total power, although there may be CPR artifacts with significant power content in higher harmonics, Figure 5.4a is an example.

The efficient elimination of the CPR artifact involves adaptive signal processing techniques because the artifact presents an important spectral overlap with human cardiac arrest rhythms, in addition to its inter-patient and inter-rescuer variability. The spectral overlap of the CPR artifact and human VF is well known, however the spectral overlap between non-shockable OHCA rhythms and the CPR artifact is also large. Figure 5.6 compares the PSD of the OHCA rhythms in our database to that of the CPR artifacts.

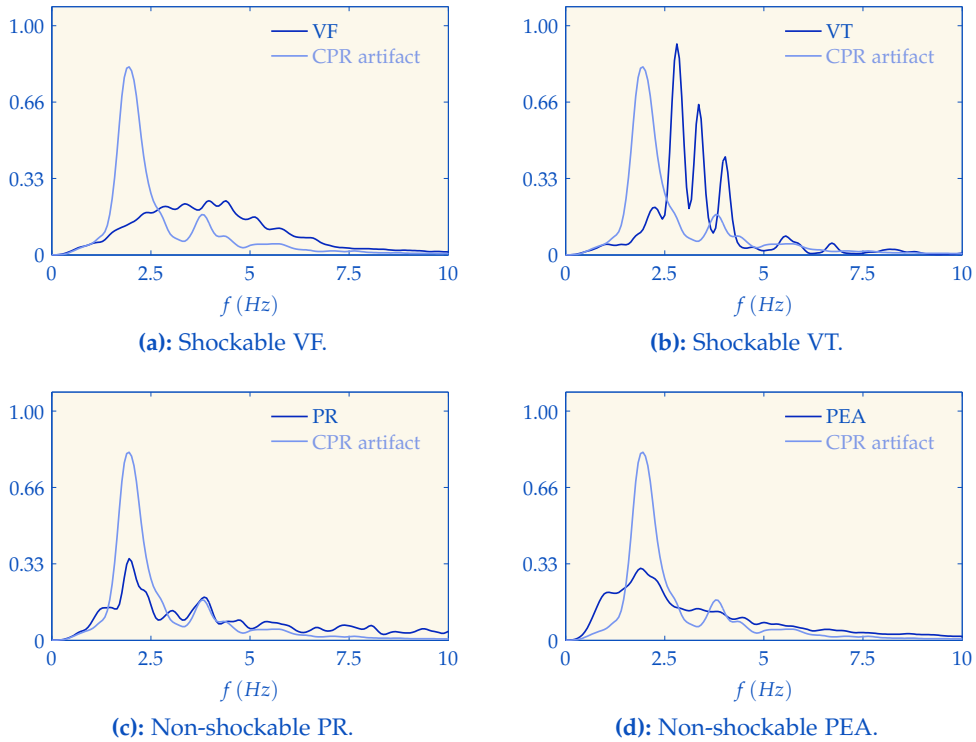


**Figure 5.6:** Normalized PSD of pure CPR artifacts and rhythms recorded in OHCA. The PSD were computed for the intervals without CPR artifact of the registers from the database described in Section 3.2. Asystole registers (no underlying rhythm) corrupted by CPR are taken as pure artifacts. The PSD was calculated using Welch’s method with 5 s Hamming windows and 50% overlap, and then averaged with equal weight for all the registers in the class.



There is a clear spectral overlap for both shockable and non-shockable OHCA rhythms, which is reflected by the proximity of the dominant frequencies of each rhythm class to the fundamental frequency of the artifact. Furthermore, the overlap is higher for non-shockable than for shockable rhythms which anticipates the challenge of artifact removal from corrupted non-shockable registers.

### 5.3.2 Adaptive filter based on the frequency of the chest compressions

This section describes a methodology to suppress the CPR artifact developed in the course of this thesis work. The method is general and can be implemented using different adaptive solutions, the LMS filter described in page 127 is one of the possible solutions, although alternative ways based on Kalman filters have also been studied.<sup>38,119</sup>

The filtering method relies on a simple hypothesis: during chest compressions, the CPR artifact can be modeled as an almost periodic signal, its fundamental frequency being that of the chest compressions. Then, the suppression of the CPR artifact depends on an accurate recording of the instantaneous frequency of the chest compressions, or alternatively, of the instants when the chest compressions are given. Let us call those instants

$$t_k = n_k T_s, \quad (5.1)$$

where  $T_s$  is the sampling period.

The interval between consecutive compressions corresponds to one oscillatory cycle. Assuming that during a cycle the frequency is constant but may vary between cycles, the instantaneous frequency and phase of the compressions are:

$$f_k = \frac{1}{T_s(n_{k+1} - n_k)} = \frac{f_s}{\Delta n_k} \quad n_k \leq n < n_{k+1}, \quad (5.2)$$

$$\phi(n) = \frac{2\pi}{\Delta n_k}(n - n_k) + k \cdot 2\pi \quad n_k \leq n < n_{k+1}. \quad (5.3)$$

The  $\{t_k\}$  instants were not directly available in the database of OHCA registers. However, they can be estimated from the additional reference channels, for instance from the compression depth signal.<sup>†</sup> Figure 5.7 shows how to locate when the chest compressions were given by locating the instants when the compression depth is at its local minimums; i. e., when the chest is

<sup>†</sup> In the original study, the modified HeartStart 4000SP AED calculated the compression depth by integrating the recordings from several accelerometers.<sup>4</sup>

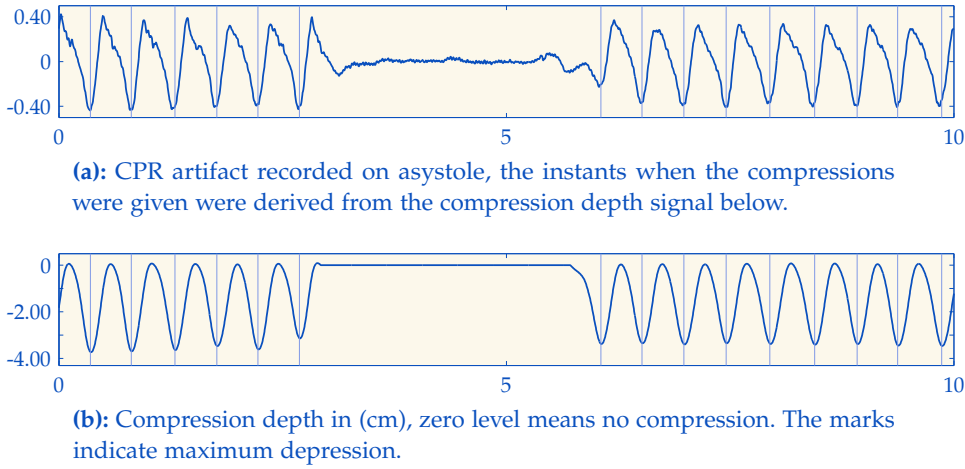


**Figure 5.7:** Estimating the frequency of the compressions from the compression depth signal. It is possible to locate the instants when the chest is fully compressed by marking the instants when the compression depth is at its local minimum.

fully compressed. These instants were automatically marked using a peak detector. In fact, it is not necessary to measure the instants when the chest is fully compressed, the frequency of the chest compressions can be equally estimated identifying other events such as the onset of each compression. Furthermore, it is possible to use other reference signals to estimate the location of these events, like the pressure or force signals recorded through pressure sensors added in the CPR compression pads.

#### *Model of the CPR artifact*

During chest compressions the artifact is regarded as a quasi-periodic interference; consequently, it can be modeled using a Fourier series representation of  $\ell = 1, \dots, N$  harmonics of time varying amplitude and phase. These values change slowly in time and track the changes in waveform from cycle to cycle. The cycle to cycle changes in the fundamental frequency are given by  $\phi(n)$ . The model of the artifact during chest compressions is then

$$\begin{aligned} \hat{x}_{comp}(n) &= \sum_{\ell=1}^N c_{\ell}(n) \cos(\ell\phi(n) + \phi_{\ell}(n)) \\ &= \sum_{\ell=1}^N a_{\ell}(n) \cos \ell\phi(n) + b_{\ell}(n) \sin \ell\phi(n). \end{aligned} \quad (5.4)$$

The time varying amplitude and phase —  $c_{\ell}(n)$  and  $\phi_{\ell}(n)$  — of each harmonic can be estimated through an adaptive filter which

tracks the evolution of the spectral composition of the artifact. This is equivalent to following the variation of the amplitudes of the in-phase and quadrature components,  $a_\ell(n)$  and  $b_\ell(n)$ .

In the course of CPR, chest compressions are interrupted for rhythm analysis or ventilations, Figure 5.8a shows a CPR artifact with a pause for ventilation. During rhythm analysis CPR is halted and there is no artifact. During ventilations the CPR artifact is a low frequency respiratory artifact, its influence is negligible (it is suppressed by the preprocessing filters) and no adaptive filtering is needed. Consequently, the CPR artifact estimated by the adaptive filter must be zero in the absence of chest compressions.

It is possible to represent intervals with and without chest compressions in a single model of the artifact by means of a signal envelope,  $A(n)$ . In the intervals without chest compressions the artifact is negligible, and the envelope must be  $A(n) = 0$ . When chest compressions are administered  $A(n) = 1$ , and the artifact is modeled through Equation 5.4. A complete model for the artifact that accounts for both types of intervals is

$$\begin{aligned}\hat{x}_{cpr}(n) &= A(n) \cdot \hat{x}_{comp}(n) \\ &= A(n) \sum_{\ell=1}^N a_\ell(n) \cos \ell\phi(n) + b_\ell(n) \sin \ell\phi(n).\end{aligned}\quad (5.5)$$

Two smooth transition periods were defined to avoid abrupt changes in the amplitude. An example of the phase and amplitude used in the model of the CPR artifact are shown in Figure 5.8 for a patient in asystole.

The period between two consecutive compressions was used to automatically distinguish ventilation and compression intervals. The current CPR guidelines recommend a compression rate of 100 cpm, a period between two consecutive compressions of more than 1 s was interpreted as a ventilation interval (the compression rate would be below 60 cpm).<sup>†</sup> This introduces a delay of 1 s in the filtering process, the time needed to decide the type of interval and the corresponding value of  $A(n)$ .

<sup>†</sup> Kramer-Johansen et al.<sup>83</sup> define pauses in chest compressions for an interval of 1.5 s without compressions.

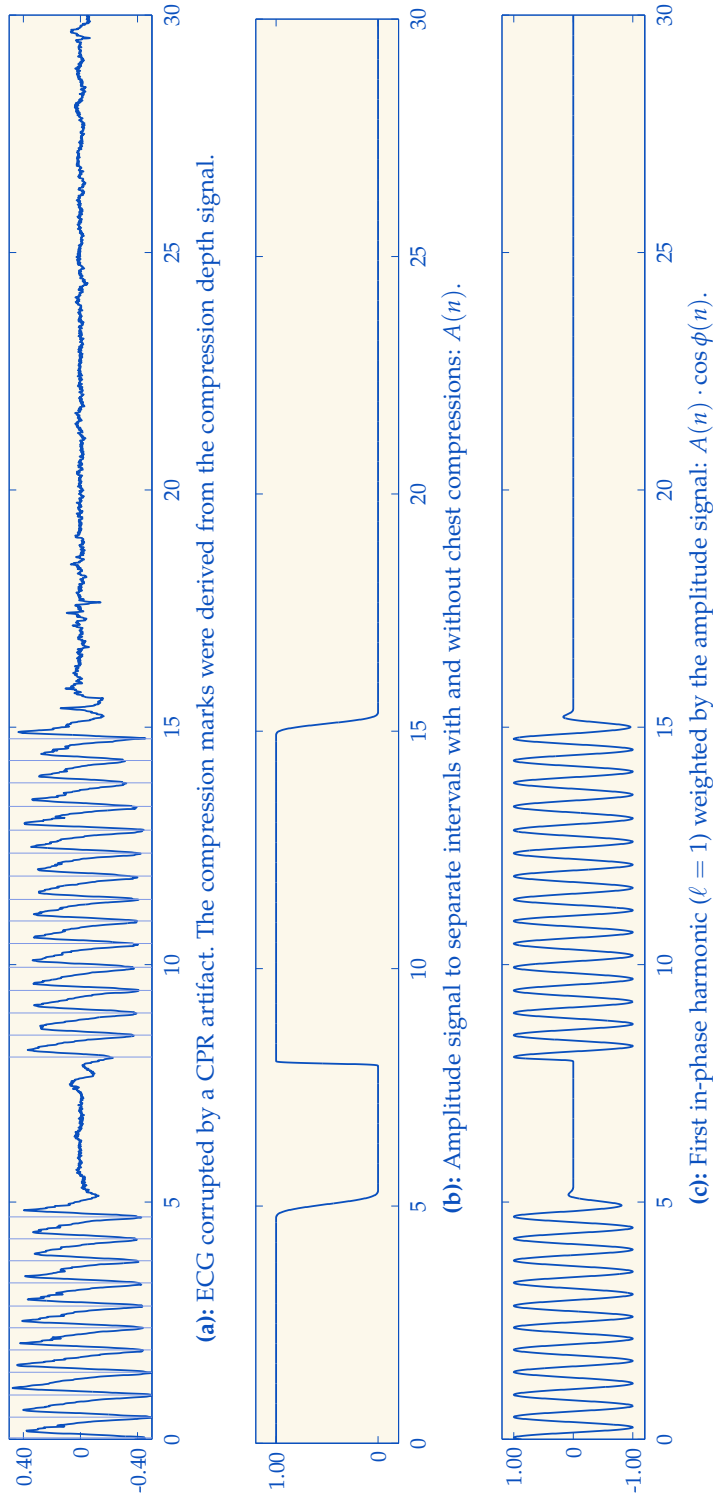


**Figure 5.8:** A representation of the amplitude  $A(n)$  and phase  $\phi(n)$  of the CPR signal model  $\hat{x}_{cpr}(n)$ . The complete signal is shown; in the initial 15 s interval a CPR artifact corrupts the ECG, in the following 15 s interval there is no artifact. Each compression cycle corresponds to a complete phase cycle, the amplitude separates ventilation and compression intervals. In the absence of compressions the CPR artifact estimated by the filter is  $\hat{x}_{cpr}(n) = 0$  because  $A(n) = 0$ .

### The LMS filter

Figure 5.9 shows the structure of the adaptive filter used to suppress an additive CPR artifact from the input ECG signal,  $x_{in}(n)$ . The artifact is first adaptively estimated by fitting the model given by Equation 5.5, and then subtracted from the input signal to produce an ECG free of artifact,  $\hat{x}_{ecg}(n)$ . The only additional information used by the adaptive scheme are the instants of the compressions needed to calculate  $A(n)$  and  $\phi(n)$ . Therefore, the estimated CPR artifact and the estimated underlying ECG are given by

$$\hat{x}_{cpr}(n) = A(n) \sum_{\ell=1}^N a_{\ell}(n) \cos \ell\phi(n) + b_{\ell}(n) \sin \ell\phi(n), \quad (5.6)$$

$$\hat{x}_{ecg}(n) = x_{in}(n) - \hat{x}_{cpr}(n). \quad (5.7)$$

The time varying in-phase and quadrature components of the artifact model —  $a_{\ell}(n)$  and  $b_{\ell}(n)$  — are the coefficients of the filter, which are updated using the LMS method. This configuration is a well-known generalization to  $N$  harmonics<sup>76,147</sup> of the classical LMS filter used to suppress a sinusoidal interference of known frequency.<sup>144</sup> The clean ECG is the LMS error signal and each harmonic has a different step size  $\mu_{\ell}$ . The filter coefficient update equations are then

$$a_{\ell}(n+1) = a_{\ell}(n) + 2\mu_{\ell}\hat{x}_{ecg}(n)A(n) \cos \ell\phi(n) \quad (5.8)$$

$$b_{\ell}(n+1) = b_{\ell}(n) + 2\mu_{\ell}\hat{x}_{ecg}(n)A(n) \sin \ell\phi(n), \quad (5.9)$$

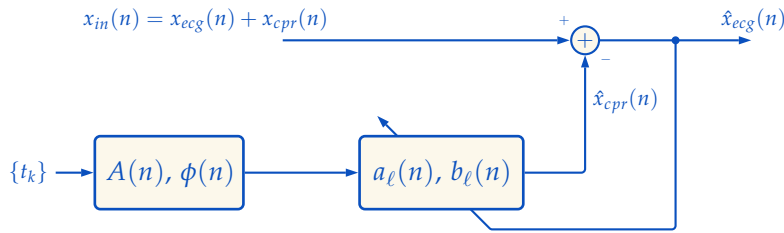


**Figure 5.9:** Diagram of the CPR suppression filter. The input signal,  $x_{in}(n)$ , is an ECG corrupted by a CPR artifact. An estimate of the artifact,  $\hat{x}_{cpr}(n)$ , is subtracted from  $x_{in}(n)$  to obtain the clean ECG,  $\hat{x}_{ecg}(n)$ . The model of the artifact is estimated based on the chest compression instants  $\{t_k\}$ , which in an OHCA scenario could be recorded through the CPR compression pads. The filter coefficients  $a_{\ell}(n)$  and  $b_{\ell}(n)$  are updated using the LMS method.

which are the update equations of  $N$  uncoupled LMS filters for the suppression of a sinusoidal interference. The initial value of the filter coefficients was made zero

$$a_\ell(0) = 0 \quad \text{and} \quad b_\ell(0) = 0. \quad (5.10)$$

Two parameters control the filtering method: the number of harmonics used to model the CPR artifact,  $N$ , and the step size of each harmonic component,  $\mu_\ell$ . To ease the design of the filter, the  $N + 1$  degrees of freedom were reduced to two —  $N$  and  $\mu_0$  — by selecting the step sizes in the following way:

$$\mu_\ell = \frac{1}{\ell} \mu_0 \quad \ell = 1, \dots, N. \quad (5.11)$$

This choice of step sizes is better understood in terms of the frequency response of the LMS filter.

When the reference signal is a pure sinusoidal of fundamental frequency  $f_0$  and amplitude  $A = 1$ , the transfer function of our LMS filter is equivalent to the cascade of  $N$  notch filters centered in the harmonics of the fundamental frequency,  $\ell f_0$ .<sup>147</sup> An example of an experimentally computed steady-state frequency response of the filter is shown in Figure 5.10.

The step size  $\mu_\ell$  of the  $\ell$ -th harmonic controls the bandwidth of the notch filter at that frequency, which is proportional to the

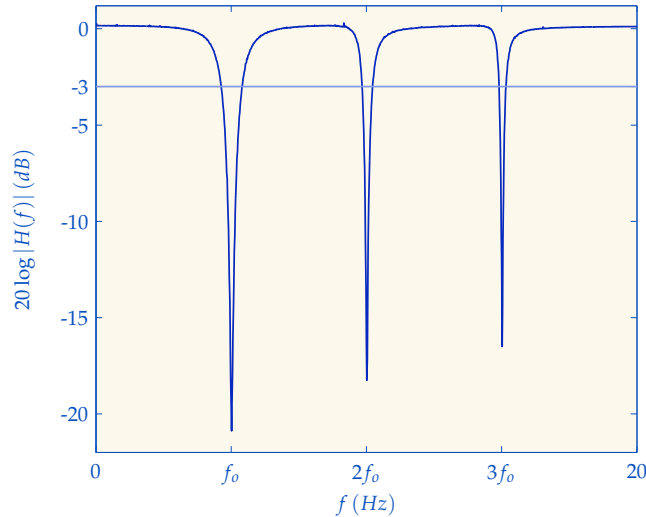


**Figure 5.10:** Experimental frequency response of the LMS filter for a gaussian white noise input, averaged for 1024 realizations. The LMS filter was configured to have  $N = 3$  harmonics,  $\mu_0 = 0.01$ , and a sinusoidal reference signal of amplitude one and constant frequency  $f_0 = 5$  Hz.

step size.<sup>147</sup> Consequently, the step size of the LMS filter,  $\mu_0$ , can be interpreted as the coarseness of the filter; higher values of  $\mu_0$  represent higher values of the bandwidth, that is a more coarse filter. By choosing a step size that decreases as the harmonic number increases (Equation 5.11), lower bandwidths are assigned to the higher harmonics of the artifact, which agrees with the experimental observations of the spectral distribution of the CPR artifact, shown in Figure 5.5.

#### Adjusting $N$ and $\mu_0$

A thorough analysis of the performance of the LMS filter for the same OHCA register database used for this thesis work is found in Irusta et al.<sup>67</sup> There, it was shown that good sensitivity and specificity scores were obtained using 5 harmonics to model the artifact, and that increasing the number of harmonics further did not improve the results at the cost of increasing the computational load. Using fewer harmonics compromises the results for the specificity.

Figure 5.11 shows the sensitivity and the specificity of the new algorithm after filtering. The values are computed as a function of  $\mu_0$ , the coarseness of the filter, for an artifact model with  $N = 5$

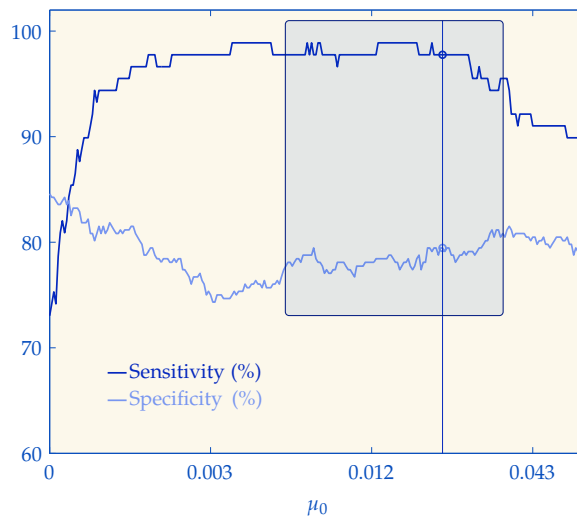


**Figure 5.11:** Sensitivity and specificity as a function of the filter coarseness  $\mu_0$  for an LMS filter with  $N = 5$  harmonics. The horizontal axis is in a nonlinear scale. The working range and working point of the LMS filter are highlighted.

harmonics. The results in Figure 5.11 demonstrate how filtering modifies the diagnosis of the new algorithm. The values for  $\mu_0 = 0$  reflect the performance for the unfiltered signal because when the step sizes are 0 the coefficients of the LMS filter are not updated and there is no filtering. The sensitivity improves rapidly as  $\mu_0$  grows for low values of  $\mu_0$ , in fact for  $\mu_0 > 1 \cdot 10^{-3}$  the sensitivity is already above 95%. Then it declines steadily for  $\mu_0 > 37 \cdot 10^{-3}$ . Conversely, for low values of  $\mu_0$ , the specificity rapidly declines as  $\mu_0$  grows, it then stabilizes to values slightly below 80% for  $\mu_0 > 6 \cdot 10^{-3}$ . We defined the working range of the LMS filter as the range of values of  $\mu_0$  when the sensitivity is consistently above 95% and the specificity is close to 80%:  $\mu_0 \sim 6 - 37 \cdot 10^{-3}$ .

### 5.3.3 Sensitivity and specificity of the new AED algorithm

Table 5.2 reports the average performance of the LMS filter in the working range for  $N = 5$ . There is a 25 point increase in the accuracy of the detection of shockable rhythms after filtering, at the expense of a 6 point drop in the detection accuracy for non-shockable rhythms. Compared with the interval with no artifact, the sensitivity slightly increases by 2 points while the specificity decreases by 19 points, far from the 97.6% obtained on the intervals without artifact. When compared with the mean results obtained by Irusta et al.<sup>67</sup> after filtering the same OHCA data with the LMS filter, we observe a 2 point increase in sensitivity but an 8 point decrease in specificity for the new algorithm. The results are different because they were obtained for another AED algorithm, which underlines the relevance of the AED algorithm in the design process of CPR suppression algorithms.

A filter coarseness that yields high sensitivity and specificity when compared with those in the working range is:  $\mu_0 = 22 \cdot 10^{-3}$ , the working point highlighted in Figure 5.11. Table 5.3 shows the

CPR unfiltered		CPR filtered <sup>a</sup>		No CPR	
Se (%)	Sp (%)	Se (%)	Sp (%)	Se (%)	Sp (%)
73.0	84.6	97.5	78.6	95.5	97.6

<sup>a</sup> Mean performance for:  $6 - 37 \cdot 10^{-3}$ .

**Table 5.2:** Average value of the sensitivity and specificity in the working range of the LMS filter for  $N = 5$ .



Rhythm type	Records			AHA goals (%)
	S	NS	Se/Sp (%) <sup>a</sup>	
<b>Shockable</b>				
VF and VT	65	24	73.0 (64.7-80.0)	> 90 <sup>b</sup>
<b>Non-shockable</b>				
PEA	23	143	86.1 (81.1-90.0)	> 95
PR	4	34	89.5 (78.1-95.6)	> 95
Asystole	18	70	79.6 (71.6-85.7)	> 95
<b>Total</b>	<b>45</b>	<b>247</b>	<b>84.6 (80.8-87.8)</b>	<b>&gt; 95</b>

<sup>a</sup> 90% CI indicated in parenthesis.  
<sup>b</sup> Performance goal for VF.

(a): Sensitivity and specificity results before filtering.

Rhythm type	Records			AHA goals (%)
	S	NS	Se/Sp (%) <sup>a</sup>	
<b>Shockable</b>				
VF and VT	87	2	97.8 (93.1-99.6)	> 90 <sup>b</sup>
<b>Non-shockable</b>				
PEA	35	131	78.9 (73.3-83.7)	> 95
PR	2	36	94.7 (84.7-98.9)	> 95
Asystole	23	65	73.9 (65.5-80.8)	> 95
<b>Total</b>	<b>60</b>	<b>232</b>	<b>79.5 (75.3-83.1)</b>	<b>&gt; 95</b>

<sup>a</sup> 90% CI indicated in parenthesis.  
<sup>b</sup> Performance goal for VF.

(b): Sensitivity and specificity results after filtering.

**Table 5.3:** Sensitivity and specificity results for the OHCA registers before and after filtering. The working point of the LMS filter was:  $N = 5$  and  $\mu_0 = 22 \cdot 10^{-3}$ .

classification results after filtering for that working point, and compares them with those obtained before filtering. There is again a significant increase in sensitivity (25 points) at the expense of a lower specificity (5 point decrease). Although it is possible to exceed the AHA specifications for the shockable rhythms after

filtering, the specificity is 15 points under AHA specifications. Furthermore, asystole and PEA are the most difficult to identify non-shockable rhythms, pulse-giving rhythms present high specificity both before and after filtering and are the only non-shockable rhythm class for which filtering improves the classification results.

To better understand the relation between the AED algorithm and the filtering process, the following figures show examples of successful and unsuccessful diagnoses before and after filtering. They were calculated for the operating point of the filter,  $N = 5$  and  $\mu_0 = 22 \cdot 10^{-3}$ . The examples demonstrate the limitations of an approach to rhythm diagnosis during chest compressions based on suppressing the CPR artifact. Although the artifact is accurately estimated in all the examples, there are still many potential sources of misclassification of the underlying rhythm, such as: rhythm changes induced by and sustained only during chest compressions, or filtering residuals.

When the signal-to-noise ratio is low — the power of the artifact is large compared with that of the underlying rhythm — the chest compression rate strongly influences the diagnosis of the algorithm. When chest compressions are given according to the guidelines — approximate compression rate of  $\sim 100$  cpm — the corrupted ECG is classified as non-shockable slow VT by the algorithm, Figure 5.12 and Figure 5.15 show two examples. Conversely, Figure 5.13 displays an episode where the chest compression rate is above 160 cpm; in this example the corrupted ECG is classified as rapid shockable VT by the algorithm. The high average chest compression rate<sup>†</sup> of the registers in the database partially explains the tendency of the algorithm to diagnose the corrupted intervals as shockable.

The accurate detection of shockable rhythms during CPR does not pose a problem. The sensitivity is well above AHA goals, although there may be occasional errors. Figure 5.14 shows an example of a misclassified VF. Filtering reveals a QRS-like spiky artifact, which is superimposed onto the VF rhythm. When the chest compressions are stopped the spiky artifact disappears and the AED algorithm correctly identifies the underlying VF.

An accurate diagnosis of non-shockable rhythms during chest compressions is unfortunately not possible. The specificity is well below AHA goals and filtering the artifact lowers it. A plausible reason that explains this degradation is that filtering the artifact produces a disorganized residual. When the residual is large compared with the underlying rhythm and its power exceeds the

<sup>†</sup> As stated in Section 5.3.1, the average chest compression rate was 121 cpm (range: 73–170 cpm)

threshold for the detection of asystole, the filtered rhythm is classified as VF. Figure 5.16 shows a typical case for asystole in which filtering reveals a large residual. For low-amplitude artifacts the amplitude of the residual is very low, and the residual is correctly classified as asystole, as shown in Figure 5.15. These residuals may also affect the accurate diagnosis of PEA during chest compressions, Figure 5.18 shows an example. Conversely, PEAs with well defined QRS complexes are more accurately identified both before and after filtering, as shown in Figure 5.17. Finally pulsed rhythms are less affected by chest compressions for two reasons: the artifact induced in perfusing rhythms is smaller (Figure 5.19) and filtering reveals the underlying QRS complexes (Figure 5.20).

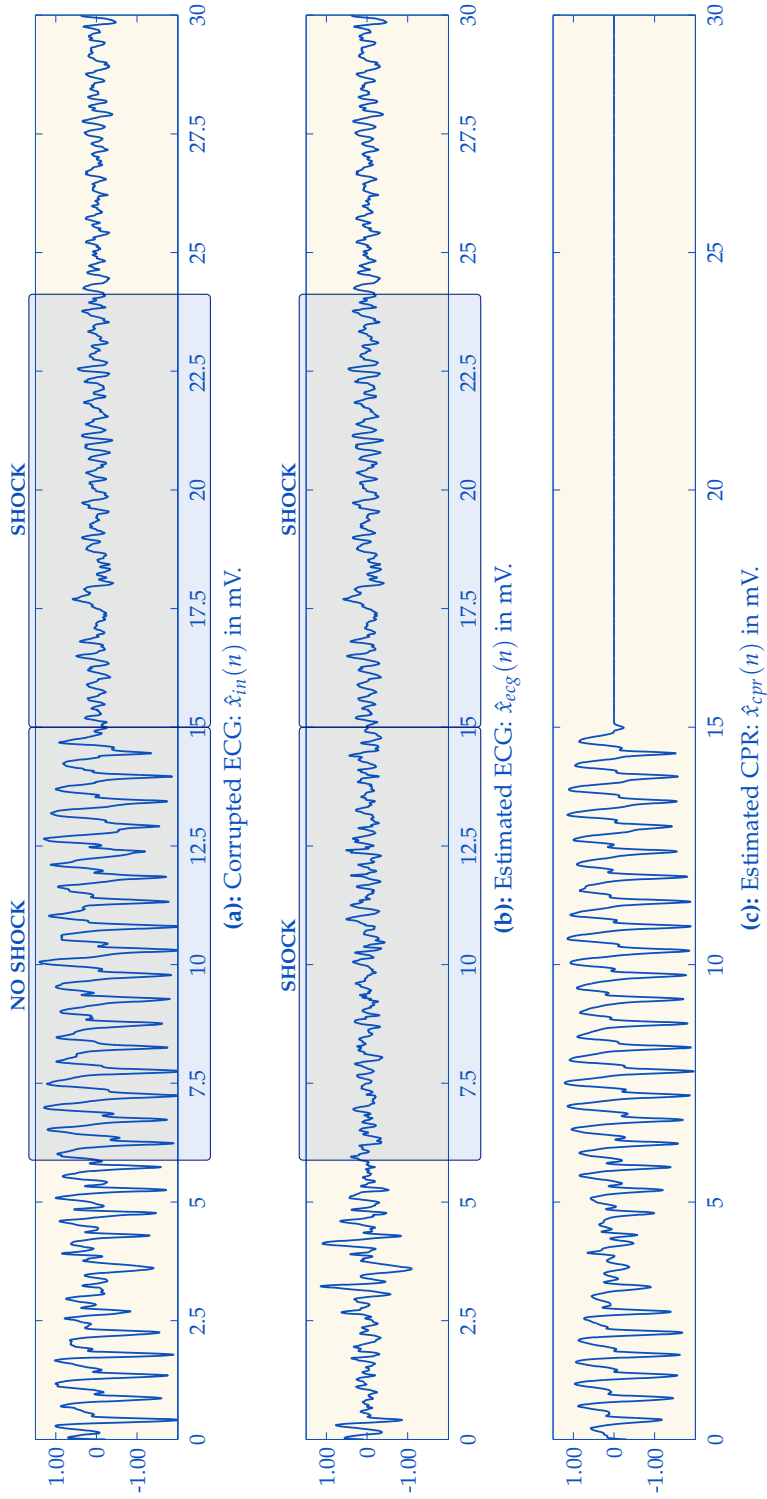


**Figure 5.12:** Example of a VF correctly diagnosed only after filtering. The underlying VF presents a small DF in the interval without CPR,  $DF=3.5\text{Hz}$ .

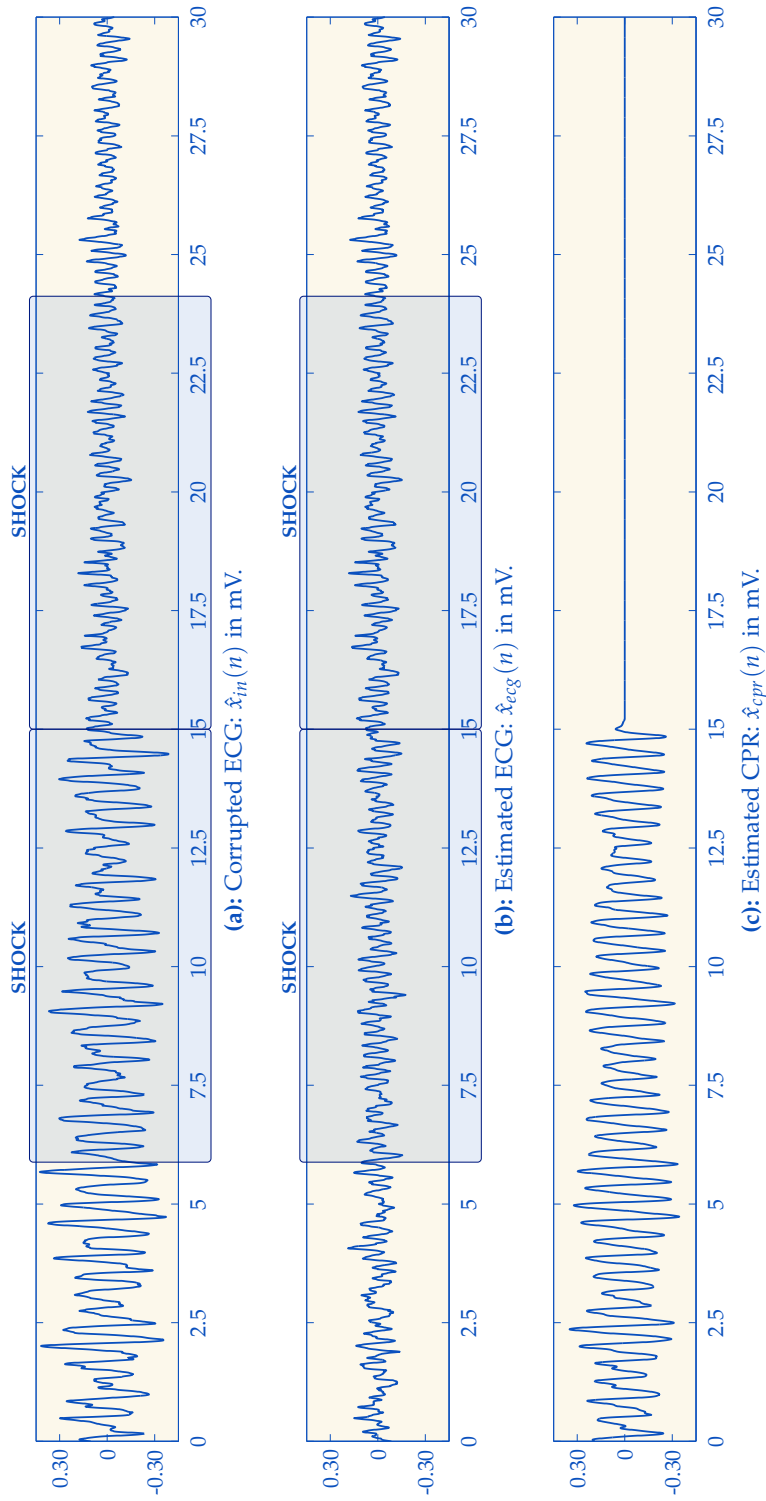


**Figure 5.13:** Example of a VF correctly diagnosed before and after filtering. CPR was administered at 160 cpm and it is classified as rVT by the algorithm.

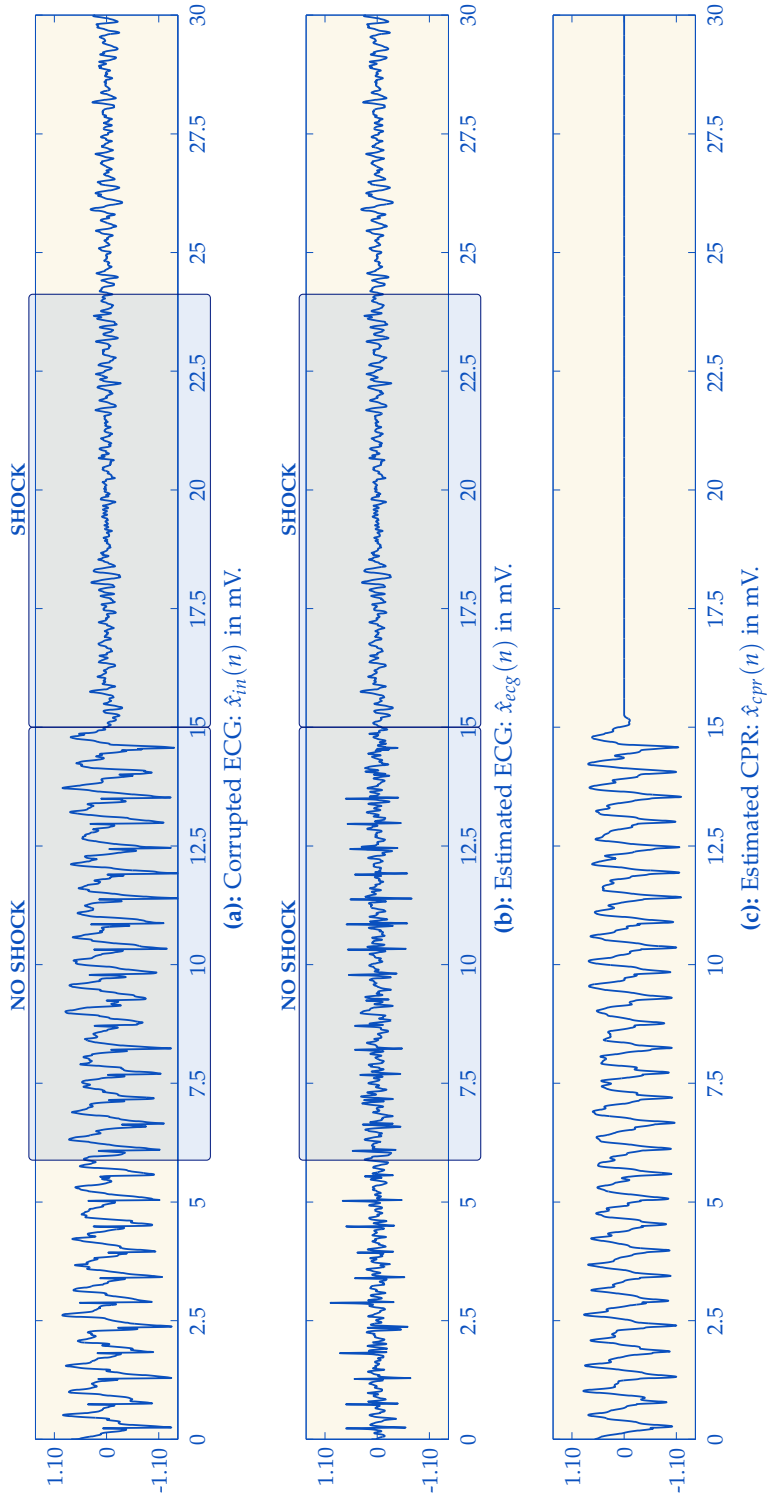


**Figure 5.14:** Example of a VF misdiagnosed before and after filtering. Filtering reveals a spiky artifact that is confused with QRS complexes, producing a no shock diagnosis.

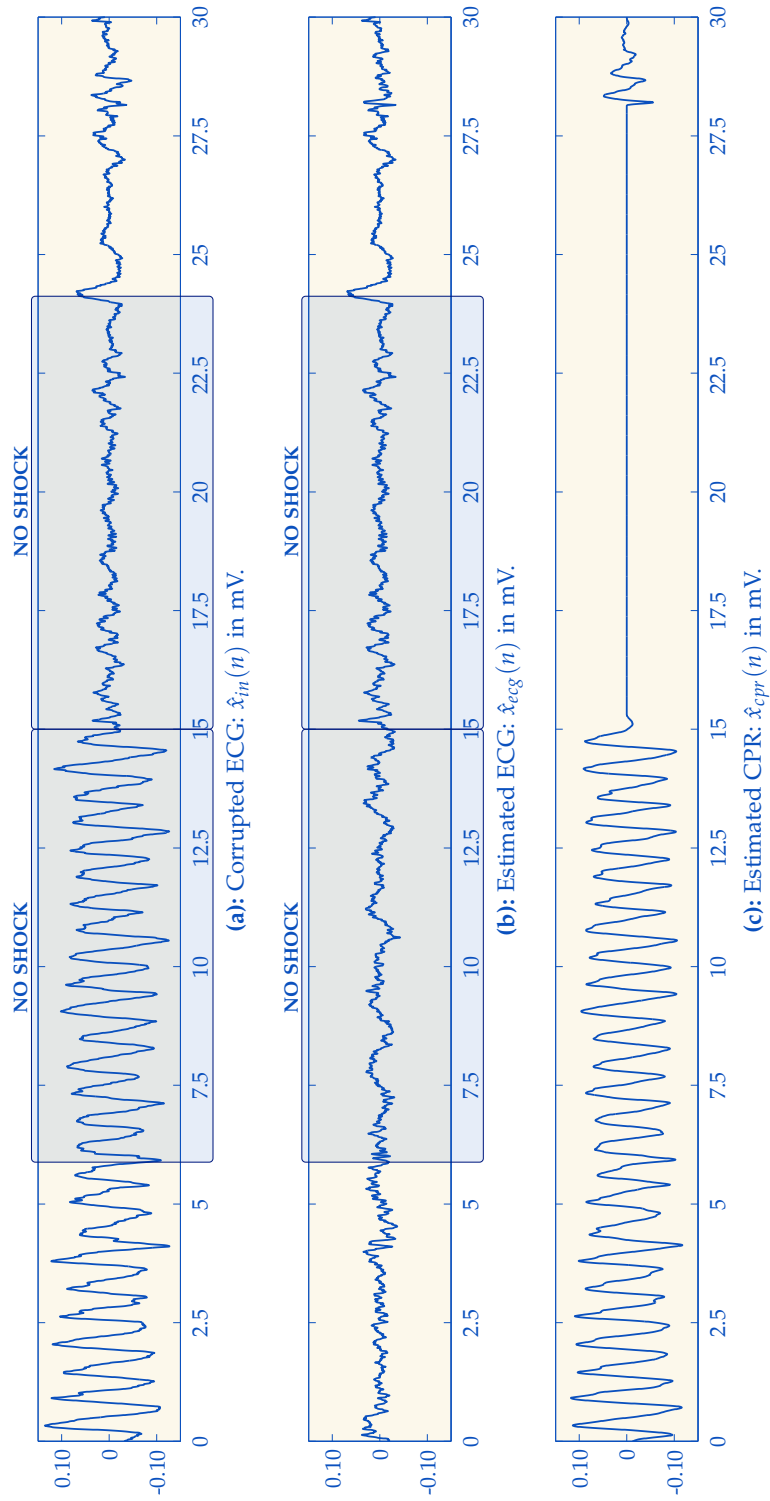


**Figure 5.15:** Example of an AS correctly diagnosed before and after filtering. CPR was administered at 105 cpm and the corrupted ECG is classified as sVT by the algorithm. The amplitude of the artifact is small and consequently the power of the disorganized residual is low and is classified as asystole.

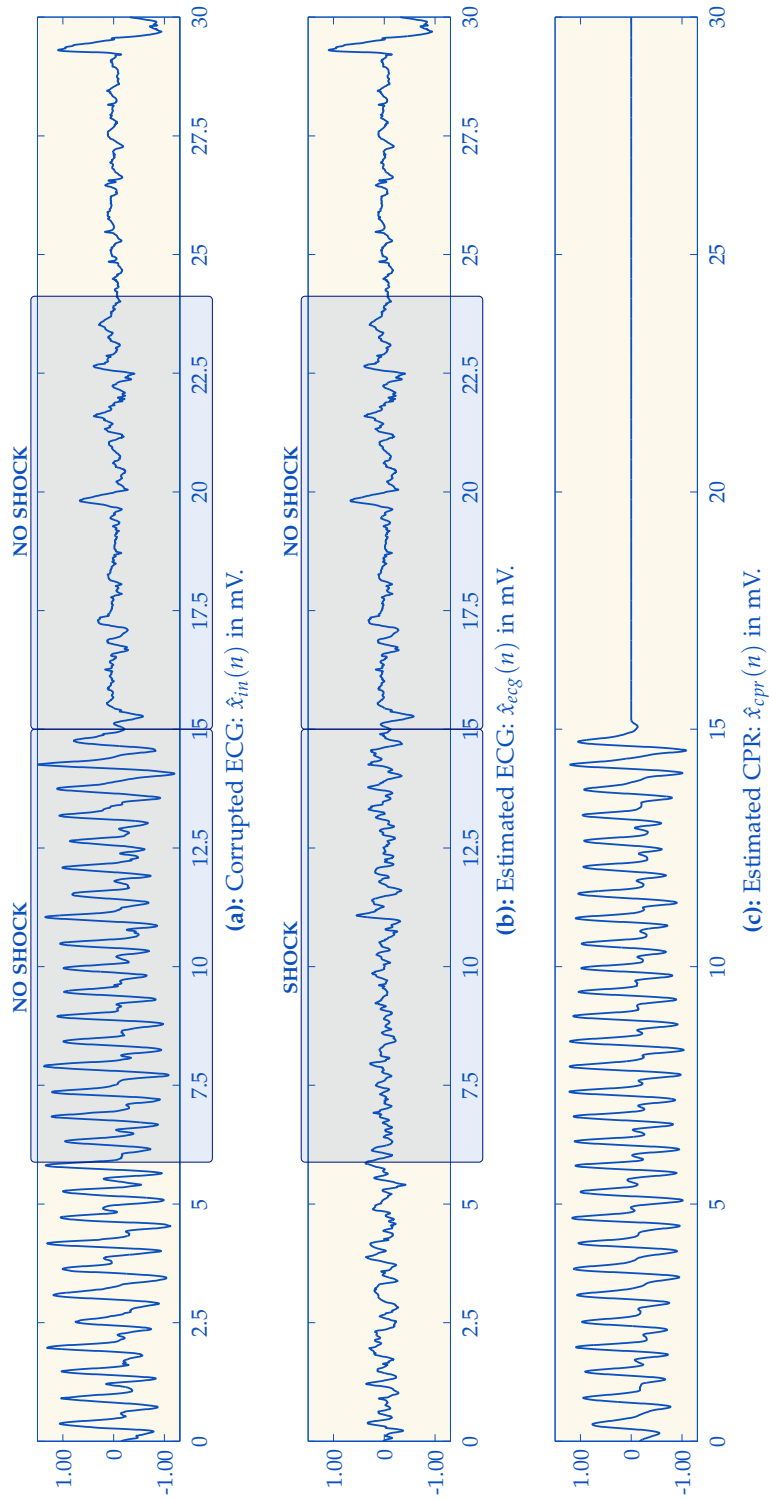


**Figure 5.16:** Example of a AS misdiagnosed after filtering. CPR was administered at 112 cpm and the corrupted ECG is classified as sVT by the algorithm. The amplitude of the artifact is large enough to produce a large amplitude disorganized residual classified as VF.



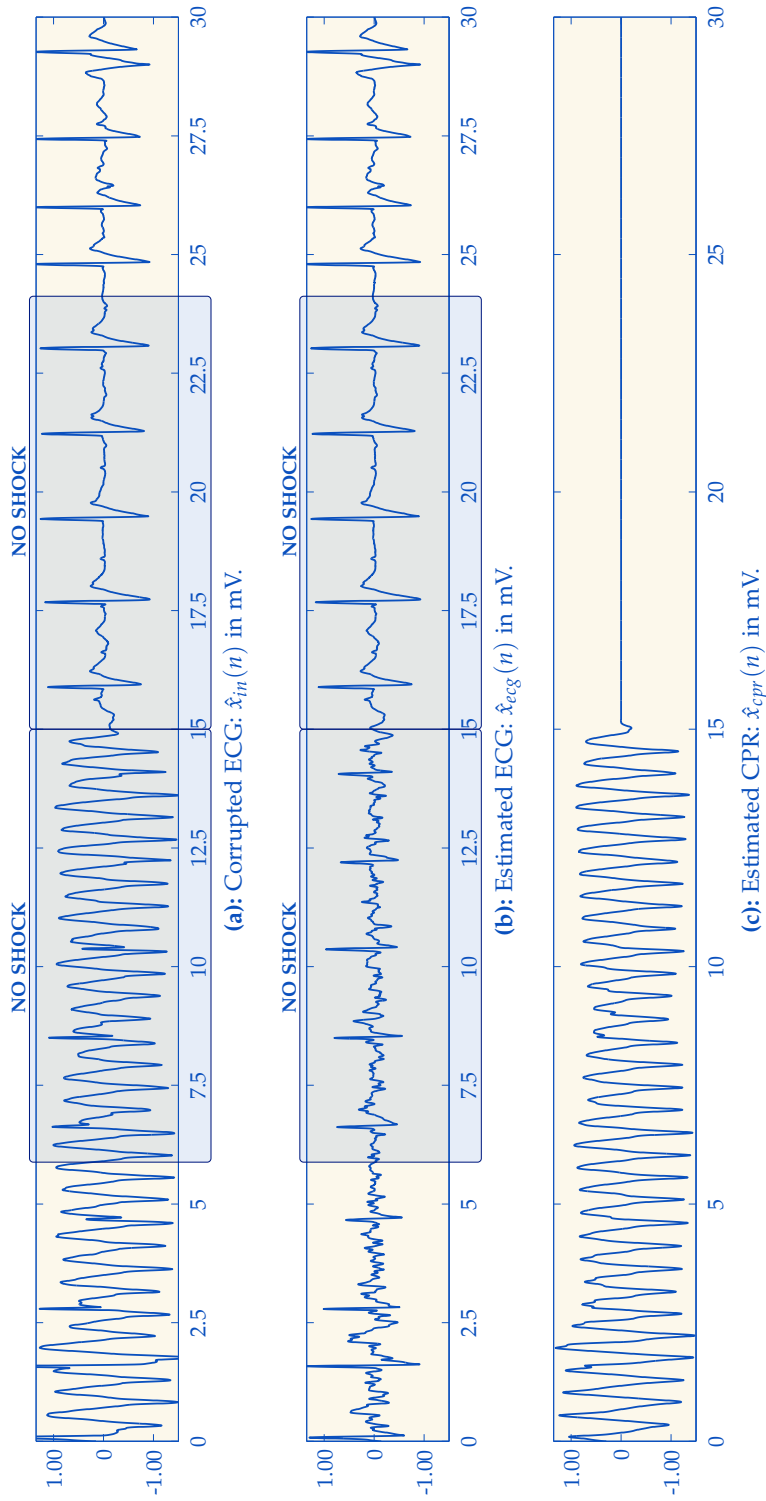


**Figure 5.17:** Example of an PEA correctly diagnosed before and after filtering. The frequency of the chest compressions was high, 127 cpm, although it is below the threshold for shockable VT. Filtering reveals the QRS complexes and the rhythm is classified as non-shockable.

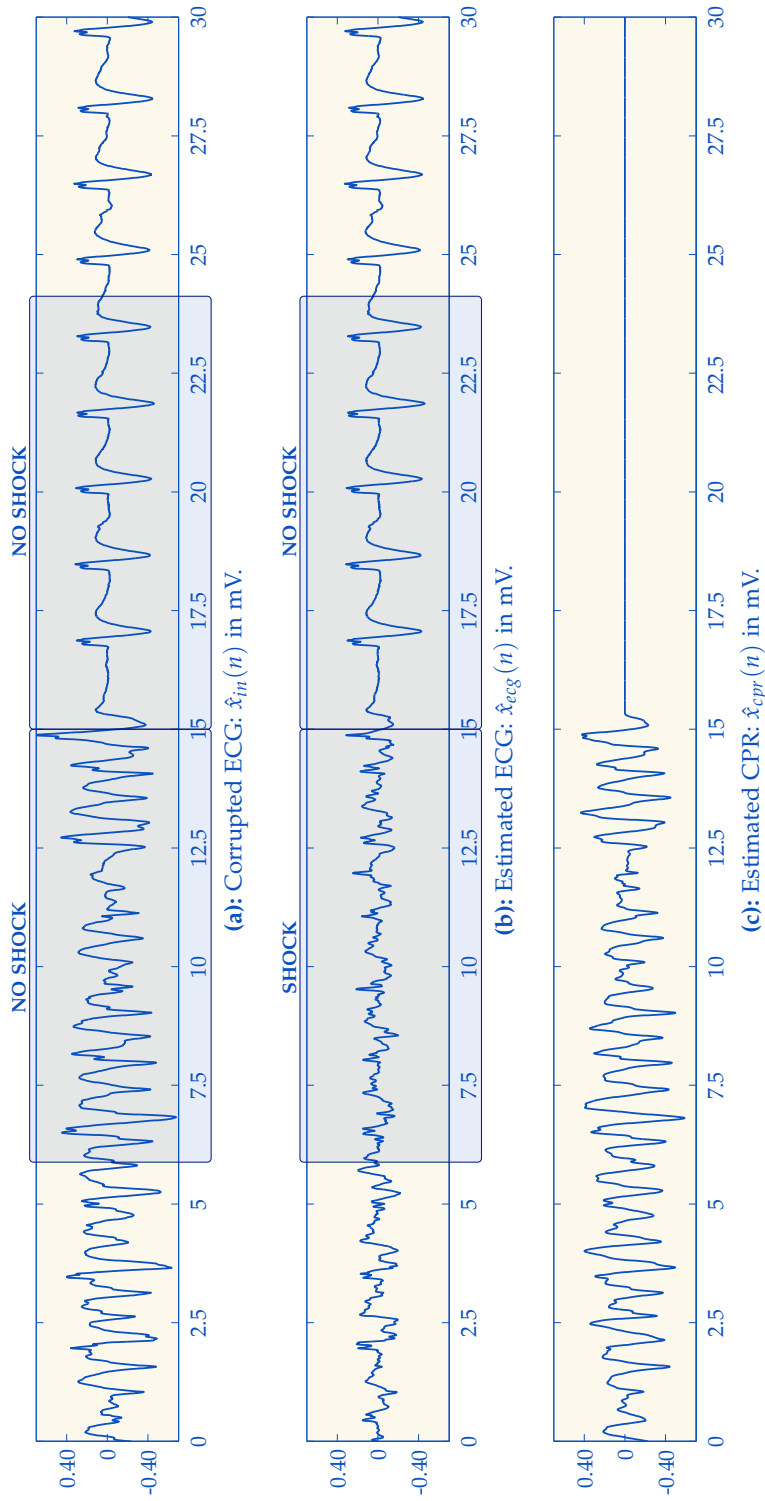


**Figure 5.18:** Example of an PEA misdiagnosed after filtering. CPR was administered at 115 cpm and the corrupted ECG is classified as sVT by the algorithm. The amplitude of the artifact is large. Although the underlying slow ventricular rhythm is partially revealed, the large disorganized residual produces the shock diagnosis.

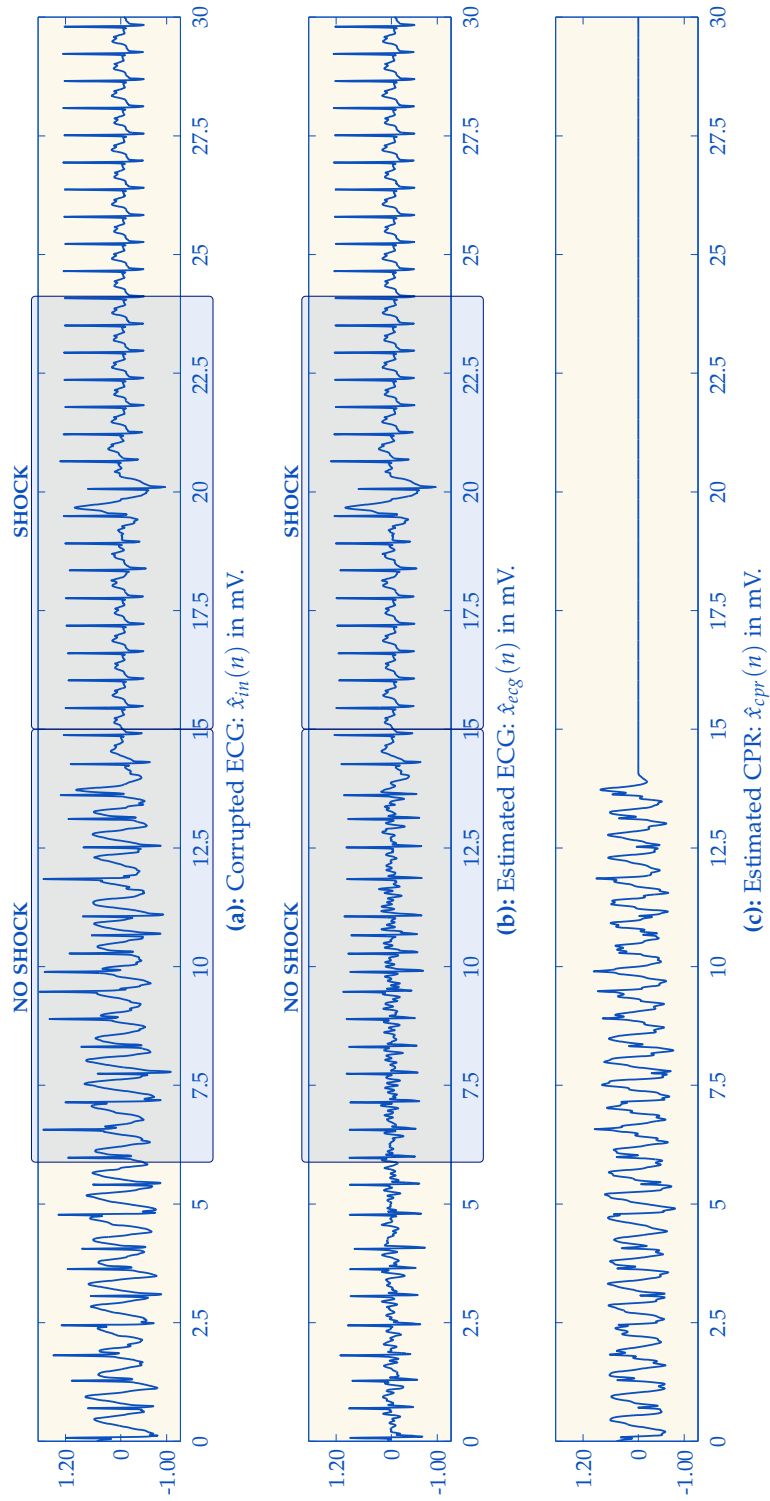


**Figure 5.19:** Example of a PR correctly diagnosed before and after filtering. QRS complexes are clearly seen before and after filtering.

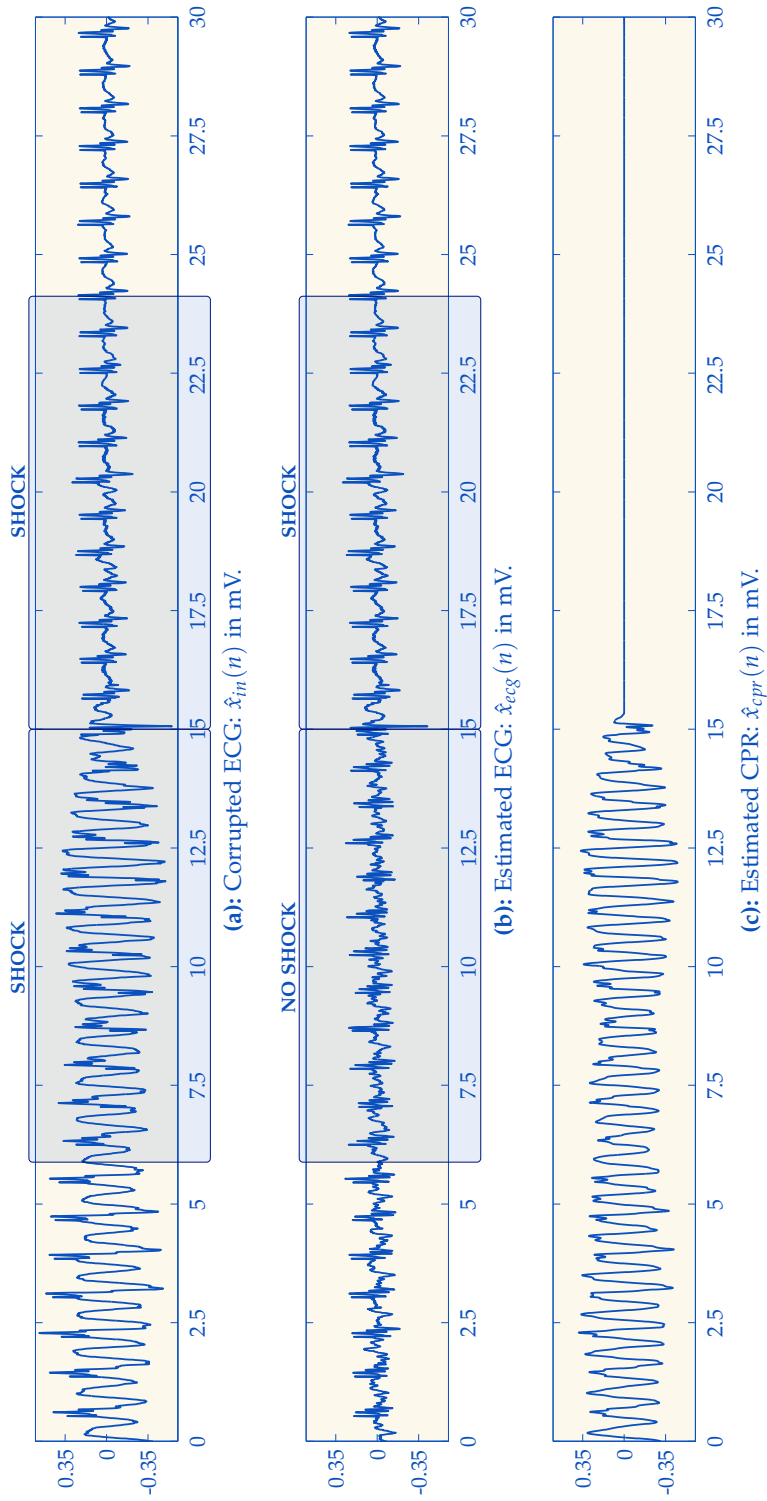


**Figure 5.20:** Example of a PR correctly diagnosed only and after filtering. CPR was administered at 150 cpm and the corrupted ECG is classified as rVT by the algorithm because the QRS complexes are not clearly seen during CPR.



## 6 | CONCLUSIONS

This chapter summarizes the main findings and contributions of this thesis work; several parts of which have been published in indexed journals (A1-A4) or presented at international conferences (C1-C11). The chapter concludes with a brief description of the future research lines opened by this work.

### Main contributions of the thesis work

The objective of this thesis work was the development and thorough testing of an AED algorithm valid for adult and pediatric patients. Its main contributions are those presented as intermediate goals in the introduction.

- *The compilation of the experimental data.* When this work started our group had an adult arrhythmia database to test AED algorithms. First, this database was revised and refined, and then a complete second database of adult arrhythmias was created through the cooperation with several Spanish EMS and hospitals. More importantly, a new database of pediatric arrhythmias to test AED algorithm was created. A large network of Spanish hospitals and cardiologists were involved in the process, which lasted three years from 2005 until late 2007. The pediatric database is comparable to the three proprietary databases known in the literature, and in combination with the two adult databases constitute a comprehensive tool to test AED algorithms in accordance with the AHA statement.
- *Parametrization of the ECG.* We have studied new ways to obtain robust rhythm identification parameters from several signal domains such as time, frequency, slope or the ACF. Furthermore, these new parameters were designed using adult and pediatric arrhythmias together.
- *Design of the AED shock advice algorithm.* Adult AED algorithms have been used to diagnose pediatric arrhythmias accurately either directly or after adjusting their thresholds

to pediatric data. In this thesis, we use a new methodology to design AED algorithms that takes pediatric and adult arrhythmias together for the design and validation of the algorithm. We have designed a new arrhythmia detection algorithm composed of four sub-algorithms, which are based on the new discrimination parameters. The algorithm will be incorporated soon to Osatu SCoop's new line of defibrillators.

- *Testing the algorithm in a resuscitation scenario.* The algorithm has been thoroughly tested using data extracted from a large and well-known database of OHCA episodes. We gained access to these data through our cooperation with Prof. Trygve Eftestøl. First, we evaluated the performance of the algorithm for clean OHCA rhythms; this is particularly interesting for non-shockable OHCA rhythms without a palpable pulse, which are very different from those covered in the AHA statement. Then, we analyzed the performance of the algorithm during CPR, both before and after suppressing the CPR artifact. We used an adaptive LMS filter developed as part of this thesis work to suppress the CPR artifact.

## Financial support

This thesis work was financially supported by the research projects listed below. They are all part of government-funded programs to support science and research, either exclusively (P1, P3) or in cooperation with Osatu SCoop (P2), the company that provided the infrastructure to create the pediatric database.

P1 *Estudio y análisis de hitos relacionados con la desfibrilación cardiaca mediante procesado digital de la señal ECG.*

Spanish ministry of Science and Technology

January 2004 – December 2007

Financing: 44800 €

P2 *Desfibrilador externo automático pediátrico.*

Basque Government and Osatu SCoop.

January 2005 – June 2007

Financing: 96000 €

P3 *Desfibrilación cardiaca en pacientes pediátricos.*

Spanish ministry of Science and Education

October 2006 – October 2009

Financing: 78650 €

## Publications

In this section we cite the contributions published in indexed journals and presented at international conferences in relation to this thesis work.

- Four communications at international conferences related to the creation of the arrhythmia databases and the comparison between pediatric and adult arrhythmias (C3, C4, C6 and C11).
- A publication in an indexed journal and a communication at an international conference related the parameters for the detection of adult and pediatric arrhythmias (A3, C8).
- A publication in an indexed journal and three communications at international conferences related to the new algorithm and its sub-algorithms (A2, C5, C7, C9).
- Two publications in indexed journals and three communications at international conferences related to the suppression of the CPR artifact (A1, A4, C1, C2 and C10).

### Indexed journals

- A1 Irusta U, Ruiz J, Ruiz de Gauna S, et al. A Least Mean-Square Filter for the Estimation of the Cardiopulmonary Resuscitation Artifact Based on the Frequency of the Compressions. *IEEE Trans Biomed Eng* 2009;56(4):1052–1062.
- A2 Irusta U, Ruiz J. An algorithm to discriminate supraventricular from ventricular tachycardia in automated external defibrillators valid for adult and paediatric patients. *Resuscitation* 2009;80(11):1229–1233.
- A3 Aramendi E, Irusta U, Pastor E, et al. ECG spectral and morphological parameters reviewed and updated to detect adult and paediatric life-threatening arrhythmia. *Physiological Measurement* 2010;31(6):749–761.
- A4 Ruiz J, Irusta U, Ruiz de Gauna S, et al. Cardiopulmonary resuscitation artefact suppression using a Kalman filter and the frequency of chest compressions as the reference signal. *Resuscitation* 2010. doi: 10.1016/j.resuscitation.2010.02.031.

## International conferences

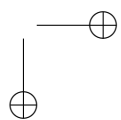
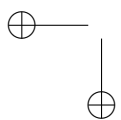
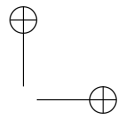
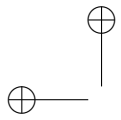
- C1 Ruiz de Gauna S, Ruiz J, Irusta U, et al. CPR Artefact Removal from VF Signals by Means of an Adaptive Kalman Filter Using the Chest Compression Frequency as Reference Signal. *Computers in Cardiology* 2005;32;175–178.
- C2 Irusta U, Ruiz de Gauna S, Ruiz J, et al. A variable step size LMS algorithm for the suppression of the CPR artefact from a VF signal. *Computers in Cardiology* 2005;32;179–182.
- C3 Aramendi E, Irusta U, Ruiz de Gauna S, et al. Comparative Analysis of the Parameters Affecting AED Specificity: Pediatric vs. Adult Patients. *Computers in Cardiology* 2006;33;445–448.
- C4 Irusta U, Aramendi E, Ruiz de Gauna S, et al. Development of a pediatric ECG rhythm database for the assessment of the rhythm analysis algorithms of automated external defibrillators. *Computers in Cardiology* 2006;33;609–612.
- C5 Irusta U, Ruiz J, Ruiz de Gauna S, et al. Sequential VT/VF discrimination algorithm based on wave mode sample entropy for adult and pediatric patients. *Computers in Cardiology* 2007;34;229–232.
- C6 Aramendi E, Irusta U, Ruiz de Gauna S, et al. Comparative analysis of the parameters affecting AED rhythm analysis algorithm applied to pediatric and adult Ventricular Tachycardia. *Computers in Cardiology* 2007; 419–422.
- C7 Irusta U, Ruiz J, Ruiz de Gauna S, et al. An algorithm to discriminate SVT from VT in pediatric AED based on spectral parameters. *Computers in Cardiology* 2008;35;925–928.
- C8 Ruiz de Gauna S, Ruiz J, Irusta U, et al. Parameters affecting shock decision in pediatric automated defibrillation. *Computers in Cardiology* 2008;35;929-932.
- C9 Irusta U, Ruiz J, Ruiz de Gauna S, et al. A pediatric shock advice algorithm based on the regularity of the detected beats. *Computers in Cardiology* 2008;35;1033–1036.
- C10 Ruiz de Gauna S, Ruiz J, Irusta U. A new CPR artefact removal method using chest compression signals. *Resuscitation* 2008;77(S1); S12.
- C11 Irusta U, Ruiz J, Aramendi E, et al. Amplitude, frequency and complexity features in paediatric and adult ventricular fibrillation. *Resuscitation* 2008;77(S1);S53.



## Future lines of research

AED algorithms have successfully been adapted for pediatric use in the following ways: adult algorithms that diagnose pediatric arrhythmias accurately,<sup>25,16</sup> pediatric specific algorithms<sup>15</sup> and universal algorithms designed including both patients groups. Our universal algorithm diagnoses clean OHCA rhythms accurately. However, it is not possible to diagnose non-shockable rhythms during chest compressions accurately; therefore, hands-off intervals have not been minimized. Several strategies can be further studied to minimize or shorten the hands-off intervals to increase survival rates.

- *Design of quick AED algorithms.* Hands-off intervals for rhythm assessment could be consistently limited to under 10 s by designing robust AED algorithms that diagnose a rhythm in 4–6 s accurately. Instead of the analysis based on three consecutive short windows, as used in this work, the new algorithms would be based on a new set of parameters calculated for a single but longer analysis window.
- *Combine AED algorithms and CPR suppression filters.* A way to accurately diagnose non-shockable rhythms during chest compressions may be to better understand the influence of the CPR suppression filter on the AED algorithm. First, the influence of the artifact and the filter on the AED parameters should be assessed. Then features derived from the corrupt and the filtered ECG could be used together to design a robust algorithm for the intervals with chest compressions. This would combine the two current strategies to rhythm analysis during CPR: filtering<sup>46,67</sup> and direct analysis of the corrupt ECG.<sup>95,86</sup>
- *Minimize the CPR artifact.* Finally, the possibility of minimizing the source of CPR artifacts should be further investigated. The amplitude of the artifact could be reduced either by recording the ECG through additional electrodes placed at locations less affected by chest compressions, or through the design of new systems to stabilize the skin-electrode contact during chest compressions.



# 7 | BIBLIOGRAPHY

- [1] The AHA Database for evaluation of ventricular arrhythmia detectors. Available at <http://www.ecri.org>
- [2] Guidelines 2000 for Cardiopulmonary Resuscitation and Emergency Cardiovascular Care. Part 4: the automated external defibrillator: key link in the chain of survival. *Circulation* 2000;102(8 Suppl); I60–I76.
- [3] Aase SO, Eftestøl T, Husøy JH, Sunde K, and Steen PA. CPR artifact removal from human ECG using optimal multichannel filtering. *IEEE Trans Biomed Eng* 2000;47(11); 1440–1449.
- [4] Aase SO and Myklebust H. Compression depth estimation for CPR quality assessment using DSP on accelerometer signals. *IEEE Trans Biomed Eng* 2002;49(3); 263–268.
- [5] Afonso V and Tompkins W. Detecting ventricular fibrillation. *IEEE Eng Med Biol Mag* 1995;14(2); 152–159.
- [6] Agresti A and Coull B. Approximate is better than "exact" for interval estimation of binomial proportions. *AmerStatist* 1998;52(2); 119–26.
- [7] al Fahoum AS and Howitt I. Combined wavelet transformation and radial basis neural networks for classifying life-threatening cardiac arrhythmias. *Med Biol Eng Comput* 1999;37(5); 566–573.
- [8] Aliot E, Nitzsché R, and Ripart A. Arrhythmia detection by dual-chamber implantable cardioverter defibrillators. A review of current algorithms. *Europace* 2004;6(4); 273–286.
- [9] Amann A, Klotz A, Niederklapfer T, et al. Reduction of CPR artifacts in the ventricular fibrillation ECG by coherent line removal. *Biomed Eng Online* 2010;9(1); 2.
- [10] Amann A, Tratnig R, and Unterkofler K. Reliability of old and new ventricular fibrillation detection algorithms for automated external defibrillators. *Biomed Eng Online* 2005;4; 60.

- [11] Amann A, Tratnig R, and Unterkofler K. Detecting Ventricular Fibrillation by Time-Delay Methods. *IEEE Trans Biomed Eng* 2007;54(1); 174–177.
- [12] Aramendi E, Irusta U, Pastor E, Bodegas A, and Benito F. ECG spectral and morphological parameters reviewed and updated to detect adult and paediatric life-threatening arrhythmia. *Physiological Measurement* 2010;31(6); 749–761.
- [13] Aramendi E, de Gauna SR, Irusta U, Ruiz J, Arcocha MF, and Ormaetxe JM. Detection of ventricular fibrillation in the presence of cardiopulmonary resuscitation artefacts. *Resuscitation* 2007;72(1); 115–123.
- [14] Atkins DL, Hartley LL, and York DK. Accurate recognition and effective treatment of ventricular fibrillation by automated external defibrillators in adolescents. *Pediatrics* 1998; 101(3 Pt 1); 393–397.
- [15] Atkins DL, Scott WA, Blaufox AD, et al. Sensitivity and specificity of an automated external defibrillator algorithm designed for pediatric patients. *Resuscitation* 2008;76(2); 168–174.
- [16] Atkinson E, Mikysa B, Conway JA, et al. Specificity and sensitivity of automated external defibrillator rhythm analysis in infants and children. *Ann Emerg Med* 2003;42(2); 185–196.
- [17] Aubert A, Denys B, Ector H, and Geest HD. Fibrillation recognition using autocorrelation analysis. *Computers in Cardiology* 1982;9; 477–480.
- [18] Bar-Cohen Y, Walsh EP, Love BA, and Cecchin F. First appropriate use of automated external defibrillator in an infant. *Resuscitation* 2005;67(1); 135–137.
- [19] Barro S, Ruiz R, Cabello D, and Mira J. Algorithmic sequential decision-making in the frequency domain for life threatening ventricular arrhythmias and imitative artefacts: a diagnostic system. *J Biomed Eng* 1989;11(4); 320–328.
- [20] Berg RA, Sanders AB, Kern KB, et al. Adverse hemodynamic effects of interrupting chest compressions for rescue breathing during cardiopulmonary resuscitation for ventricular fibrillation cardiac arrest. *Circulation* 2001;104(20); 2465–2470.

- [21] Berger RD, Palazzolo J, and Halperin H. Rhythm discrimination during uninterrupted CPR using motion artifact reduction system. *Resuscitation* 2007;75(1); 145–152.
- [22] Biarent D, Bingham R, Richmond S, et al. European Resuscitation Council guidelines for resuscitation 2005. Section 6. Paediatric life support. *Resuscitation* 2005;67(Suppl 1); S97–133.
- [23] Bossaert LL. Fibrillation and defibrillation of the heart. *Br J Anaesth* 1997;79(2); 203–213.
- [24] Cabello D, Barro S, Salceda JM, Ruiz R, and Mira J. Fuzzy K-nearest neighbor classifiers for ventricular arrhythmia detection. *Int J Biomed Comput* 1991;27(2); 77–93.
- [25] Cecchin F, Jorgenson DB, Berul CI, et al. Is arrhythmia detection by automatic external defibrillator accurate for children?: sensitivity and specificity of an automatic external defibrillator algorithm in 696 pediatric arrhythmias. *Circulation* 2001;103(20); 2483–2488.
- [26] Chen S. Complexity-Measure-Based Sequential Hypothesis Testing for Real-Time Detection of Lethal Cardiac Arrhythmias. *EURASIP Journal on Advances in Signal Processing* 2007; 2007(3); h1–h8.
- [27] Chen S, Thakor NV, and Mower MM. Ventricular fibrillation detection by a regression test on the autocorrelation function. *Med Biol Eng Comput* 1987;25(3); 241–249.
- [28] Chen SW. A two-stage discrimination of cardiac arrhythmias using a total least squares-based prony modeling algorithm. *IEEE Trans Biomed Eng* 2000;47(10); 1317–1327.
- [29] Chen SW, Clarkson PM, and Fan Q. A robust sequential detection algorithm for cardiac arrhythmia classification. *IEEE Trans Biomed Eng* 1996;43(11); 1120–1125.
- [30] Chugh SS, Jui J, Gunson K, et al. Current burden of sudden cardiac death: multiple source surveillance versus retrospective death certificate-based review in a large U.S. community. *J Am Coll Cardiol* 2004;44(6); 1268–1275.
- [31] Clayton RH and Murray A. Linear and non-linear analysis of the surface electrocardiogram during human ventricular fibrillation shows evidence of order in the underlying mechanism. *Med Biol Eng Comput* 1999;37(3); 354–358.

- [32] Clayton RH, Murray A, and Campbell RW. Comparison of four techniques for recognition of ventricular fibrillation from the surface ECG. *Med Biol Eng Comput* 1993;31(2); 111–117.
- [33] Clayton RH, Murray A, and Campbell RW. Recognition of ventricular fibrillation using neural networks. *Med Biol Eng Comput* 1994;32(2); 217–220.
- [34] Clifford AC. Comparative assessment of shockable ECG rhythm detection algorithms in automated external defibrillators. *Resuscitation* 1996;32(3); 217–225.
- [35] Cobb LA, Fahrenbruch CE, Olsufka M, and Copass MK. Changing incidence of out-of-hospital ventricular fibrillation, 1980–2000. *JAMA* 2002;288(23); 3008–3013.
- [36] Cobb LA, Fahrenbruch CE, Walsh TR, et al. Influence of cardiopulmonary resuscitation prior to defibrillation in patients with out-of-hospital ventricular fibrillation. *JAMA* 1999;281(13); 1182–1188.
- [37] Cummins RO, Eisenberg MS, Hallstrom AP, and Litwin PE. Survival of out-of-hospital cardiac arrest with early initiation of cardiopulmonary resuscitation. *Am J Emerg Med* 1985;3(2); 114–119.
- [38] de Gauna SR, Ruiz J, and Irusta U. A new CPR artefact removal method using chest compression signals. *Resuscitation* 2008;77(Suppl 1); S12 – S12.
- [39] de Gauna SR, Ruiz J, Irusta U, Aramendi E, Eftestøl T, and Kramer-Johansen J. A method to remove CPR artefacts from human ECG using only the recorded ECG. *Resuscitation* 2008;76(2); 271–278.
- [40] de Luna AB, Coumel P, and Leclercq JF. Ambulatory sudden cardiac death: mechanisms of production of fatal arrhythmia on the basis of data from 157 cases. *Am Heart J* 1989;117(1); 151–159.
- [41] Deakin CD, Nolan JP, and Council ER. European Resuscitation Council guidelines for resuscitation 2005. Section 3. Electrical therapies: automated external defibrillators, defibrillation, cardioversion and pacing. *Resuscitation* 2005; 67(Suppl 1); S25–S37.

- [42] Diack AW, Welborn WS, Rullman RG, Walter CW, and Wayne MA. An automatic cardiac resuscitator for emergency treatment of cardiac arrest. *Med Instrum* 1979;13(2); 78–83.
- [43] Doniger SJ and Shariieff GQ. Pediatric dysrhythmias. *Pediatr Clin North Am* 2006;53(1); 85–105.
- [44] Edelson DP, Abella BS, Kramer-Johansen J, et al. Effects of compression depth and pre-shock pauses predict defibrillation failure during cardiac arrest. *Resuscitation* 2006;71(2); 137–145.
- [45] Eftestøl T, Sunde K, and Steen PA. Effects of interrupting precordial compressions on the calculated probability of defibrillation success during out-of-hospital cardiac arrest. *Circulation* 2002;105(19); 2270–2273.
- [46] Eilevstjønn J, Eftestøl T, Aase SO, Myklebust H, Husøy JH, and Steen PA. Feasibility of shock advice analysis during CPR through removal of CPR artefacts from the human ECG. *Resuscitation* 2004;61(2); 131–141.
- [47] Eisenberg M, Bergner L, and Hallstrom A. Epidemiology of cardiac arrest and resuscitation in children. *Ann Emerg Med* 1983;12(11); 672–674.
- [48] Ewy GA. Cardiocerebral resuscitation: a better approach to cardiac arrest. *Curr Opin Cardiol* 2008;23(6); 579–584.
- [49] Fitzgibbon E, Berger R, Tsitlik J, and Halperin HR. Determination of the noise source in the electrocardiogram during cardiopulmonary resuscitation. *Crit Care Med* 2002; 30(4 Suppl); S148–S153.
- [50] DF39, Automatic External Defibrillators and Remote-Control Defibrillators. Technical Report, Association for the Advancement of Medical Instrumentation 1993.
- [51] Fukunaga K. Introduction to statistical pattern recognition. Academic Press, second edition 1990.
- [52] Ge D, Srinivasan N, and Krishnan SM. Cardiac arrhythmia classification using autoregressive modeling. *Biomed Eng Online* 2002;1; 5.
- [53] Gerein RB, Osmond MH, Stiell IG, Nesbitt LP, Burns S, and Group OPALSS. What are the etiology and epidemiology of out-of-hospital pediatric cardiopulmonary arrest in Ontario, Canada? *Acad Emerg Med* 2006;13(6); 653–658.

- [54] Hall M, Frank E, Holmes G, Pfahringer B, Reutemann P, and Witten I. The WEKA data mining software: An update. *ACM SIGKDD Explorations Newsletter* 2009;11(1); 10–18.
- [55] Hallstrom A, Rea TD, Sayre MR, et al. Manual chest compression vs use of an automated chest compression device during resuscitation following out-of-hospital cardiac arrest: a randomized trial. *JAMA* 2006;295(22); 2620–2628.
- [56] Handley AJ, Koster R, Monsieurs K, et al. European Resuscitation Council guidelines for resuscitation 2005. Section 2. Adult basic life support and use of automated external defibrillators. *Resuscitation* 2005;67(Suppl 1); S7–23.
- [57] Herbschleb J, Heethaar R, van der Tweel I, Zimmerman A, and Meijler F. Signal analysis of ventricular fibrillation. *Computers in Cardiology* 1979;6; 49–54.
- [58] Hickey RW, Cohen DM, Strausbaugh S, and Dietrich AM. Pediatric patients requiring CPR in the prehospital setting. *Ann Emerg Med* 1995;25(4); 495–501.
- [59] Holmberg M, Holmberg S, and Herlitz J. Effect of bystander cardiopulmonary resuscitation in out-of-hospital cardiac arrest patients in Sweden. *Resuscitation* 2000;47(1); 59–70.
- [60] Holmberg M, Holmberg S, and Herlitz J. Incidence, duration and survival of ventricular fibrillation in out-of-hospital cardiac arrest patients in Sweden. *Resuscitation* 2000;44(1); 7–17.
- [61] Hongxuan Z and Yisheng Z. Qualitative chaos analysis for ventricular tachycardia and fibrillation based on symbolic complexity. *Med Eng Phys* 2001;23(8); 523–528.
- [62] Huang H, Xie H, and Wang Z. The analysis of VF and VT with wavelet-based Tsallis information measure. *Physics Letters A* 2005;336; 180–187.
- [63] Husøy JH, Eilevstjønn J, Eftestøl T, Aase SO, Myklebust H, and Steen PA. Removal of cardiopulmonary resuscitation artifacts from human ECG using an efficient matching pursuit-like algorithm. *IEEE Trans Biomed Eng* 2002;49(11); 1287–1298.
- [64] IEC60601-2-4: Medical electrical equipment - Part 2-4: Particular requirements for the safety of cardiac defibrillators. Technical Report, IEC 2005.



- [65] Irusta U, Aramendi E, Ruiz de Gauna S, et al. Development of a pediatric ECG rhythm database for the assessment of the rhythm analysis algorithms of automated external defibrillators. *Computers in Cardiology* 2006;33; 609–612.
- [66] Irusta U and Ruiz J. An algorithm to discriminate supraventricular from ventricular tachycardia in automated external defibrillators valid for adult and paediatric patients. *Resuscitation* 2009;80(11); 1229–1233.
- [67] Irusta U, Ruiz J, de Gauna SR, Eftestol T, and Kramer-Johansen J. A Least Mean-Square Filter for the Estimation of the Cardiopulmonary Resuscitation Artifact Based on the Frequency of the Compressions. *IEEE Trans Biomed Eng* 2009;56(4); 1052–1062.
- [68] Irusta U, Ruiz J, Ruiz de Gauna S, and Aramendi E. An algorithm to discriminate SVT from VT in pediatric AED based on spectral parameters. *Computers in Cardiology* 2008; 35; 925–928.
- [69] Jacobs I, Nadkarni V, Bahr J, et al. Cardiac arrest and cardiopulmonary resuscitation outcome reports: update and simplification of the Utstein templates for resuscitation registries. *Circulation* 2004;110(21); 3385–3397.
- [70] Jekova I. Comparison of five algorithms for the detection of ventricular fibrillation from the surface ECG. *Physiol Meas* 2000;21(4); 429–439.
- [71] Jekova I. Shock advisory tool: Detection of life-threatening cardiac arrhythmias and shock success prediction by means of a common parameter set. *Biomedical Signal Processing and Control* 2007;2; 25–33.
- [72] Jekova I, Dushanova J, and Popivanov D. Method for ventricular fibrillation detection in the external electrocardiogram using nonlinear prediction. *Physiol Meas* 2002;23(2); 337–345.
- [73] Jekova I and Krasteva V. Real time detection of ventricular fibrillation and tachycardia. *Physiol Meas* 2004;25(5); 1167–1178.
- [74] Jekova I and Mitev P. Detection of ventricular fibrillation and tachycardia from the surface ECG by a set of parameters acquired from four methods. *Physiol Meas* 2002;23(4); 629–634.

- [75] Jenkins J and Caswell S. Detection algorithms in implantable cardioverter defibrillators. *Proc IEEE* 1996;84(3); 428–445.
- [76] Jr JG. Adaptive noise canceling applied to sinusoidal interferences. *IEEE Trans Acoust, Speech, Signal Process* 1977;25(6); 484–491.
- [77] Kaspar and Schuster. Easily calculable measure for the complexity of spatiotemporal patterns. *Phys Rev A* 1987; 36(2); 842–848.
- [78] Kellum MJ, Kennedy KW, Barney R, et al. Cardiocerebral resuscitation improves neurologically intact survival of patients with out-of-hospital cardiac arrest. *Ann Emerg Med* 2008;52(3); 244–252.
- [79] Kellum MJ, Kennedy KW, and Ewy GA. Cardiocerebral resuscitation improves survival of patients with out-of-hospital cardiac arrest. *Am J Med* 2006;119(4); 335–340.
- [80] Kerber RE, Becker LB, Bourland JD, et al. Automatic external defibrillators for public access defibrillation: recommendations for specifying and reporting arrhythmia analysis algorithm performance, incorporating new waveforms, and enhancing safety. *Circulation* 1997;95(6); 1677–1682.
- [81] Khadra L, al Fahoum AS, and al Nashash H. Detection of life-threatening cardiac arrhythmias using the wavelet transformation. *Med Biol Eng Comput* 1997;35(6); 626–632.
- [82] Khadra L, Al-Fahoum AS, and Binajjaj S. A quantitative analysis approach for cardiac arrhythmia classification using higher order spectral techniques. *IEEE Trans Biomed Eng* 2005;52(11); 1840–1845.
- [83] Kramer-Johansen J, Edelson DP, Losert H, Köhler K, and Abella BS. Uniform reporting of measured quality of cardiopulmonary resuscitation (CPR). *Resuscitation* 2007;74(3); 406–417.
- [84] Kramer-Johansen J, Myklebust H, Wik L, et al. Quality of out-of-hospital cardiopulmonary resuscitation with real time automated feedback: a prospective interventional study. *Resuscitation* 2006;71(3); 283–292.
- [85] Krasteva V and Jekova I. Assessment of ECG frequency and morphology parameters for automatic classification of life-threatening cardiac arrhythmias. *Physiol Meas* 2005;26(5); 707–723.

- [86] Krasteva V, Jekova I, Dotsinsky I, and Didon JP. Shock advisory system for heart rhythm analysis during cardiopulmonary resuscitation using a single ECG input of automated external defibrillators. *Ann Biomed Eng* 2010;38(4); 1326–1336.
- [87] Kuisma M, Suominen P, and Korpela R. Paediatric out-of-hospital cardiac arrests—epidemiology and outcome. *Resuscitation* 1995;30(2); 141–150.
- [88] Kuo S and Dillman R. Computer detection of ventricular fibrillation. *Computers in Cardiology* 1978;5; 347–349.
- [89] Köhler BU, Hennig C, and Orglmeister R. The principles of software QRS detection. *IEEE Eng Med Biol Mag* 2002;21(1); 42–57.
- [90] König B, Bengler J, and Goldsworthy L. Automatic external defibrillation in a 6 year old. *Arch Dis Child* 2005;90(3); 310–311.
- [91] Langer A, Heilman MS, Mower MM, and Mirowski M. Considerations in the development of the automatic implantable defibrillator. *Med Instrum* 1976;10(3); 163–167.
- [92] Langhelle A, Eftestøl T, Myklebust H, Eriksen M, Holten BT, and Steen PA. Reducing CPR artefacts in ventricular fibrillation in vitro. *Resuscitation* 2001;48(3); 279–291.
- [93] Larsen MP, Eisenberg MS, Cummins RO, and Hallstrom AP. Predicting survival from out-of-hospital cardiac arrest: a graphic model. *Ann Emerg Med* 1993;22(11); 1652–1658.
- [94] Lempel A and Ziv J. On the Complexity of Finite Sequences. *IEEE Trans Inf Theory* 1976;22(1); 75–81.
- [95] Li Y, Bisera J, Geheb F, Tang W, and Weil MH. Identifying potentially shockable rhythms without interrupting cardiopulmonary resuscitation. *Crit Care Med* 2008;36(1); 198–203.
- [96] Li Y and Tang W. Techniques for artefact filtering from chest compression corrupted ECG signals: good, but not enough. *Resuscitation* 2009;80(11); 1219–1220.
- [97] Luu M, Stevenson WG, Stevenson LW, Baron K, and Walden J. Diverse mechanisms of unexpected cardiac arrest in advanced heart failure. *Circulation* 1989;80(6); 1675–1680.

- [98] Marengo JP, Wang PJ, Link MS, Homoud MK, and Estes NA. Improving survival from sudden cardiac arrest: the role of the automated external defibrillator. *JAMA* 2001; 285(9); 1193–1200.
- [99] Martin DR, Gavin T, Bianco J, et al. Initial countershock in the treatment of asystole. *Resuscitation* 1993;26(1); 63–68.
- [100] Minami K, Nakajima H, and Toyoshima T. Real-time discrimination of ventricular tachyarrhythmia with Fourier-transform neural network. *IEEE Trans Biomed Eng* 1999; 46(2); 179–185.
- [101] Mogayzel C, Quan L, Graves JR, Tiedeman D, Fahrenbruch C, and Herndon P. Out-of-hospital ventricular fibrillation in children and adolescents: causes and outcomes. *Ann Emerg Med* 1995;25(4); 484–491.
- [102] Moody GB, Mark RG, and Goldberger AL. PhysioNet: a Web-based resource for the study of physiologic signals. *IEEE Eng Med Biol Mag* 2001;20(3); 70–75.
- [103] Murray A, Clayton RH, and Campbell RW. Assessment of the ventricular fibrillation detection algorithm in the semi-automatic Cardio-Aid defibrillator. *Resuscitation* 1995;29(2); 113–117.
- [104] Myerburg RJ. Sudden cardiac death: exploring the limits of our knowledge. *J Cardiovasc Electrophysiol* 2001;12(3); 369–381.
- [105] Myerburg RJ and Castellanos A. Emerging paradigms of the epidemiology and demographics of sudden cardiac arrest. *Heart Rhythm* 2006;3(2); 235–239.
- [106] Nadkarni VM, Larkin GL, Peberdy MA, et al. First documented rhythm and clinical outcome from in-hospital cardiac arrest among children and adults. *JAMA* 2006;295(1); 50–57.
- [107] Noc M, Weil MH, Tang W, Sun S, Pernat A, and Bisera J. Electrocardiographic prediction of the success of cardiac resuscitation. *Crit Care Med* 1999;27(4); 708–714.
- [108] Nolle F, AB KR, and Zencka. Power Spectrum Analysis of Ventricular Fibrillation and Imitative Artifacts. *Computers in Cardiology* 1980;7; 209–212.

- [109] Nygard M and Hulting J. Recognition of ventricular fibrillation utilizing the power spectrum of the ECG. *Computers in Cardiology* 1977;4; 393–397.
- [110] O'Rourke MF, Donaldson E, and Geddes JS. An airline cardiac arrest program. *Circulation* 1997;96(9); 2849–2853.
- [111] Owis MI, Abou-Zied AH, Youssef ABM, and Kadah YM. Study of features based on nonlinear dynamical modeling in ECG arrhythmia detection and classification. *IEEE Trans Biomed Eng* 2002;49(7); 733–736.
- [112] Page RL, Joglar JA, Kowal RC, et al. Use of automated external defibrillators by a U.S. airline. *N Engl J Med* 2000; 343(17); 1210–1216.
- [113] Polikaitis A, Arzbaeher R, Bump T, and Wilber D. Probability density function revisited: improved discrimination of VF using a cycle length corrected PDF. *Pacing Clin Electrophysiol* 1997;20(8 Pt 1); 1947–1951.
- [114] Povoas HP, Weil MH, Tang W, Bisera J, Klouche K, and Barbatsis A. Predicting the success of defibrillation by electrocardiographic analysis. *Resuscitation* 2002;53(1); 77–82.
- [115] Ravelli F and Antolini R. Complex dynamics underlying the human electrocardiogram. *Biol Cybern* 1992;67(1); 57–65.
- [116] Rea TD, Eisenberg MS, Sinibaldi G, and White RD. Incidence of EMS-treated out-of-hospital cardiac arrest in the United States. *Resuscitation* 2004;63(1); 17–24.
- [117] Rheinberger K, Steinberger T, Unterkofler K, Baubin M, Klotz A, and Amann A. Removal of CPR artifacts from the ventricular fibrillation ECG by adaptive regression on lagged reference signals. *IEEE Trans Biomed Eng* 2008;55(1); 130–137.
- [118] Rossano JW, Quan L, Kenney MA, Rea TD, and Atkins DL. Energy doses for treatment of out-of-hospital pediatric ventricular fibrillation. *Resuscitation* 2006;70(1); 80–89.
- [119] Ruiz J, Irusta U, de Gauna SR, and Eftestol T. Cardiopulmonary resuscitation artefact suppression using a Kalman filter and the frequency of chest compressions as the reference signal. *Resuscitation* 2010; doi:10.1016/j.resuscitation.2010.02.031.

- [120] Samson RA, Berg RA, Bingham R, et al. Use of automated external defibrillators for children: an update: an advisory statement from the pediatric advanced life support task force, International Liaison Committee on Resuscitation. *Circulation* 2003;107(25); 3250–3255.
- [121] Schuckers S. Approximate entropy as a measure of morphologic variability for ventricular tachycardia and fibrillation. *Computers in Cardiology* 1998;25; 265–268.
- [122] Schuckers S and Raphisak P. Distinction of arrhythmias with the use of approximate entropy. *Computers in Cardiology* 1999;26; 347–350.
- [123] Schwartz PJ, Garson A, Paul T, et al. Guidelines for the interpretation of the neonatal electrocardiogram. A task force of the European Society of Cardiology. *Eur Heart J* 2002;23(17); 1329–1344.
- [124] Sirbaugh PE, Pepe PE, Shook JE, et al. A prospective, population-based study of the demographics, epidemiology, management, and outcome of out-of-hospital pediatric cardiopulmonary arrest. *Ann Emerg Med* 1999;33(2); 174–184.
- [125] Small M, Yu D, Simonotto J, Harrison R, Grubb N, and Fox K. Uncovering non-linear structure in human ECG recordings. *Chaos, Solitons and Fractals* 2002;13(8); 1755–1762.
- [126] Snyder D and Morgan C. Wide variation in cardiopulmonary resuscitation interruption intervals among commercially available automated external defibrillators may affect survival despite high defibrillation efficacy. *Crit Care Med* 2004;32(9 Suppl); S421–S424.
- [127] Steen S, Liao Q, Pierre L, Paskevicius A, and Sjöberg T. The critical importance of minimal delay between chest compressions and subsequent defibrillation: a haemodynamic explanation. *Resuscitation* 2003;58(3); 249–258.
- [128] Strohmenger HU, Lindner KH, and Brown CG. Analysis of the ventricular fibrillation ECG signal amplitude and frequency parameters as predictors of countershock success in humans. *Chest* 1997;111(3); 584–589.
- [129] Strohmenger HU, Lindner KH, Keller A, Lindner IM, and Pfenninger EG. Spectral analysis of ventricular fibrillation and closed-chest cardiopulmonary resuscitation. *Resuscitation* 1996;33(2); 155–161.

- [130] Sun Y, Chan KL, and Krishnan SM. Life-threatening ventricular arrhythmia recognition by nonlinear descriptor. *Biomed Eng Online* 2005;4(1); 6.
- [131] Takata TS, Page RL, and Joglar JA. Automated external defibrillators: technical considerations and clinical promise. *Ann Intern Med* 2001;135(11); 990–998.
- [132] Thakor N, Zhu YS, and Pan KY. Ventricular tachycardia and fibrillation detection by a sequential hypothesis testing algorithm. *IEEE Trans Biomed Eng* 1990;37(9); 837–843.
- [133] Valenzuela TD, Roe DJ, Cretin S, Spaite DW, and Larsen MP. Estimating effectiveness of cardiac arrest interventions: a logistic regression survival model. *Circulation* 1997;96(10); 3308–3313.
- [134] Valenzuela TD, Roe DJ, Nichol G, Clark LL, Spaite DW, and Hardman RG. Outcomes of rapid defibrillation by security officers after cardiac arrest in casinos. *N Engl J Med* 2000; 343(17); 1206–1209.
- [135] Waalewijn RA, Nijpels MA, Tijssen JG, and Koster RW. Prevention of deterioration of ventricular fibrillation by basic life support during out-of-hospital cardiac arrest. *Resuscitation* 2002;54(1); 31–36.
- [136] Waalewijn RA, Tijssen JG, and Koster RW. Bystander initiated actions in out-of-hospital cardiopulmonary resuscitation: results from the Amsterdam Resuscitation Study (ARRESUST). *Resuscitation* 2001;50(3); 273–279.
- [137] Wang Y, Zhu YS, Thakor NV, and Xu YH. A short-time multifractal approach for arrhythmia detection based on fuzzy neural network. *IEEE Trans Biomed Eng* 2001;48(9); 989–995.
- [138] Weaver WD, Hill D, Fahrenbruch CE, et al. Use of the automatic external defibrillator in the management of out-of-hospital cardiac arrest. *N Engl J Med* 1988;319(11); 661–666.
- [139] Weisfeldt ML and Becker LB. Resuscitation after cardiac arrest: a 3-phase time-sensitive model. *JAMA* 2002;288(23); 3035–3038.
- [140] Weisfeldt ML, Kerber RE, McGoldrick RP, et al. Public access defibrillation. A statement for healthcare professionals from

- the American Heart Association Task Force on Automatic External Defibrillation. *Circulation* 1995;92(9); 2763.
- [141] Werther T, Klotz A, Granegger M, et al. Strong corruption of electrocardiograms caused by cardiopulmonary resuscitation reduces efficiency of two-channel methods for removing motion artefacts in non-shockable rhythms. *Resuscitation* 2009;80(11); 1301–1307.
- [142] Werther T, Klotz A, Kracher G, et al. CPR Artifact Removal in Ventricular Fibrillation ECG Signals Using Gabor Multipliers. *IEEE Trans Biomed Eng* 2009;56(2); 320–327.
- [143] White RD, Bunch TJ, and Hankins DG. Evolution of a community-wide early defibrillation programme experience over 13 years using police/fire personnel and paramedics as responders. *Resuscitation* 2005;65(3); 279–283.
- [144] Widrow B, Jr JG, McCool J, et al. Adaptive noise cancelling: Principles and applications. *Proc IEEE* 1975;63(12); 1692–1716.
- [145] Wik L, Hansen TB, Fylling F, et al. Delaying defibrillation to give basic cardiopulmonary resuscitation to patients with out-of-hospital ventricular fibrillation: a randomized trial. *JAMA* 2003;289(11); 1389–1395.
- [146] Wik L, Kramer-Johansen J, Myklebust H, et al. Quality of cardiopulmonary resuscitation during out-of-hospital cardiac arrest. *JAMA* 2005;293(3); 299–304.
- [147] Xiao Y and Tadokoro Y. LMS-based notch filter for the estimation of sinusoidal signals in noise. *Signal Processing* 1995;46(2); 223–231.
- [148] Young KD and Seidel JS. Pediatric cardiopulmonary resuscitation: a collective review. *Ann Emerg Med* 1999;33(2); 195–205.
- [149] Yu T, Weil MH, Tang W, et al. Adverse outcomes of interrupted precordial compression during automated defibrillation. *Circulation* 2002;106(3); 368–372.
- [150] Zhang XS, Zhu YS, Thakor N, and Wang ZZ. Detecting ventricular tachycardia and fibrillation by complexity measure. *IEEE Trans Biomed Eng* 1999;46(5); 548–555.
- [151] Zheng ZJ, Croft JB, Giles WH, and Mensah GA. Sudden cardiac death in the United States, 1989 to 1998. *Circulation* 2001;104(18); 2158–2163.



- [152] Zipes DP and Wellens HJ. Sudden cardiac death. *Circulation* 1998;98(21); 2334–2351.